Nonlinear modeling of the seismic response of masonry structures: critical review and open issues towards engineering practice

Submitted to Bulletin of Earthquake Engineering – SI: URM nonlinear modeling – Benchmark project

NONLINEAR MODELING OF THE SEISMIC RESPONSE OF MASONRY STRUCTURES: CRITICAL REVIEW AND OPEN ISSUES TOWARDS ENGINEERING PRACTICE

Serena Cattari[1*], Bruno Calderoni[2], Ivo Caliò[3], Guido Camata[4], Stefano de Miranda[5], Guido Magenes[6], Gabriele Milani[7], Anna Saetta[8]

[1] *Department of Civil, Chemical and Environmental Engineering (DICCA), University of Genoa, Via Montallegro 1, 16145 Genoa, Italy*

e-mail: serena.cattari@unige.it

[2] *Department of Structures for Engineering and Architecture (DIST). University of Naples Federico II, Via Claudio 21. 80125 – Napoli*

e-mail: bruno.calderoni@unina.it

[3] *Dipartimento di Ingegneria Civile e Architettura (DICAR), University of Catania, Via Santa Sofia 64, 95125 Catania, Italy*

e-mail: ivo.calio@unict.it

[4] *Department of Engineering and Geology (INGEO). University "G. d'Annunzio" of Chieti Pescara*

e-mail: guido.camata@unich.it

[5] *Department of Civil, Chemical, Environmental, and Materials Engineering (DICAM), University of Bologna, Viale del Risorgimento 2, Bologna 40136, Italy*

e-mail: stefano.demiranda@unibo.it

[6] *Department of Civil and Architectural Engineering (DICAR), University of Pavia, Via Adolfo Ferrata 3, 27100 Pavia, Italy*

e-mail guido.magenes@unipv.it

[7] *Department of Architecture, Built Environment and Construction Engineering (A.B.C.) Technical University of Milan (Politecnico di Milano) Piazza Leonardo da Vinci 32, 20133 Milan*

e-mail: gabriele.milani@polimi.it

[8] *Department of Architecture and Arts (DCP), University Iuav of Venice, Tolentini 191, 30135 Venezia, Italy*

e-mail: anna.saetta@iuav.it

*Corresponding author

Abstract

This paper provides a comphrensive review of the critical aspects of nonlinear modeling for evaluating the seismic response of masonry structures, emphasizing the issues relevant to engineering practice. Currently, the specialized technical community shares the opinion that, for a performance-based approach, numerical models are the only tools sufficiently effective to support the seismic assessment of existing buildings. However, their potential often falls short when attempting to accurately describe the behavior of masonry structures. In fact, these structures feature highly complex architectural configurations, different masonry types, and various structural solutions, meaning that extra care is required in numerical modeling. This is especially true when the modelers do not have a solid background in the software chosen and may not be practiced using the vast variety of options offered by the software houses. They are often unaware of the consequences that questionable

modeling choices may have on the results obtained by the models. These extremely complex topics are treated in the paper from an engineering practice perspective, providing an in-depth overview of the challenging issues related to the use of different modeling strategies. The paper covers strategies ranging from the Equivalent Frame approach (used widely in common engineering practice) to more refined techniques like 2D and 3D FE procedures based on continuous, discrete, and micro-mechanical approaches. Critical aspects in the modeling of both in- and out-of-plane responses of masonry, as well as the critical issues in wall-to-wall connections and diaphragm roles are investigated. All the examined issues are clarified through numerical examples highlighting also how a consistent and integrated use of different procedures may be beneficial. Finally, some of most relevant challenging issues concerning the use of numerical models in seismic assessments with the nonlinear static approach are presented and discussed.

Keywords: *masonry structures; modeling strategies; equivalent frame approach; continuum approach; discrete approach; wall-to-wall connection; diaphragms modeling; nonlinear analyses*

1 Introduction

At present, numerical models represent an essential tool that practitioners and researchers can utilize when analysing and interpreting the results of the simulation of the structural response of buildings. The ability of numerical models to correctly reproduce the actual seismic behavior of buildings is fundamental for the effective assessment of seismic risk analyses and the supporting of mitigation policies. Such a requisite is essential, in general, for existing buildings and, especially, for the unreinforced masonry (URM) ones.

Masonry buildings are distinctly multifaceted in terms of:

- Architectural configurations. A large variety in the layouts is observed not only in ordinary buildings, but also in monumental ones (like palaces, churches, fortresses, towers, see Lagomarsino et al. 2011 for a classification in seismic areas), as well as in aggregate masonry structures, which are quite ubiquitous in historical city centers.
- Masonry typologies. A rough classification distinguishes between “regular” and “irregular” masonry types, but it is well-known that there are many other factors, such as mortar quality, blocks type and shape, bond pattern, and transversal connections in multi-leaf walls (just to mention a few) that affect the overall seismic response of a building (as discussed, for example, in Borri et al. 2015, Cardani and Binda 2015, Krzan et al. 2015).
- Structural solutions for carrying gravity loads, such as the presence of different lintel typologies above the openings, segmental arches, timber/steel or reinforced concrete beams, etc.
- Structural solutions that influence the global behavior. For instance, the presence (or lack) of tensile resistant elements at floor level, steel tie rods or r.c. beams, diaphragms (*e.g.*, vaults, timber floors, r.c. slabs, iron beams and hollow bricks capped by r.c. slabs) and their connection to the walls, as well as the wall-to-wall interconnections.

From the previous considerations, it emerges how any numerical model, to be used in engineering practice, should be versatile enough to effectively describe a wide variety of masonry structures,

maintaining the ability to satisfactorily predict their actual behavior, and still being relatively simple to use.

Many surveys after past earthquakes (see for example D'Ayala and Paganoni 2011, Penna et al. 2014a, Sorrentino et al. 2019) have shown how all the above-mentioned factors play a decisive role in defining the actual seismic response of URM buildings. Such factors are usually associated to two main categories of response: the in-plane one and the occurrence of local mechanisms (mainly associated to out-of-plane failures of single parts). More specifically, a large amount of data, made available by the Italian Department of Civil Protection through the Da.D.O platform (Dolce et al. 2019) on the observed seismic damage, has been recently used in statistical studies aimed at deriving empirical fragility curves (*e.g.*, Rosti et al. 2021, Del Gaudio et al. 2019, Lagomarsino et al. 2021). Such data gave the possibility of quantitatively addressing the influence that combined factors, like masonry quality (regular or irregular), type of diaphragms (flexible or rigid), and the systematic presence (or lack thereof) of connecting devices (*e.g.*, tie rods/tie r.c. beams) can have on the seismic response of masonry buildings. In fact, the results in terms of fragility curves have highlighted that masonry quality has a significant role on the seismic response, that there is a general tendency for vulnerability to decrease with increasing diaphragm stiffness (provided the quality of masonry is above a minimum), and, moreover, that there is a positive role of the presence of connecting devices. In addition, as discussed in De Felice (2011), it is known how the role of masonry quality is crucial in determining the actual morphology of damage associated to the out-of-plane response. In case of poor mortar quality, characterized by a low connection between leaves, it is needed to verify if the out-of-plane response can be due to the rigid-block idealization or to a masonry crumbling.

It is clear that in order to interpret such complex phenomena, first of all the analysts should have a sound knowledge of the recurring failure modes that may occur in order to properly identify the key features of the structure examined and, consequently, to address the modeling choices. Moreover, even if this paper is essentially numerical oriented, it cannot be disgregarded that an appropriate knowledge phase also constitutes the preliminary but crucial requisite to support the modeling choices, addressing at the same time the matter of uncertainties (as discussed for example in Cattari et al. 2015a). In most of the cases, such phase presupposes the integration of various tools, e.g. historical analysis, in-depth visual structural in-situ surveys and experimental tests. Recent emblematic examples are illustrated for example in Lorenzoni et al. (2020), Ponte et al. (2021) and Camara et al. (2021), where it is stressed how nowadays the issue has to be faced more and more from a multidisciplinary perspective.

Instead, concerning the models, they must be effectively versatile and accurate in their ability to describe all possible behaviors and the cause-effect relationship with the corresponding structural

solutions and masonry typologies. Concerning the last aspect, there are many possible strategies that can be adopted. In the literature, studies devoted to the classification of the most widely adopted modeling strategies already exist (see, for example, Lourenço 2002, Roca et al. 2010, D'Altri et al. 2020a). In some of them, such a classification is provided as a function of architectural type (*e.g.*, in Lagomarsino and Cattari 2015a, for monumental buildings), and going into the detail on the state of the art for specific approaches (*e.g.*, in Quagliarini et al. 2017 for the equivalent frame approaches). Taking advantage of such robust background, the main goal of this paper is instead to provide the reader with a wide perspective on how to model effectively URM structures from a seismic and engineering practice point of view. To this aim, the use of various modeling strategies is critically reviewed in order to investigate how different solutions can be applied to simulate the above-mentioned phenomena and also highlighting the potential of integrating their use. Several numerical examples are illustrated and discussed to better demonstrate how the treated issues can influence the outcome of seismic verification. Many of them have been selected from the results of a wide research program, synthetically named in the following as "*URM nonlinear modeling* – Benchmark project" (Cattari and Magenes 2021). The latter has been carried out, starting in 2014, by several research units coordinated by the Authors of this paper and involved in the ReLUIS project (*Rete dei Laboratori Universitari di Ingegneria Sismica* - Italian Network of University Seismic Laboratories). As a matter of fact, the project gave the whole research group the opportunity to gain insight into various critical issues in modeling strategies and in the interpretation of the seismic response of URM buildings. The selection proposed in the paper relates to the challenging issues of URM modeling derived from this experience and has been integrated with the expertise on the topic by the Authors.

More in detail, the paper examines models working at different scales, that can be preliminarily classified into the following two main categories:

- Equivalent Frame (EF) models, defined at structural element scale identifying one-dimensional macroscopic structural elements, namely piers and spandrels, where all nonlinearity is concentrated, and whose size (length) is in the order of magnitude of the interstory height or the size of the openings (doors, windows). These elements are one-dimensional in the sense that they are mainly formulated as beam-column elements. Piers are the elements with a vertical axis, designed primarily to resist gravity loads and, in case of an earthquake, to transfer significant horizontal actions from the foundation to the elevation. Spandrels are masonry beams characterized by a horizontal axis, connecting contiguous piers. The elements are mutually interconnected by rigid links representing crossing areas between piers and spandrels.

- Models with a more “refined” discretization with 2D or 3D elements, in which masonry may be described through different degrees of accuracy using for instance: the following approaches: (1) fictitious homogeneous materials (also known as macro-scale modeling) by adopting a continuous mesh of 2D or 3D finite elements (FE) with isotropic or anisotropic laws; (2) discrete elements strategies, based on 2D or 3D macro-elements; and meso-scale (or micro-mechanical) approaches, in which the single components (mortar joints and blocks) are modeled separately. In this paper, the adjective “refined” aims at synthetically grouping a class of models that, differently from EF models, do not strictly require any *a priori* identification of piers and spandrels and that can describe the structure at macro or micro scale. For the sake of brevity, these models are referred to in this paper as “refined”, in a relative comparison with equivalent frame approaches.

Regardless the adopted modeling approach, another essential key feature is its capability to accurately reproduce the nonlinear response typical of masonry structures. Actually, masonry is characterized by very low tensile strength, which causes the onset of cracking phenomena for low levels of stress and, therefore, a nonlinear behavior even at early stages of incremental analyses and for low levels of loading, especially in the presence of horizontal actions. That being said, this requisite is essential in the seismic engineering field when dealing with the performance-based assessment (PBA). Figure 1 illustrates a possible classification of the element types used in EF and refined models as a function of the different approaches adopted for describing the nonlinearity (*i.e.,* distinguishing the concentrated or distributed nonlinearity). The selection of models represented in Figure 1 refers to the options more commonly adopted also in the engineering practice and available in commercial software. Figure 1 is not intended to be exhaustive of all possible solutions implemented at research level, like for example the block-based approach or other ones discussed in sub-paragraphs of Section 2.4. Moreover, as discussed in more detail in Section 2.1, solutions a, b and c of Figure 1 are typical of EF models, while the others are more commonly adopted in refined models. Such classification can also adapt to the different components that constitute the buildings (*i.e.*, vertical –*walls*, horizontal- *diaphragms*, and connections).

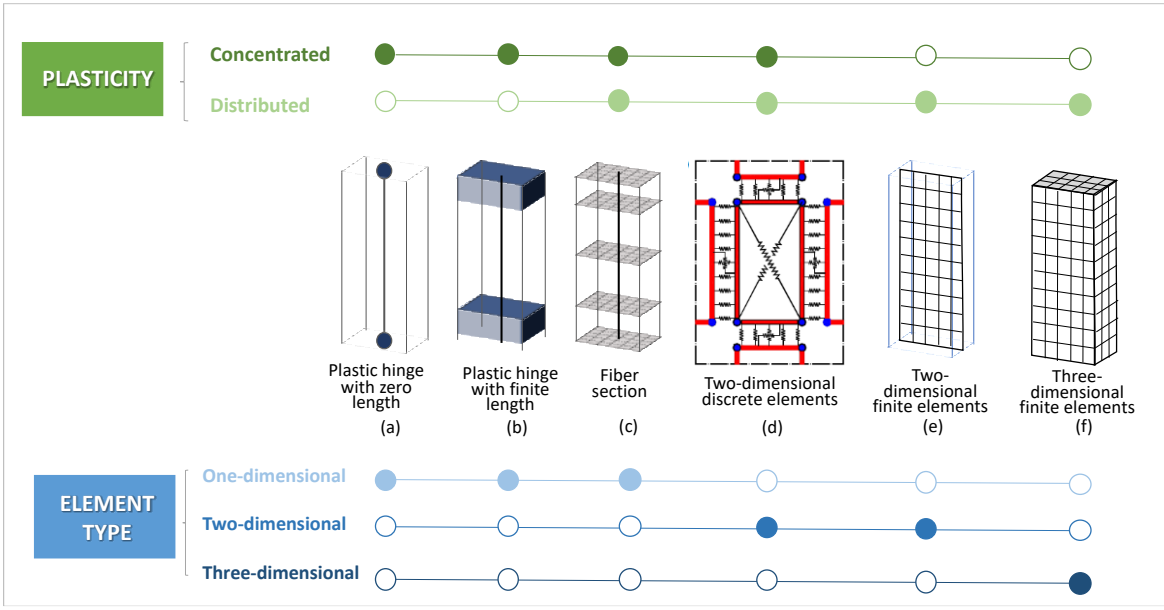

Figure 1 – Possible classification of models commonly adopted by professionals and researchers for the seismic analysis of URM structures

Within this general context and to pursue the aforementioned goals, the paper is organized into two main parts. The first gives an overview of challenging issues in URM modeling, focusing on criticalities aspects related to:

- the modeling of structural elements (piers and spandrels) in EF models (Section 2.1) and the main issue of the proper calibration of parameters for a consistent cross-comparison between EF and refined models (Section 2.2.);
- the rules adopted to *a priori* define piers and spandrels and the challenges still open in the case of irregular layout of openings (Section 2.3);
- the modeling of wall-to-wall connections (Section 2.4);
- the modeling of the out-of-plane response of masonry walls (Section 2.5);
- the modeling of the diaphragms (Section 2.6).

All the topics mentioned above are relevant whatever the method of analysis adopted for seismic assessment (linear, nonlinear, static, or dynamic). Conversely, the second part investigates some concerns related to the use of URM models within the specific field of seismic verification carried out through nonlinear static analysis (NLSA). Among the possible alternatives, the paper focuses only on the static method since it currently represents the most widespread approach adopted not only by professionals but also by the scientific community. In particular, three topics related to the NLSA are discussed: issues related to convergence and algorithmic aspects (Section 3.1), the application of horizontal loads (Section 3.1) and the definition of displacement thresholds on the pushover curve (Section 3.2). Since the focus in the paper is given only on the static approach, issues related to the description of the nonlinear behaviour are essentially limited to the monotonic field.

2 Overview on challenging issues of URM modeling in engineering practice

2.1 Critical issues for pier and spandrel modeling

The rigorous identification of pier and spandrel elements is strictly necessary in the modeling phase only when dealing with EF models (as introduced in Section 1); however, it also turns out to be essential for refined approaches when the final aim is the seismic verification performed according to the procedures defined by the codes. In fact, seismic codes (*e.g.* NTC18 (2018), EC8-3 CEN (2005), ASCE 41-17 (2017), NZSEE (2017)) provide limit conditions that, for both strength and displacement capacity, commonly refer to quantities and parameters associated with the scale of masonry panels/walls rather than with the scale of the material, i.e.: generalized forces (V -shear, M -bending moment and N-axial load) for strength, and drift (δ) values for deformation and displacement capacity. Thus, if the analysis is carried out by means of refined models, the panel drift demand should be compared with the limits defined by the technical codes. In addition, the use of refined models will require the calculation of the generalized forces through the integration of the nodal forces and the selection of the position where the displacements are monitored. On the other hand, it is evident that the definition of what "piers and spandrels" are in a wall is purely conventional and in principle not required in refined models. The observation of the damage pattern predicted by the refined model may be useful in guiding the *a posteriori* identification of the structural elements, similar to the basis of rules usually adopted in EF models, as discussed in more detail in Section 2.3.

First of all, regardless of the approach adopted, the correct modeling and interpretation of the piers and spandrels seismic behavior requires proper knowledge of the possible failure modes which can occur under seismic actions, namely those associated with diagonal shear cracking, bed joint sliding, or flexural response (*i.e.*, rocking or crushing). As well known, failure modes are usually interpreted according to simplified analytical strength criteria, as specified in detailed reviews like those presented in (Magenes and Calvi 1997, Calderini et al. 2009), for piers, and in (Beyer and Mangalathu 2013), for spandrels. The width-to-height slenderness ratio, the applied axial force, the boundary conditions and the strength properties play fundamental roles in defining the structural capacity of these elements. Different combinations of such factors can lead to different failure modes. Moreover, in the case of spandrels, the lintel typology and the presence of other tensile resistant elements at floor level have to be added to the aforementioned list of factors. A differentiation between piers and spandrels, although conventional, is convenient, given the different role that they play in the "load path" under the application of both vertical and horizontal loads. Piers are subjected to significant compressive axial forces due to gravity, whereas for

spandrels, the axial forces are often negligible, except when other tensile resistant elements or very stiff diaphragms are present.

Figure 2 illustrates the different possible idealizations made for the shear force – displacement behavior of a panel through the adoption of the various modeling strategies synoptically shown in Figure 1.

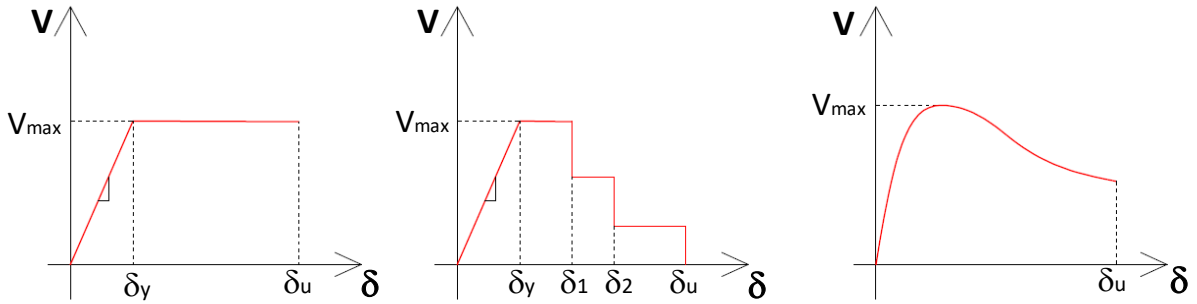

(a) (b) (c)

Figure 2 – Possible idealization of the shear behavior of URM panels obtained through: (a/b) nonlinear beams with lumped plasticity; (c) fiber model or refined 2D- or 3D- models. Where: V shear force, δ displacement or drift, V_{max} maximum shear force of the panel, δ_u ultimate displacement/drift capacity, δ_y displacement/drift capacity at yielding.

The simplest idealization refers to the nonlinear beam scheme with lumped plasticity. It represents the most common solution in EF models implemented in commercial software packages. If zero-length hinges are used, three different hinges are usually placed along the vertical beam element (which represents the pier): two flexural hinges at the edges of the beam and, assuming that the shear force is constant along the pier, the third one (shear hinge) can be in any position along the beam (usually in the middle). The force (moment or shear) - displacement (chord rotation or drift) relationship of the element generally results in an elastic-plastic behavior (similarly to what depicted in Figure 2a), with or without a softening branch that may be characterized by a stepped drop behavior in strength (similarly to that depicted in Figure 2b, as explicitly mentioned for example in CNR DT212 2014). This model is usually based on the following assumptions: the interaction between the axial force and the bending moment is accounted for through simplified approaches, or sometimes neglected, and no accurate shear-flexure interaction failure mechanisms are accounted for.

As far as the initial stiffness is concerned, usually conventional secant values are assumed. An alternative for the flexural behavior idealized through a hinge is the finite length approach, which, in the majority of cases, is based on the so-called fiber approach. In this case, the progressive degradation in the first branch of the response (before the attainment of the maximum shear strength, V_{max}), associated with a progressive flexural cracking of the sections, can be explicitly modeled (Figure 2c).

According to this general framework and focusing the attention on EF models, various proposals have been presented in the literature: the nonlinear beam model with lumped (*e.g.*, Magenes and Della Fontana 1998, Lagomarsino et al. 2013, Cattari and Lagomarsino 2013, Vanin et al. 2020a) or spread plasticity (*e.g.*, Belmouden and Lestuzzi 2007); the use of nonlinear springs in series or in parallel (*e.g.*, Chen et al. 2008); the fiber approach (*e.g.*, Raka et al. 2015); or other hybrid macro-elements that combine the use also of a mechanical approach (*e.g.*, Penna et al. 2014b, Bracchi et al. 2021, Bracchi and Penna 2021). Some of the aforementioned models include also specific formulations to simulate the influence of strengthening, e.g. with FRP strips (Grande et al. 2011). Although an exhaustive review on this topic is out of the scope of the paper, it is possible to highlight some distinctive features of the available literature: i) the adoption of a mechanical or phenomenological approach to describe the nonlinear response; ii) a less or more accurate kinematic relationship among variables (*e.g.* able to take into account the coupling between the axial displacement and the rotation due to flexural cracking that is responsible of the uplift phenomenon in piers dominated by a flexural failure mode); iii) the formulation of an appropriate hysteretic response, essential for performing nonlinear cyclic pushover and dynamic analyses.

Conversely, refined models can usually describe more accurately the progressive degradation of both stiffness and strength (Figure 2c). The counterpart is the increase of the computational burden needed and a larger number of parameters to set in the constitutive laws characterizing the material behavior, as for example the need to introduce a fracture energy parameter, in FEM based approaches, for governing the softening branch. Section 2.2 addresses this issue in-depth for the purpose of performing a calibration of parameters able to guarantee, as much as possible, cross-consistency in the use of EF and refined models in practical applications.

The modeling of spandrels deserves some additional attention. In fact, although such elements can be considered as secondary (their failure does not usually imply the attainment of an ultimate limit state of the structure), they significantly affect the static scheme of piers, as a function of their strength and stiffness properties, with possible situations ranging from the weak-spandrel-strong-piers (WSSP) behavior to the strong-spandrel-weak-piers (SSWP) behavior. In the case of weak spandrels (low stiffness or low resistance – leading to WSSP), piers tend to behave as cantilever-like elements, mainly dominated by the flexural failure mode. On the contrary, as the stiffness and strength of the spandrels increase (until the idealized case of SSWP), a frame-like behavior of the wall arises, piers are more affected by shear failure modes. These issues, together with the role of horizontal coupling elements in determining the overall response of URM walls and buildings, has been already preliminary investigated in the earliest works of ‘90 (Magenes and Della Fontana 1998, Magenes et al. 2000). In such works, based on nonlinear EF models, it has been shown that, as expected, the effects of the variation in some basic properties and modeling hypotheses of URM

spandrels and coupling beams would significantly change the response of multistorey masonry structures in terms of base shear capacity and overall failure mechanism, calling for further research, in particular experimental (at that time almost completely absent).

Most of the design/assessment codes explicitly recommend including spandrels in the modeling phase only if an effective lintel (*i.e.*, properly anchored at the end sections and able to support the weights above it) is present. As testified by the experimental campaigns available in the literature (*e.g.*, Beyer and Dazio 2012, Graziotti et al. 2012), spandrel behavior is significantly affected by the interaction with the lintel. Moreover, the post-peak softening phase strongly depends on the lintel type and presents a steep degradation in the case of segmental arch systems and a more gradual softening in the presence of timber/steel lintels (as also discussed in Beyer 2012). The spandrel-lintel modeling interaction phenomena is treated in a very different way passing from EF to refined models. In fact, in the first case (EF models), according to a phenomenological approach, it is usually accounted for in an indirect way by properly calibrating the properties of plastic hinges (*e.g.*, introducing in the nonlinear behaviour of the beam a residual strength after the peak). Conversely, in the second case (refined models), both elements must be meshed separately, introducing some complexities in the definition of the nonlinear model but avoiding the a priori distinction between piers and spandrels. In refined models lintels should be able to slip, in order to avoid the transfer of fictitious stresses to the surrounding masonry. This behavior can be achieved by inserting an interface or a weak layer between masonry and lintel, as shown in Figure 3a. Thus, Figure 3b shows that, in this way, the damage behavior is predicted correctly; clearly, this behavior cannot be captured if no slip is possible between lintel and masonry.

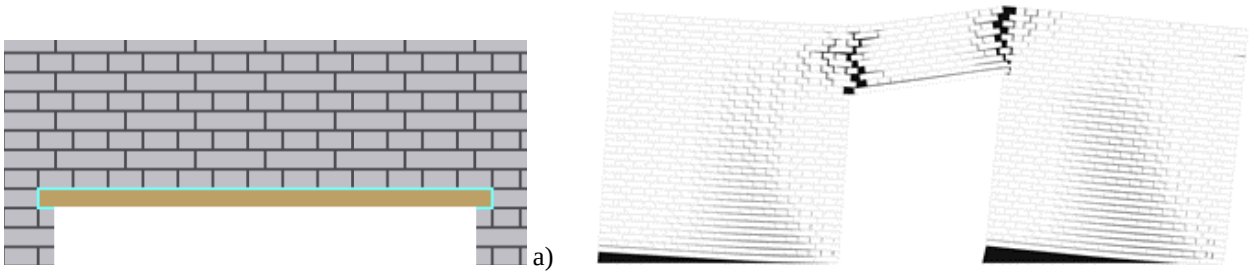

Figure 3 –Example of lintel-spandrel interaction simulated by a micro-mechanical approach: a) interface between masonry spandrel and lintel (in cyan); b) simulated response

Another relevant issue is the capability of the model to reproduce the actual failure mechanisms that may occur in the spandrel, also as a function of its interaction with other tensile resistant elements, possibly coupled (*i.e.* tie rods or r.c. ring beams). This is particularly relevant for a reliable simulation of the flexural behavior in EF models. In fact, in the past, the common approach was to adopt the same analytical criteria adopted for piers, leading to an unrealistic (if compared

with the observed seismic damage) predominance of the flexural failure mode in weak URM spandrels (*i.e.*, not coupled to other tensile resistant elements). Conversely, recent codes (*e.g.*, NZSEE 2017, MIT 2019), based on the latest experimental evidence, propose to consider the contribution of an equivalent horizontal tensile strength ($f_{t,sp}$) of the spandrel that can be produced, even in absence of other coupled tensile resistant elements, by virtue of the interlocking phenomena generated at the end sections of spandrel with the adjacent masonry portions (*e.g.*, Cattari and Lagomarsino 2008a, Beyer 2012, Krzan et al. 2015). Such a contribution tends to become more relevant in the presence of a regular bond masonry pattern, good quality mortar joints and adjacent masonry portions subjected to high vertical stresses (*i.e.*, the positive effect is much more evident for lower levels than for upper floors). The inclusion of the $f_{t,sp}$ contribution in the spandrel modeling may significantly alter the response of URM walls as depicted for illustrative purposes, in Figure 4, where such parameter has been computed according to various formulations available in the literature (*e.g.*, Cattari and Lagomarsino 2008a, Beyer 2012). The figure also shows the effect produced by the insertion of a steel tie rod coupled to the spandrel; more details can be found in Cattari and Beyer (2015).

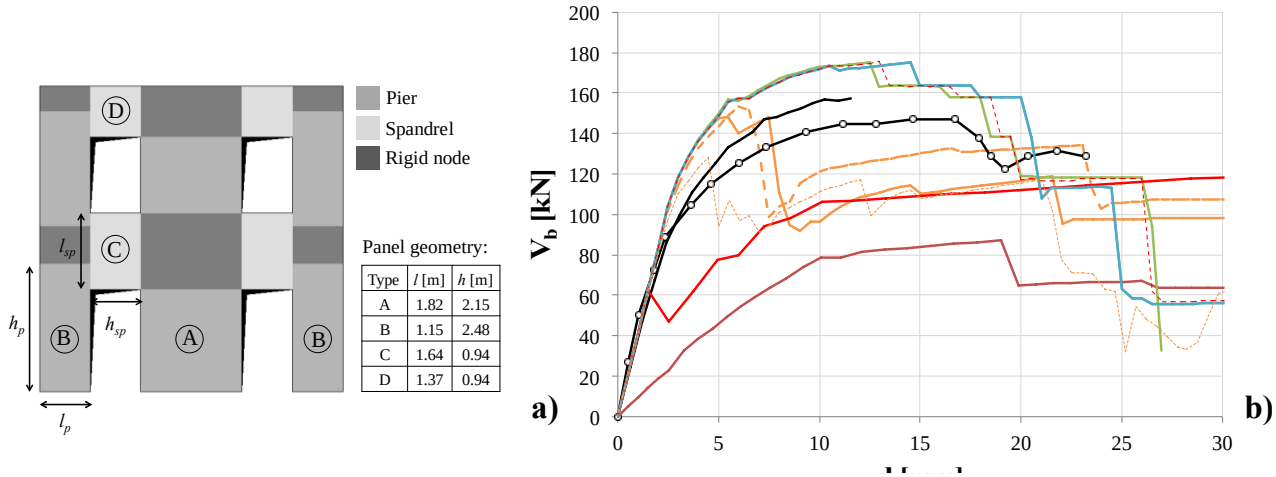

Case	Flexural strength criterion (*)	Computation of $f_{t,sp}$		Residual strength(+)	Steel beams
	Flexural	Horiz. joints	Head joints		
I-a	NTC 2008	No	No	Conv.	No
I-b	NTC 2008	No	No	Conv.	Yes
II-a	Beyer 2012	Yes	Yes	Mech.	No
II-b	Beyer 2012	Yes	Yes	Mech.	Yes
II-c	Cattari & Lagomarsino 2008	Yes	No	Mech.	No
III-a	Beyer 2012	Yes	No	Mech.	Yes
IV-a	Beyer 2012	Yes (*0.7*)	Yes (*0.7*)	Mech.	Yes
IV-b	Beyer 2012	Yes (*0.5*)	Yes (*0.5*)	Mech.	Yes

(*) For the shear response it has been assumed a criterion consistent with that of Mann and Müller (1980) for interpreting the *Diagonal Shear Cracking*. In Cases IV a reduced value of the cohesion and the friction coefficient has been adopted coherently with the assumption of a poor quality of spandrel masonry (by adopting a reduction factor equal to 0.7 or 0.5).

(+) "Conv" means that the residual strength of spandrels have been conventionally assumed by adopting $\beta_{E3}=\beta_{E4}= 50$, while "Mech." means that the residual strength has been defined on the basis of the mechanical criteria proposed in Beyer (2012).

c)

Figure 4 – Effect of accounting for the equivalent tensile strength of the spandrel ($f_{t,sp}$) and the presence of a coupled tensile resistant element in the seismic response of a two-story URM wall (adapted from Cattari and Beyer 2015)

When a tensile resistant element is coupled to the spandrel, all modeling strategies are unanimous in predicting a predominance of the shear failure modes. In EF models, such an outcome is a consequence of the analytical strength criteria adopted, that usually are based on the development of a diagonal strut in the spandrel. In refined models, the appearance of the strut depends on the explicit interaction with the steel tie-rod or the r.c. beam that also significantly alters the axial force acting along the spandrel.

Figure 5 shows the variation of the behavior of a multi-story URM wall passing from the case of weak URM spandrels (Figure 5 a and d) to a model that considers the addition of elastic floor beams at each level (except the roof level) (Figure 5 b and e) and, finally, to a model that considers nonlinear concrete floor beams and elastic lintel beams (Figure 5 c and f). In the case of very weak masonry, the achievement of the tensile strength on the spandrel can lead to a full separation of the wall in different portions, since no constraint is a priori assumed. A very consistent response is simulated by a discrete macro-element approach (DMEM, Figure 5a/b/c) and a micro-mechanical approach, respectively (Figure 5d/e/f). For further details, interested readers may refer to Occhipinti et al. (2021). Such behavior, which can also be exhibited by continuous FE and mesoscale approaches, is also influenced by the actual position of the r.c. or floor beams modeled. More specifically, in the DMEM method, spandrels are modeled with a single or a mesh of macro-elements depending on the presence of lintels or floor beams. Each macro-element can simulate the shear-diagonal and/or the flexural response of the spandrels, including the tensile capacity of masonry in the horizontal direction, when appropriate. The presence of floor beams or lintels is considered in their correct position by introducing an inelastic frame element interacting with the macro-elements (Occhipinti et al. 2021).

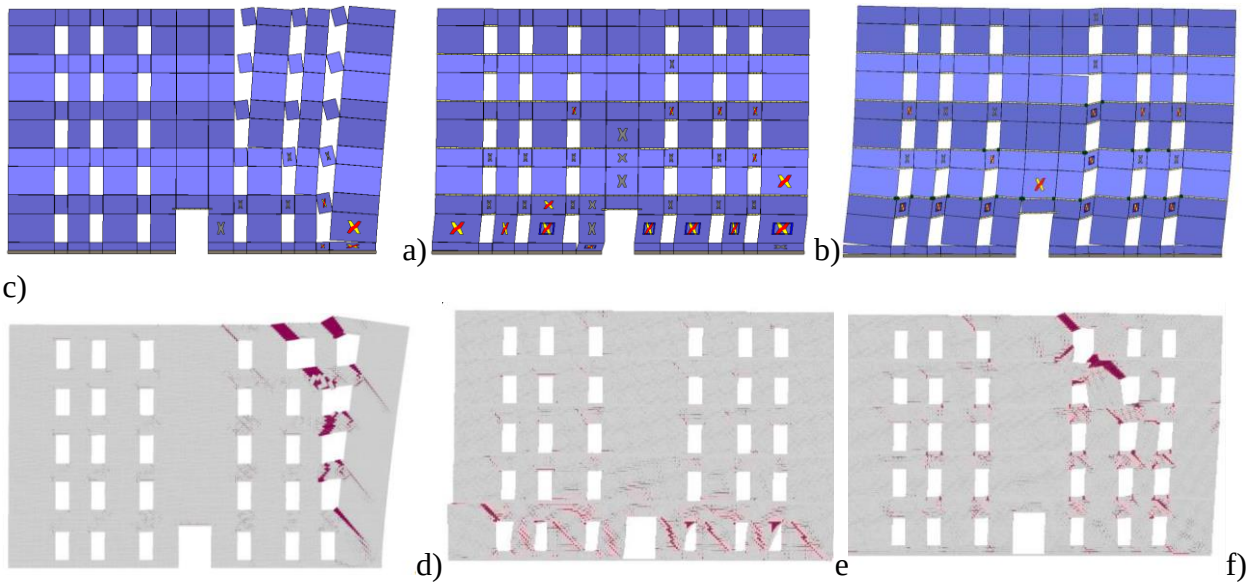

Figure 5 – Response of a multi-story URM wall varying some modeling options for spandrels: a), d) weak spandrels; b), e) elastic floor beams at each level except the roof level; c), f) nonlinear concrete floor beams and elastic lintel beams coupled to spandrels (adapted from Occhipinti et al. 2021)

Another problematic point is the correct evaluation of the axial load acting in the spandrel. This aspect is usually roughly approximated in EF models (due to oversimplifications usually made in the modeling of the floors), while a more reliable prediction is provided by refined models (when the interaction with all the other structural elements is properly simulated).

Finally, other modeling solutions aimed at more accurately predicting the spandrel response are under development by researchers, based on experimental and numerical tests (Calderoni et al. 2019a). In the framework of the EF approach, in order to better simulate the spandrel behavior within the masonry wall without losing the easiness of the frame model, an alternative EF hybrid scheme has recently been proposed (Sandoli et al. 2020a). In this scheme, the piers are modeled with one-dimensional vertical frame elements, while the spandrels are modeled with strut and tie truss elements (acting only in compression or in tension, respectively, and exhibiting nonlinear behavior) instead of equivalent nonlinear beams (Figure 6). This EF hybrid scheme (Sandoli et al. 2020b) gives the following advantages with respect to a "classic" EF scheme (especially when effective tensile-resistant elements are present in the spandrels):

- the axial force in the diagonal strut (which is related to the structural engagement of the spandrel) is expressly evaluated up to the diagonal strut failure, giving the control of the internal stress state of the spandrel;
- the partialization of the end cross-sections due to material cracking is considered through the dimensions of the equivalent diagonal strut (*i.e.*, effective compressed area at the panel edges) and its position inside the panel, defined according to a specific theoretical formulation (Calderoni et al. 2011);
- the tensile axial force in the ties is directly given by the analysis, and different positions of ties, r.c. ring beams, and different typologies of ties (bonded continuously to the masonry or unbonded, *i.e.*, connected to the wall at the edges only) can be easily accounted for;
- it allows for the identification of the component (*i.e.*, compressed masonry and/or tensile-resistant element) triggering the spandrel failure, and consequently, the overall failure mechanisms of the entire equivalent frame can be better identified, also in terms of displacements.

However, this type of hybrid modeling is, at present, not readily available in commercial EF software for the analysis of masonry buildings, but needs to be specifically implemented by the user through available general purpose software using nonlinear frame and truss elements.

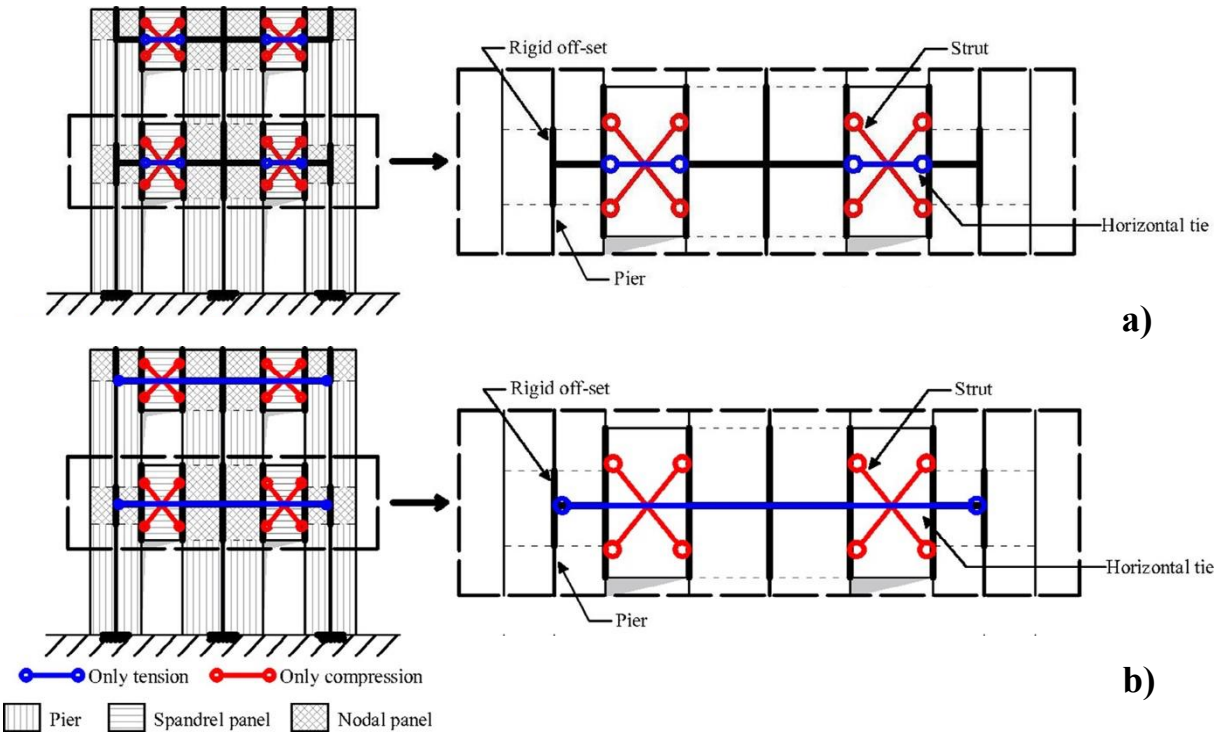

Figure 6 – Hybrid EF model in the case of: a) bonded ties; b) un-bonded ties (adapted from Sandoli et al. 2020a)

2.2 Parameters calibration for a consistent cross-comparison between refined and equivalent frame models

This section discusses some calibration and modeling issues in the nonlinear analysis of URM structures. A consistent cross-comparison between different numerical strategies with reference to specific modeling aspects is reported in the following sub-sections.

2.2.1 Basics and target for the calibration procedure

In this sub-section, some issues related to the calibration of mechanical parameters are addressed to guarantee, as much as possible, cross-consistency between refined and EF models. The topic is particularly useful for practitioners since, in most cases, the adopted reference mechanical properties of masonry types directly refer to the scale of masonry panels and are ready-to-use in the simplified analytical strength criteria mentioned in Section 2.1. Typical reference values may be found in Codes (*e.g.*, MIT 2019) or in the literature (*e.g.*, Augenti et al. 2012, Krzan et al. 2015, Vanin et al. 2017, Morandi et al. 2018, Rezaie et al. 2020, Boschi et al. 2021). The same mechanical parameters are also those derivable from in situ experimental tests, after their proper interpretation and the careful treatment of data, which often constitutes another delicate point of the assessment (*e.g.*, as discussed in Brignola et al. 2009, for the diagonal compression test).

As a consequence, in the case of an EF approach, these parameters can be directly adopted as input data without needing any specific calibration of the panel. On the contrary, for refined approaches, which usually refer to the material scale, the basic material parameters, espressed in terms of elastic modula, tensile and compressive strength and fracture energies, have to be considered.

The main steps expected in this calibration phase are summarized in Figure 7 and consist of the following points:

1. Definition of the "target behaviour" for the calibration. Keeping in mind that both EF models and refined models aim to reproduce the same masonry, consistent with code-defined parameters, first a choice is made of the most relevant simplified code-based strength criteria to be adopted to describe the main failure modes expected in a pier for the masonry typology of interest. Then the target behavior is set, as a consequence of such definition of the mechanical parameters, *i.e.*, strength parameters (like those marked in red in Figure 7-step 1) and stiffness properties as well as those necessary for the description of the post-peak behavior of panels (like those of the drift thresholds and corresponding strength drops associated to different damage conditions). In Figure 7, among the possible behaviours, the flexural response (V_u^F) and the diagonal shear cracking (V_u^{DC}) are shown together with some common strength criteria adopted in codes, based on the compressive strength (f_m) and the shear strength (τ_0), respectively, as mechanical parameters. Of course, the post-peak behavior can be more or less complex, as depicted in Figure 2, as a function of the "target behavior" assumed.
2. Identification of the main parameters on which the constitutive laws of the refined model employed are based. As an example, Figure 7-step 2 depicts an isotropic plastic-damaging 3D continuum model based on the proposal by Lee and Fenves (1998) and implemented in the Finite Element FE commercial software ABAQUS. The parameters investigated in the following step 3 are highlighted in red. In particular, they consist of: the tensile strength of the material (f_t) and the uniaxial compressive stress corresponding to the point of initial yield (f_{ch}); the values of uniaxial compressive strain corresponding to the reaching of the maximum strength (ε_{cm}) and to the end of the softening branch (ε_{cu}). Different choices on such parameters may lead to various alternative options of the behaviour (e.g. Type A, B and C indicated in Figure7-step 2), whose repercussions may be investigated through targeted parametric analyses. Obviously, such parameters have to be particularized to the constitutive law adopted in the different cases.
3. Execution of sensitivity and parametric analyses aimed at least to evaluate *i*) the maximum lateral strength of the panel (V_{max}) and *ii*) the associated base shear – top displacement (V_b–d_{top}) curves (Figure 7-step 3). The analysis has to involve a set of piers characterized by various in-plane aspect ratios (λ) and various boundary conditions subjected to various different values of the applied axial load (N or σ/f_m ratio). Such a step aims to optimize the calibration of the parameters to reasonably match the "target behaviour" set in step 1.

4. Overall verification of the effectiveness of the set of parameters chosen at the end of step 3.

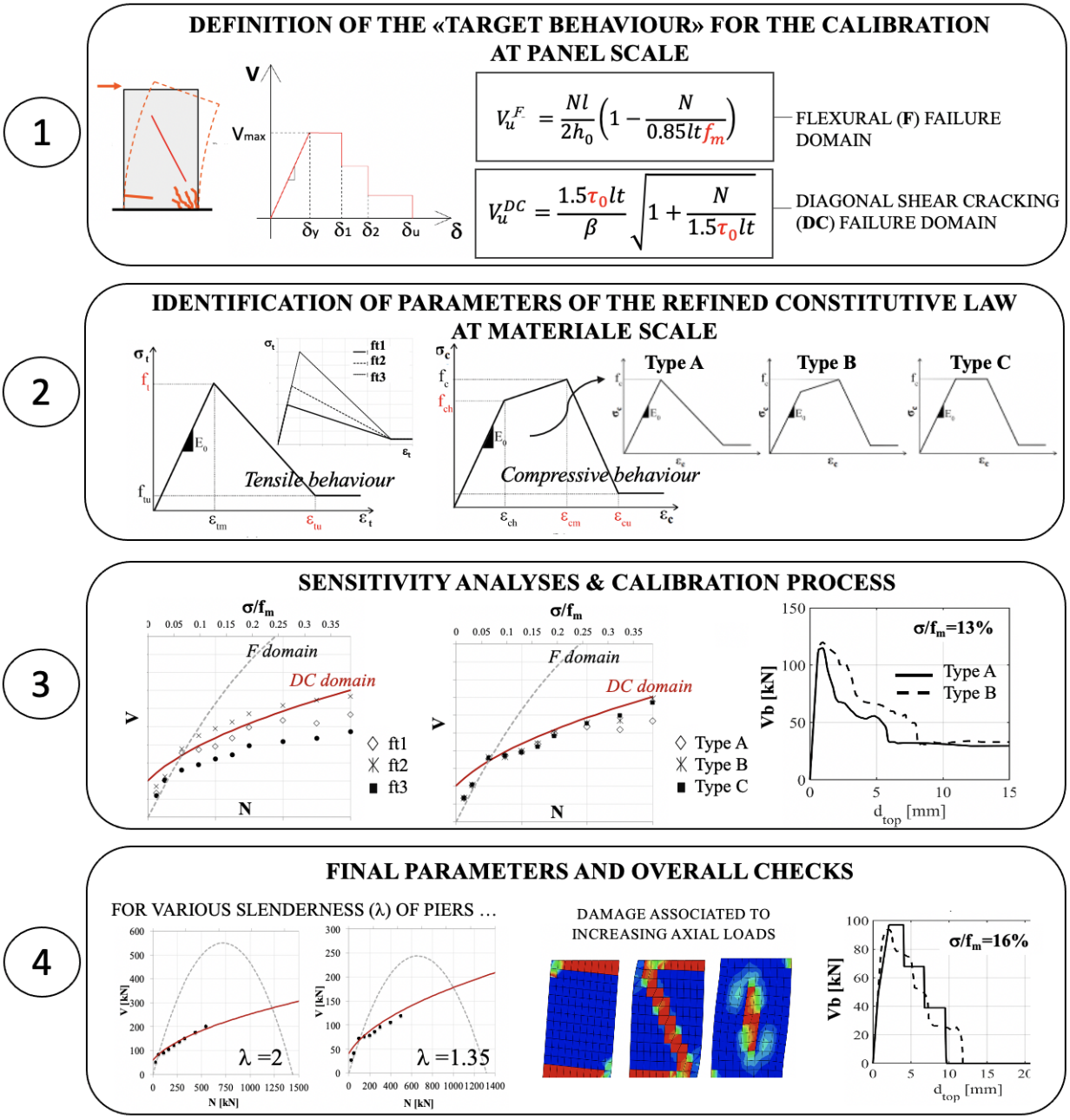

Figure 7 – Schematic flowchart of the calibration process for guaranteeing the cross consistency of parameters used at material and panel scales

A detailed exemplification of the aforementioned calibration procedure is described in D'Altri et al. (2021), where the differences resulting in the use of five constitutive laws of refined models are investigated, and in Cattari et al. (2021a), where specific reference to the aforementioned constitutive law and implemented in ABAQUS is made.

It is worth underlining that a perfect calibration between the simplified and the refined models in all the regions of the failure domain of panels is in general not possible. In fact, while in the EF approach, the flexural and shear behavior are completely decoupled, being associated with failure

criteria based on independent parameters, this does not happen in the refined FE approaches based on continuum mechanics, where the mechanical parameters ruling the flexural response can also affect the shear behavior (for example the tensile strength, see also Section 2.2.2). However, a rather good correspondence can be obtained if the calibration is performed by considering a limited portion of the strength domain of the piers within the range of variation of the normal stress for practical application. The latter can be estimated as the expected range of variation occurring in the panels of the structure under examination after the execution of some preliminary analyses.

Step 3 is carried out by varying specific parameters of the constitutive law characterizing the continuum material in order to find the best solution for the calibration in terms of:

- *elastic stiffness*, to reproduce the initial elastic behavior of masonry piers;
- *strength*, to reproduce the failure domain of the piers considered, defined according to the analytical strength criteria adopted in the EF approach;
- *displacement capacity*, to simulate, for different values of the applied axial load, the post-peak behavior of the piers described through the assigned drift thresholds and corresponding strength drops;
- *post-peak behavior*, including damage and degradation.

A reliable description of the post-peak response of masonry piers subjected to shear is a challenging task since it is extremely variable and it depends on many factors (*e.g.*, masonry type, masonry bond/texture, axial load ratio, failure mode, etc.).

The drift limits and strength degradation parameters assigned as reference for the selected masonry type can be directly assumed as input data in the EF models. Conversely, when the masonry panel is modeled at the material scale, numerical simulations may produce a softening behaviour characterized by a more or less gradual strength and stiffness degradation, due to the progressively occurred damage and the specificity of the adopted parameters. With the final goal of guranteening a cross-consistency between simplified and refined models, the aim of the calibration is to approach the envelope represented by the simplified code-prescribed piecewise-linear behavior assumed at the panel scale.

In the EF approach, with panels described by nonlinear beams based on a phenomenological approach, the calibration process is straightforward, being univocally determined as the failure mode associated with the minimum between the flexural and shear strength for the current value of the axial load. As mentioned in Section 2.1, in the EF models, the ultimate drift (or those associated with the progressing strength decay in the case of multi-linear laws) is conventionally defined according to Codes (e.g., EC8-3 CEN (2005), MIT 2019, ASCE 41-17 2017), recommendations (CNR DT 212/2013 (2014)) or literature proposals based on a large dataset of experimental campaigns (Vanin et al. 2017, Morandi et al. 2018). Moreover, in general, in EF

models, a sudden transition between prevailing flexural and prevailing shear response occurs, thus also implying a sudden transition in the displacement capacity associated with the considered element. As a rule, the utilization of hybrid modes is not managed by such an approach, apart from very few cases like that in (Cattari and Lagomarsino 2013) and exemplified in (Cattari et al. 2018, Brunelli et al. 2021), where, for hybrid modes average values of the drift thresholds are proposed on the basis of a heuristic criterion. In this proposal, the hybrid mode is detected as a function of the axial load acting on the panel, when it is in the transition region of the domain in which the strengths predicted by the flexural and shear analytical criteria are very close.

On the other hand, in the case of the refined approach, the assignment of a precise failure mode to a given panel is not needed since the collapse mechanisms are related to the adopted constitutive law for the continuum and not a priori identified according to the panel geometry and masonry material properties. The identification of the failure type can be considered as unequivocal only in the presence of pure flexural response (with the sole flexural cracking of the end sections). In all other cases, the formation of shear diagonal cracks is almost always associated with a more or less pronounced flexural cracking of the end sections, thus indicating failure modes that appear to be closer to hybrid situations rather than pure shear failures. Therefore, when using a refined approach, the obtained damage pattern, which is usually more complex and closer to reality, has to be properly interpreted case by case. This can be done, in general, only on the basis of qualitative analyses or conventional criteria (as discussed in Castellazzi et al. 2021).

Moreover, the post-peak response in material-scale models (*e.g.*, continuum models) is ruled by the fracture energy and has, in general, a less regular behavior than the simplified EF models, and more similar to the experimental one. The issue is to some extent controversial since, on the one hand, the ultimate drift is a panel-scale property but, on the other hand, the fracture energy is a material-scale property. Accordingly, it appears very complex (or nearly impossible) to calibrate fracture energies in order to have a constant target ultimate drift and vice versa. Indeed, while most codes (*e.g.*, Eurocode 8-2 CEN (2005), NTC18 (2018), ASCE 41-13 2017) conventionally assume ultimate drifts *a priori* defined and invariant with the acting axial load (except for the SIA 266 (2015)), the resulting ultimate drift obtained in continuum models, and so ruled by the fracture energy, typically depends on the axial load ratio (Figure 8 –*b).* Indeed, the influence of other factors on the drift capacity in addition to the axial load, like boundary conditions, slenderness, and masonry type, is still debated in the literature (see Petry and Beyer 2014, Wilding and Beyer 2018, Dolatshahi et al. 2018) and the fixed drift limits defined in design codes are only lower bounds of quite scattered experimental results.

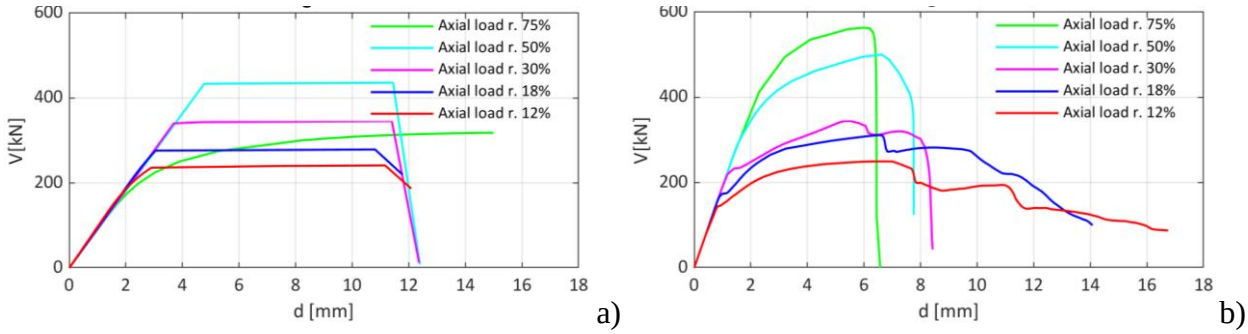

Figure 8 – Masonry panel force-displacement response: (a) modeling strategy with a priori definition of ultimate drift where the ultimate drift depends only on the failure mode, and (b) material-scale modeling strategy where the resulting ultimate drift is influenced by the axial load ratio (adapted from D'Altri et al. 2021)

2.2.2 Additional issues on the use of isotropic and orthotropic material models

When homogeneous isotropic material models are used to model masonry, a criticality arises in stiffness calibration. In an isotropic linear elastic continuum, the following well-known relationship between the three elastic constants E (Young's modulus), G (shear modulus), and ν (Poisson's coefficient) holds: $G = \frac{E}{2(1+\nu)}$. However, given the anisotropic and heterogeneous nature of masonry, the use in such a relationship of values of E and G deduced from experimental tests or literature studies, would produce values of ν that are clearly unrealistic if related to an elastic homogenous isotropic material (*e.g.*, greater than 0.5 instead of typical values between 0.15 and 0.3). Therefore, it does not always appear feasible to directly use measured (or suggested from literature) E and G values and derive a realistic value of ν from the isotropic relationship. Accordingly, a possible strategy could be to use a realistic value of ν for masonry (*e.g.*, 0.2) and to choose only one of the two measured (or suggested) moduli (E or G) to be adopted in the analysis, depending on the geometry, loading and boundary conditions of the structure, as suggested in D'Altri et al. (2021).

Moreover, in isotropic material models, although strength could be distinguished between compression and tension, only one value of uniaxial tensile strength and one value of uniaxial compressive strength can be defined. Conversely, masonry generally shows anisotropic strength (Page 1981). For example, the tensile strength perpendicular to bed joints could be significantly lower than the tensile strength parallel to bed joints (see Figure 9), their ratio reaching in some cases values near 5 (Lourenço 1997). Accordingly, isotropic material models cannot account for these differences, and only one value of tensile strength has to be used. However, it appears possible to calibrate the tensile strength of the material (*e.g.*, following the procedure suggested in Section 2.2.1 and exemplified in D'Altri et al. 2021) in order to keep the level of approximation included within engineering practice tolerance.

A further limitation on the use of isotropic models is related to the difficulties in choosing suitable mechanical parameters for modeling the typical failure mechanisms of masonry panels. The definition of tensile and compressive strength in continuous isotropic models controls the collapse response of a masonry panel subjected to vertical and horizontal loads: a correct calibration of the flexural collapse mechanism, according to experimental results, does not guarantee a corresponding calibration of the shear failure, which is generally related to different values of tensile strength. This aspect is deeply discussed in D'Altri et al. (2021) along with more detailed practical approaches to solve the issue.

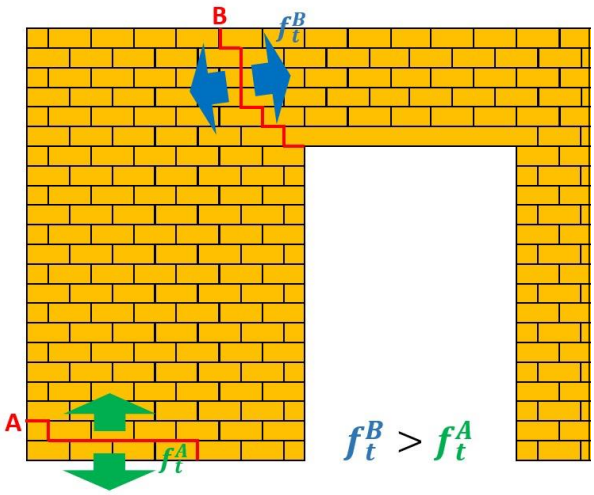

Figure 9 – Anisotropic nature of the masonry tensile strength.

Concerning orthotropic continuum models, the orthotropy of masonry can be introduced either by using standard nonlinear isotropic models, but adopting a micro-modeling approach (also called textured continuum models, D'Altri et al. 2020b) or by using equivalent homogenous orthotropic nonlinear models.

The first approach directly leads to an orthotropic behavior without involving the use of orthotropic constitutive laws; however, it does not immediately provide the mechanical behavior of masonry at the macro scale. The orthotropy is naturally introduced by the explicit modeling of the texture (Berto et al. 2004, Petracca et al. 2016 and 2017a). This approach, however, leads to very demanding models, and consequently to high computational costs.

The second approach, instead, is much faster, but it requires the use of an orthotropic nonlinear constitutive model, that cannot be easily found in most finite element modeling codes. Additionally, it would require the introduction of further material parameters that are not always available to the analyst. An example is represented by the orthotropic damage model proposed by Berto et al. (2002) where the material parameters can be calibrated from a suitable set of experimental tests on full-scale masonry panels or from the mechanical behavior of the components (brick and mortar) through homogenization techniques or micro-modeling analysis.

A detailed state-of-art on the equivalent homogenization approach is out of the scope of the paper and the interested reader may refer to (Belytschko et al. 2008, Bosco et a. 2015, Cavalagli et al. 2013, Kouznetsova et al.2004, De Bellis et al. 2011, Zucchini and Lourenco 2009, Berke et al. 2014, Sacco 2009, Mercatoris and Massart 2011, Massart et al. 2007), to name a few.

An alternative approach is to use an orthotropic mapper. It is a simple material wrapper that converts a fictitious isotropic material into an equivalent orthotropic one, based on the orthotropic elastic tensor and the ratios of the isotropic and orthotropic strengths (implemented in OpenSees, see for instance Pelà et al. 2013). Furthermore, the mapping parameters can be easily obtained by an initial analysis of an RVE (Representative Volume Element) of the masonry material (see Figure 10*).*

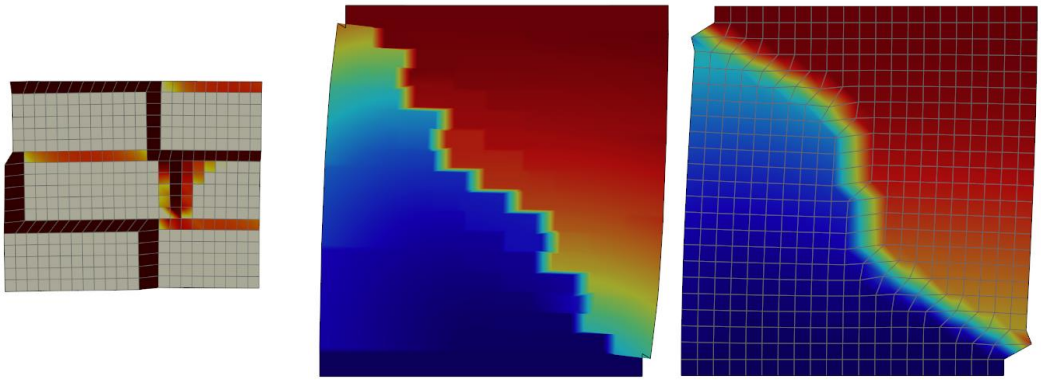

a) b)

Figure 10 – (a) RVE response for calibration; (b) Reference micro-model; (c) Equivalent homogenous orthotropic macro-model.

In the DMEM model, the mechanical calibration of the interface is based on a fiber discretization (Caliò and Pantò 2014) that allows for the definition of different mechanical properties in the vertical and horizontal directions of the panel, as summarized in Figure 11. As reported in the figure, for each direction it is needed to define the elastic modulus *E*, the tangential modulus *G*, the tensile and compressive strength σ_t and σ_c and the tensile and compressive fracture energies G_t and G_c. The pedeces *h* and *v* in each symbol identify the horizontal and vertical directions respectively. Once these parameters have been assigned, the calibration of the nonlinear orthogonal links of the interfaces follows a straithforward procedure related to the number of links and to the panel geometry. In Table 1, the mechanical characterization of the orthogonal nonlinear links of the interfaces (called *N-Links*) is expressed as a function of the main material parameters of the masonry wall.

This model allows for the separate calibration of the shear and flexural behaviors, which are not based on continuum mechanics.

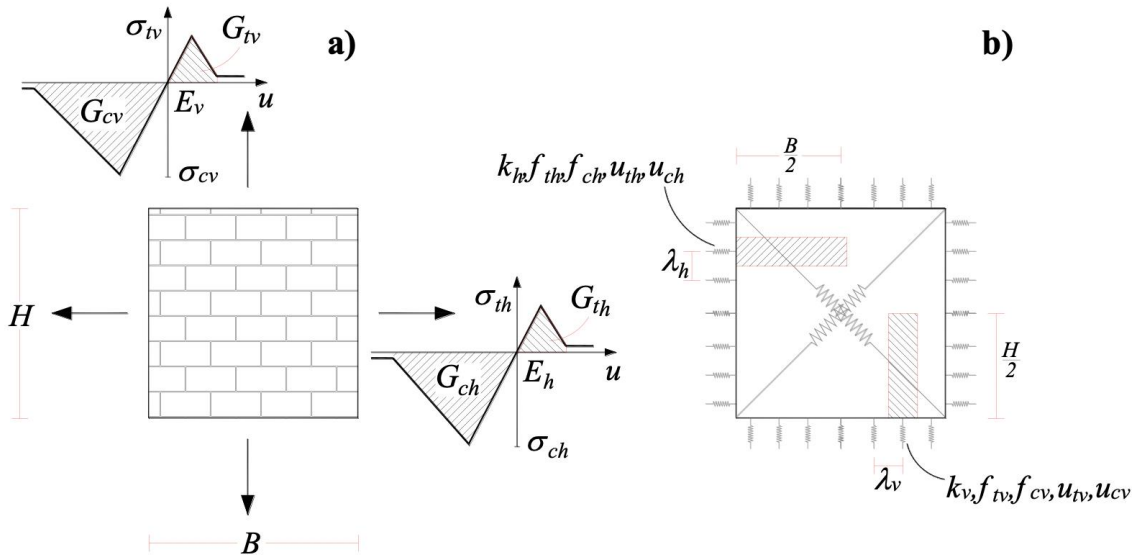

Figure 11 –Mechanical characterization of an orthotropic masonry panel: (a) constitutive laws and (b) calibration of the orthogonal Nlinks (adapted from Pantò et al., 2017a).

In general, it should be highlighted that continuum orthotropic models are less sensitive than isotropic models to the range of variation of the normal stress for the calibration.

Finally, in the case of continuum constitutive models with strain-softening, the most problematic issue is related to the strain localization and mesh dependency and is worth mentioning.

Table 1. Mechanical calibration of the orthogonal *N-links* for a rectangular panel with depth *s*

Direction	*elastic stiffness* *horizontal* K_h *vertical* K_v	*compressive strength* *horizontal* f_{ch} *vertical* f_{ch}	*tensile strength* *horizontal* f_{th} *vertical* f_{th}	*ultimate compressive displacement* *horizontal* u_{ch} *vertical* u_{cv}	*ultimate tensile displacement* *horizontal* u_{th} *vertical* u_{tv}
horizontal	$K_h = 2\frac{E_h \lambda_h s}{B}$	$f_{ch} = \sigma_{ch} \lambda_h s$	$f_{th} = \sigma_{th} \lambda_h s$	$u_{ch} = 2\frac{G_{ch}}{\sigma_{ch}}$	$u_{th} = 2\frac{G_{th}}{\sigma_{th}}$
vertical	$K_v = 2\frac{E_v \lambda_v s}{H}$	$f_{cv} = \sigma_{cv} \lambda_v s$	$f_{tv} = \sigma_{tv} \lambda_v s$	$u_{cv} = 2\frac{G_{cv}}{\sigma_{cv}}$	$u_{tv} = 2\frac{G_{tv}}{\sigma_{tv}}$

The first dependency concerns the amount of dissipated energy. Upon the onset of strain localization, the strain localizes into a narrow band of elements. In the numerical model the width of such band is not ruled by parameters with clear physical meaning and is related to the characteristic size of the finite element. The amount of dissipated energy will therefore change as the mesh size changes. The second dependency concerns the direction of the crack. When the strain localizes into a band of finite elements, the boundaries of those elements will act (erroneously) as real boundaries, trapping the strain inside them, thus forcing the crack to follow the direction of the mesh rather than the real expected crack direction.

To overcome the aforementioned problems, many algorithms were proposed in the literature. Some effective strategies to tackle strain-localization issues, at present quite widespread and nowadays considered classic, belong to the wide family of Non-Local and Gradient-Enhanced models. They are relatively popular in masonry applications, but not necessarily the most effective ones, especially when compared with other emerging numerical techniques. For instance, notable examples with great potential to capture strong discontinuities are Finite Elements with elemental (E-FEM) or nodal enrichments (X-FEM), see for instance Oliver et al. (2006). Their application to masonry is subjected to continuous evolution to increase robustness and their progressive diffusion in the scientific community is expected to grow rapidly. A variety of other specialized techniques exist, e.g. Enhanced Assumed Strain (EAS) and mixed FEM. Among the others, crack tracking algorithms deserve to be acknoldged, because of their promising efficiency and stability in the analysis of real scale structural elements up to collapse (see Saloustros et al. 2018, 2019). The use of tracking algorithms in combination with smeared crack approaches constitutes probably the simplest solution to improve remarkably the prediction of the crack propagation direction, avoiding the well know drawback of obtaining mesh-biased results (see Figure 12*).*

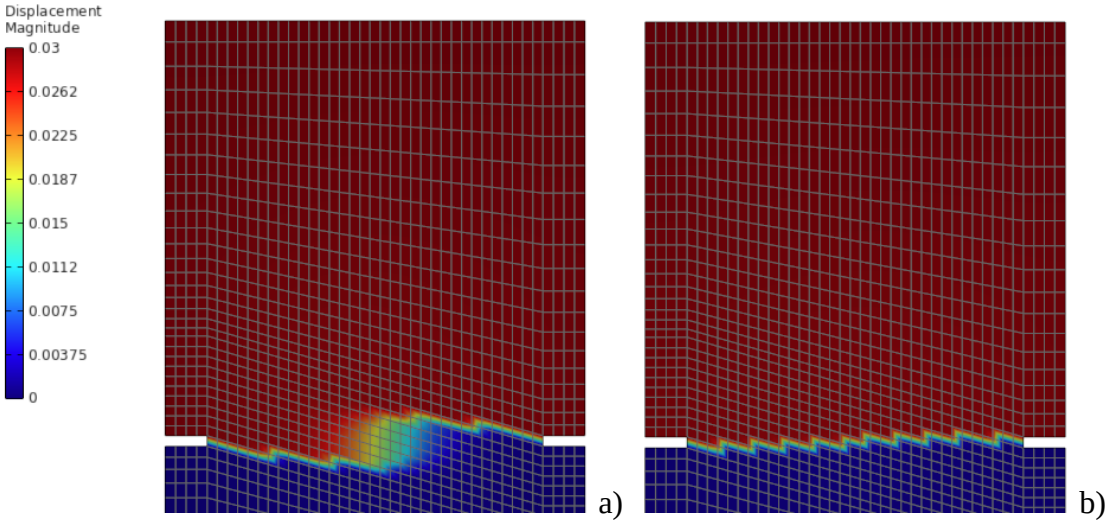

Figure 12 – a) Standard compatible FEM, the crack follows the mesh direction. b) Incompatible-modes FEM, the crack follows the expected direction (based on the work of Simo and Rifai 1990)

2.3 Critical issues in the idealization criteria of masonry walls according to EF approach

The rules adopted for the identification of the geometry of pier and spandrel elements are empirical or based on limited experimentations and/or few numerical simulations. At present, an exhaustive (*i.e.*, conclusive in providing unanimous scientific agreement) validation of their reliability is missing in the literature, and codes also do not usually provide specific indications about the criteria to use, leaving the analyst free to choose.

Most available rules are focused on piers and, specifically, to the definition of their effective height (H_{eff}), which represents a key modeling parameter in the EF approach. Figure 13 illustrates the

most popular approaches available in the literature; some of them are nowadays available in commercial software packages specifically oriented to the seismic assessment of URM buildings. Dolce (1991) proposed a simplified formula based on a series of linear elastic finite element analyses on 20 different pier–spandrel systems, derived by considering a principle of statistic equivalence between the elastic stiffness of EF and FE models. Moreover, a limit inclination of 30° was introduced for the cracks that start at the right or left corner of the openings and propagate towards the opposite pier edges. The proposed formula is a function of a geometrical parameter *h'* (indicated in Figure 13b by way of example for one of piers), defined as the distance between the midpoints of the lines connecting the vertices of two consecutive openings; according to Dolce these lines have a limit inclination of 30°. The final effective height of the pier (H_{eff}) is then obtained by properly incrementing *h'*, accounting for the deformability of masonry above and below the pier through an analytical expression that includes also the interstorey height.

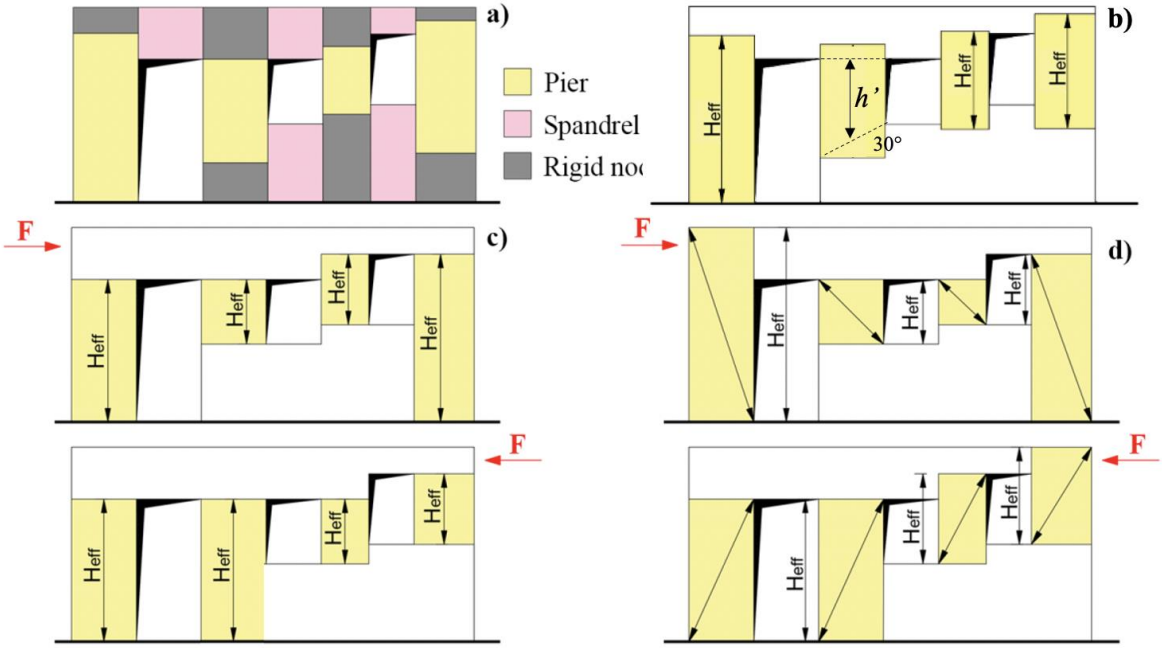

Figure 13. (a) EF idealization of a masonry wall - pier's effective height according to Lagomarsino et al. (2013); different criteria for the pier's effective height: (b) Dolce (1991), (c) Augenti (2006), (d) Moon (2006)

The Tremuri software has implemented (Lagomarsino et al. 2013) a criterion similar to that of Dolce's proposal but without the limitation of the maximum inclination of cracks (Figure 13a). According to this criterion, pier elements are defined starting from the height of adjacent openings. When these latter are perfectly aligned, the height is assumed equal to that of the openings. Conversely, in presence of openings with different heights or external piers, the height is assumed as the average of those of the adjacent openings or as the average between the inter-story height

712 and the height of the opening. Furthermore, some works adopt a criterion similar to that proposed
713 in Tremuri integrating the limitation of 30° proposed by Dolce (Bracchi et al. 2015, Rota et al.
714 2014).
715 Other rules, available in the literature, take into account that the cyclic nature of the earthquake
716 motion can induce a different failure pattern depending on the direction of the seismic forces, thus
717 leading to a pier geometry that changes with the loading orientation. In particular, in Augenti
718 (2006), on the basis of the damage observed in residential and school buildings after past
719 earthquakes (Augenti and Parisi 2010), it is proposed to assume the pier effective height equal to
720 the height of the opening that follows the pier in the direction of the seismic load (Figure 13c).
721 Considering the results of quasi-static lateral loading tests on a full-scale 2-story URM building
722 (Yi et al 2006), Moon et al (2006) proposed a pier effective height equal to the height over which
723 a compression strut is likely to develop (Figure 13d). The compression strut is assumed to develop
724 at the steepest possible angle joining the opposite free vertical edges of the pier; that is, the likely
725 strut is that, among the others, which offers the minimum lateral resistance. This criterion is
726 explicitly recommended in (NZSEE 2017). However, it is useful to highlight that the adoption of
727 these two latter criteria requires alternative models for monotonic analyses along the X and Y
728 directions, with a significant increase in the computational effort. The alternative could be the
729 adoption of structural elements able to adapt the height according to the direction (positive or
730 negative) of the horizontal loads; however, this option, at least to the Authors' knowledge, is not
731 currently implemented in any commercial software package operating under the EF approach.
732 The analysis of the literature highlights that, while several criteria are proposed for the definition
733 of the geometry of the piers, few indications are available for spandrels. While they can be easily
734 obtained by considering the portions of masonry included between two vertically aligned openings
735 for regular walls, their definition may become problematic in irregular layouts. An empirical
736 criterion that provides indications also in the presence of irregularities is proposed in Lagomarsino
737 et al. (2013). According to this rule, the idea is to conventionally assume a mean value for the
738 effective length of spandrel elements as a function of the overlapping part between the openings
739 at the two levels; when no overlap is present, or there are no openings at all, it is suggested to
740 assume that portion of masonry as a rigid area.
741 Various studies demonstrate how the criteria adopted for the geometry of the equivalent frame
742 idealization of walls may represent, for analysists, one of the most significant uncertainties in the
743 seismic assessment of complex existing buildings, corresponding to a high potential source of
744 dispersion on the achievable results (see for example Bracchi et al. 2015, Manzini et al. 2021,
745 Ottonelli et al. 2021).

The issue of defining the effective height of piers is also particularly challenging when the layout of the openings is irregular (*i.e.,* in the presence of openings with different heights on the same story or with a different number/position varying the level), which unfortunately represents a recurrent situation often observed in real cases. In recent years, many researchers have focused their attention on exploring the issue. Parisi and Augenti's (2013) work is one of the first to tackle such problem, proposing a classification of the different types of irregularities recurrent in masonry buildings and some irregularity indexes aimed at quantifying them. Other works (Berti et al. 2017, Siano et al. 2017, Siano et al. 2018, Camilletti et al. 2018, Camilletti 2019) aim to evaluate the accuracy of the EF approach when applied to irregular masonry walls by means of comparisons with refined modeling techniques in linear and nonlinear fields. In Calderoni et al. (2017) some suggestions for the application of the EF model to specific cases of irregular masonry walls are provided, even if they are not exhaustive. Despite that, the issue is still debated and open in the literature.

Adopting only the actual damage observed (*i.e.,* a purely empirical approach) as a reference for the definition and validation of these rules is complicated due to the huge variety of possible configurations. Thus, the numerical results carried out through analyses performed with refined models may be very useful and an essential support for validation aims. Some examples are discussed in the following by showing the results of a very detailed comparison between a refined model based on the use of the isotropic plastic-damaging 3D model implemented in ABAQUS and the EF model implemented in Tremuri software (Lagomarsino et al. 2013) by using the multilinear constitutive law proposed by Cattari and Lagomarsino (2013). The calibration procedure illustrated in Figure 7 and discussed in section 2.2 has been adopted to guarantee cross-consistency between the two approaches. Figure 14 presents the outcome of such a calibration for a panel characterized by a slenderness ratio equal to 2 and a fixed-fixed static scheme. For further details, interested readers may refer to (Camiletti 2019, Cattari et al. 2021a).

In particular, pushover analyses have been carried out on 2D models of various URM walls characterized by different opening layouts, very regular (Figure 15) or aimed at introducing different types of irregularity (Figure 16, named as B1 and BC).

For each wall, four EF models have been set by adopting the equivalent frame idealization rules proposed in Augenti (2006), Dolce (1991), Lagomarsino et al. (2013), and Moon et al. (2006). The comparison between the two modeling strategies is made at different levels in terms of: (i) overall pushover curve, (ii) damage pattern, (iii) generalized forces (either single values corresponding to specific steps of the analysis or their full variation during the analysis).

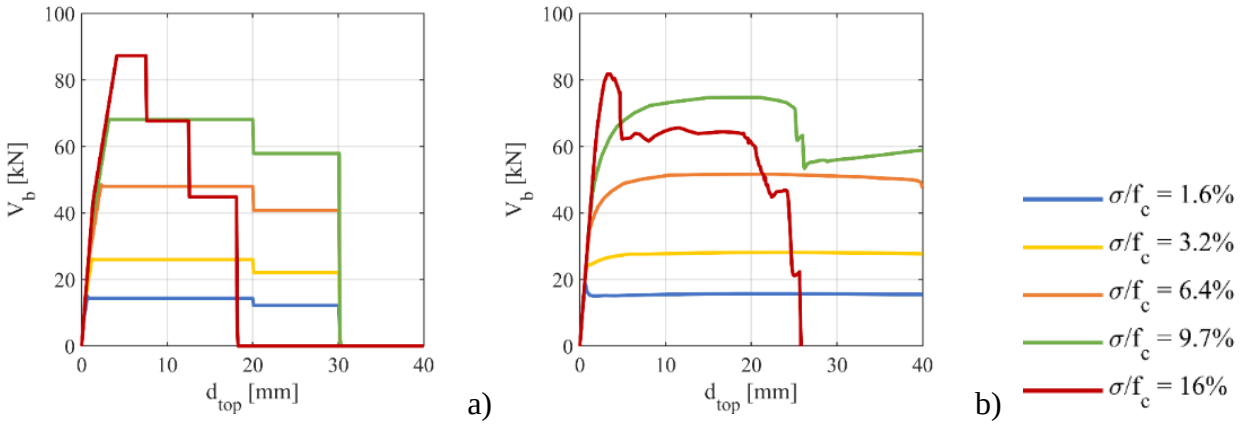

Figure 14 – Base shear-top displacement curves obtained on a single panel for different values of the applied axial load with the EF model, based on the multilinear constitutive law implemented in Tremuri program, (a) and with the FE model, based on the isotropic plastic-damaging 3D model implemented in ABAQUS (b). These models are those used for the results presented in Figures 15 and 16.

Results on the very regular wall (Figure 15), whose geometry, load, and masonry type are inspired by the "Door wall" tested by Magenes et al. (1995), show a very good agreement on all the parameters checked and confirm that in this case, the dispersion of results in adopting different rules is almost negligible (see also Cattari et al. 2021a).

Concerning the other two cases investigated, at ground level, they introduce: (i) piers characterized by a different height (case B1, Figure 16a1) and (ii) a very small opening (case BC, Figure 16a2). The equivalent frame idealization of the wall B1 highlights that the application of the above-mentioned rules is already capable of producing in such an apparently simple case a higher dispersion in the effective height of piers than the very regular case of Figure 15. Wall BC benchmark gives rise to the issue that accounting for all the openings present, independently by their dimensions, may produce very squat piers (see Figure 16b2). Since the evaluation of the drift is greatly influenced by the height, an acritical application of such rules may potentially result in a significant underestimation of the ultimate displacement capacity of the structure; that is shown in Figure16c through the comparison of the pushover curves obtained by the EF models compared with the target defined by the FE model (results refer to the positive direction). The same risk may also occur in the B1 case when the rules proposed by Moon et al. (2006) and Augenti (2006) are adopted (Figure16b1). The comparison in terms of evolution of generalized force progressively worsens, moving from case B1 to BC (Figure 16d). Finally, the analysis of the damage pattern, particularly in case BC, confirms how the sudden drop off in the overall base shear is due to the premature attainment of the collapse condition in the central squat pier. The diagonal crack developed in the FE model suggests that, in this case, the very small opening is not able to significantly affect the stress distribution in this masonry portion that, instead, behaves like a single pier. In order to confirm such an outcome, a more reliable result is obtained in the EF model when the small opening is completely neglected (see the light-blue curve in Figure 16c of case BC).

Even these results cannot conclusively define standardized rules to adopt, they only highlight the potential of a cross-use of refined and EF models to this purpose in the future (see also Cattari et al. 2021a).

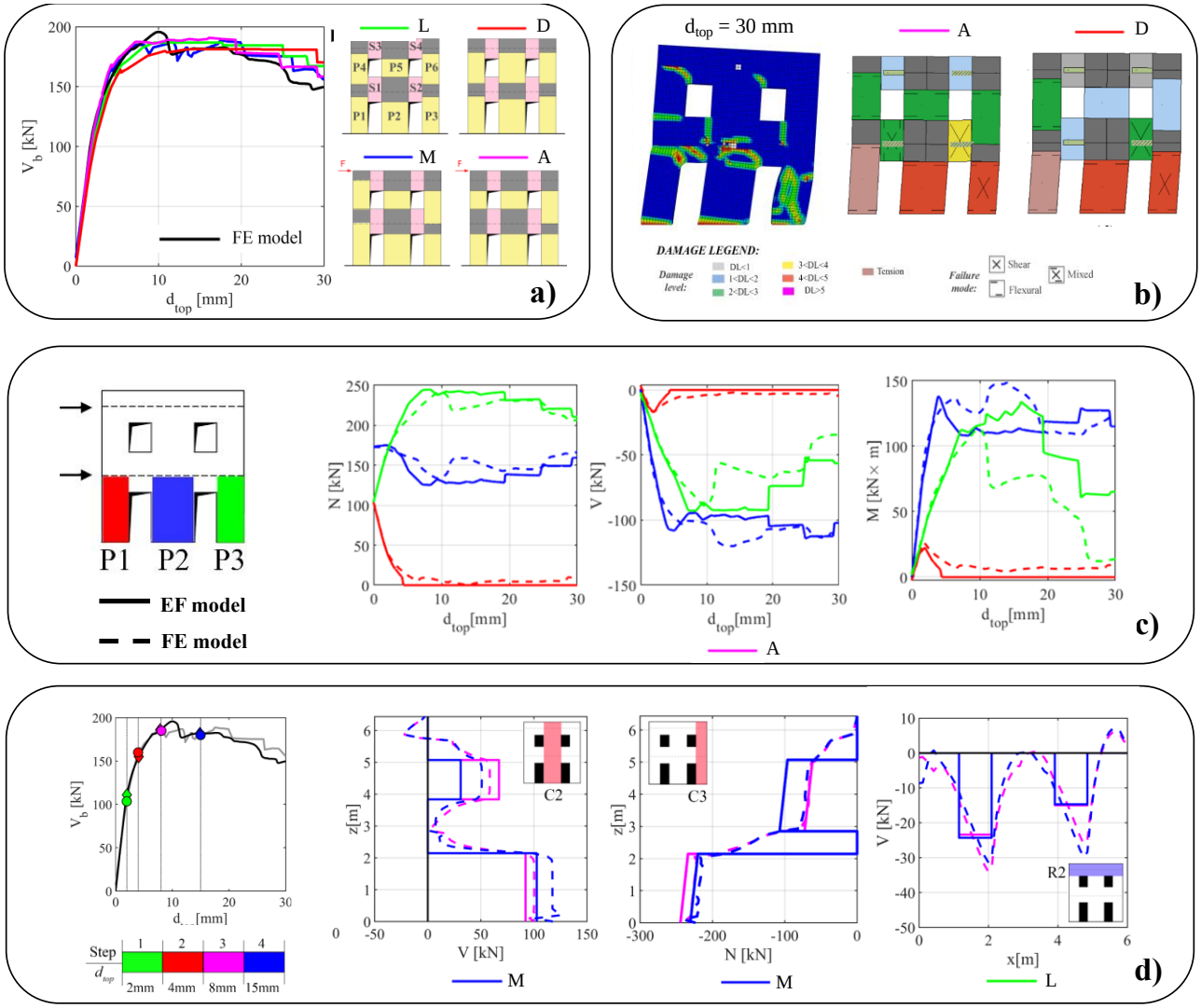

Figure 15 – Comparison between EF and EF models for a regular wall: a) pushover curves and frame idealization according to various rules (L, D, M, and A stand respectively for Lagomarsino et al. 2013, Dolce 1991, Moon et al. 2006 and Augenti 2006); b) damage pattern; c) evolution of the axial load in the piers at ground level; d) generalized forces for given steps of the pushover curve (adapted from Cattari et al. 2021a)

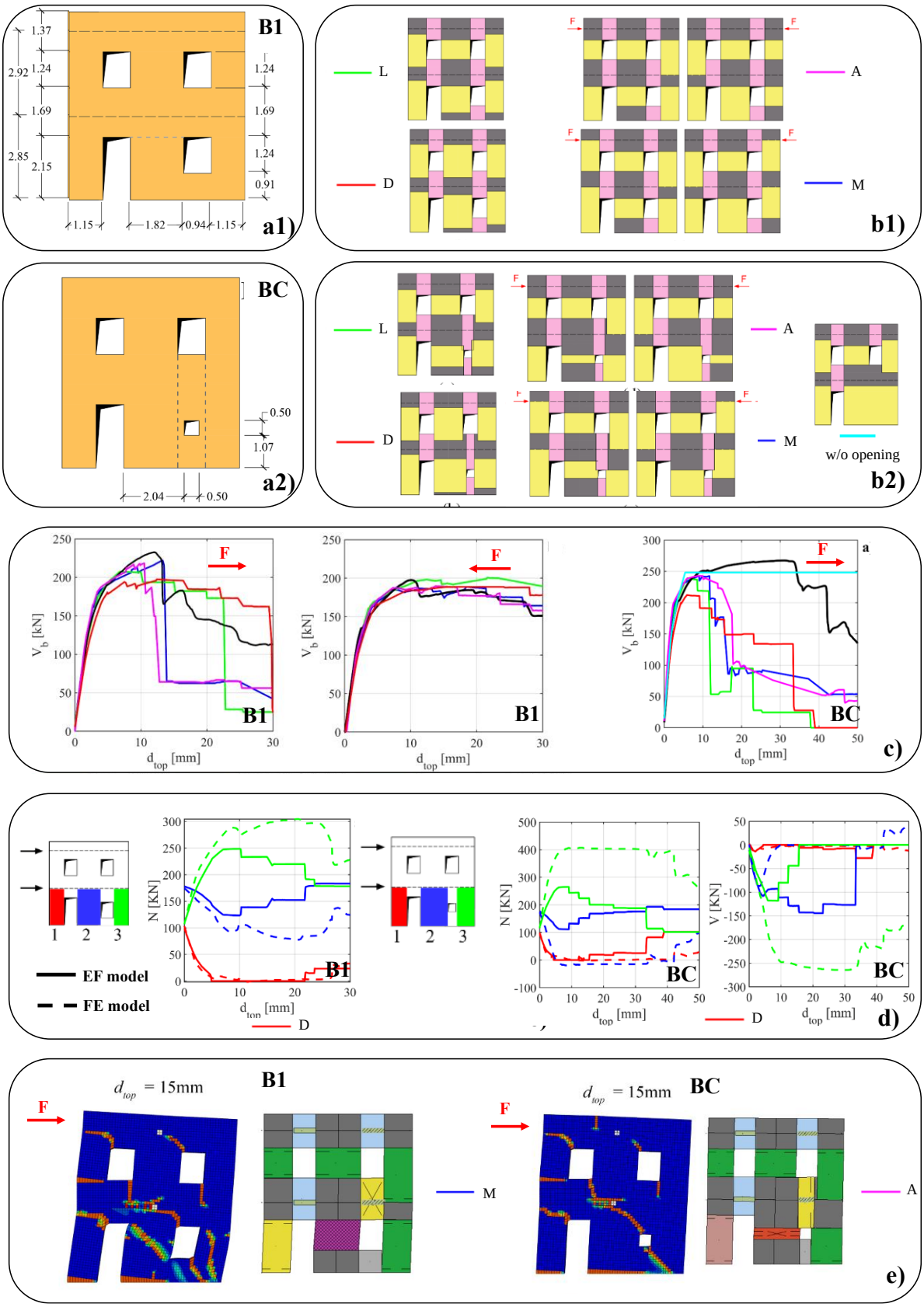

Figure 16 – Comparison between EF and EF models for a wall with different height piers at ground level (B1) and a wall with a very small opening at ground level (BC) : a1/a2) wall geometry; b1/b2) frame idealization according to various rules (L, D, M and A stand respectively for Lagomarsino et al. 2013, Dolce 1991, Moon et al. 2006 and Augenti 2006); c) pushover curves; d) evolution of the axial load in the piers at ground level; e) damage pattern. Figures adapted from Camiletti 2019.

2.4 Critical issues in the modeling of wall-to-wall connections

In order to build a 3D model and perform a global analysis, URM walls have to be properly connected, and different levels of effectiveness for the wall-to-wall connections should be accounted for to reproduce the large variety of existing buildings.

If the connection among walls is good, a possible redistribution of forces among intersecting piers may occur, generating the so-called "flange effect" (*i.e.*, forming piers with L-, C-, T-, or I-shaped cross-sections). The presence of such flanges can influence the in-plane response of the walls in terms of failure modes, maximum strength, and displacement capacity. As a consequence, the performance of the whole building, as highlighted, for instance, by experimental campaigns conducted on both single URM panels (Russell and Ingham 2010, Russell et al. 2014, Khanmohammadi et al. 2014, Sajid et al. 2018) and simple mock-ups (Costley and Abrams 1996, Paquette and Bruneau 2003, Moon et al. 2006) may vary too. Also, numerical simulations confirm experimental results (see Milosevic et al. 2020, Ottonelli et al. 2021, Tomic et al. 2021). For the aforementioned reasons, it is fundamental that the models employed for the design or the assessment can adequately account for these effects.

As depicted in Figure 17, such aspects may be accounted for in different ways depending on the modeling strategy.

While continuum models typically simulate a perfect connection (Figure 17b), only micromodels and block-based (i.e. a modelling approach where the masonry microstructure is explicitly modeled, and each microscopic behavior is described by its own nonlinear continuum constitutive model) models can consider the actual masonry texture, *i.e.*, the actual toothing between orthogonal walls (see Figure 17a). As an example, Figure 18 shows the numerical behavior of orthogonal walls with toothing obtained with a continuum micromodel considering bricks and mortar (Figure 18a) and a damaging block-based model (Figure 18b) separately.

In the plane discrete macro-element models (Caliò et al. 2012), the wall-to-wall connection is governed by corner elements that are endowed with interfaces and allow for the limitation of the coupling of orthogonal walls by adopting specific limit values, related to tensile and shear forces, according to specific constitutive laws. This approach can potentially grasps the typical nonlinear behaviour at the wall-to-wall connections with the development of a vertical crack due to detachment or sliding between the attached walls. In the three-dimensional macro-modeling (Figure 17c), this strategy also allows to consider the detachment between orthogonal walls when an out-of-plane mechanism is activated (Pantò et al. 2016, see also Section 2.6). The same strategy can be applied at the meso-scale: in this case, a block-based model can account for the actual masonry texture and, if efficiently calibrated, can provide a satisfactory prediction of the experimental response (Cannizzaro et al. 2017).

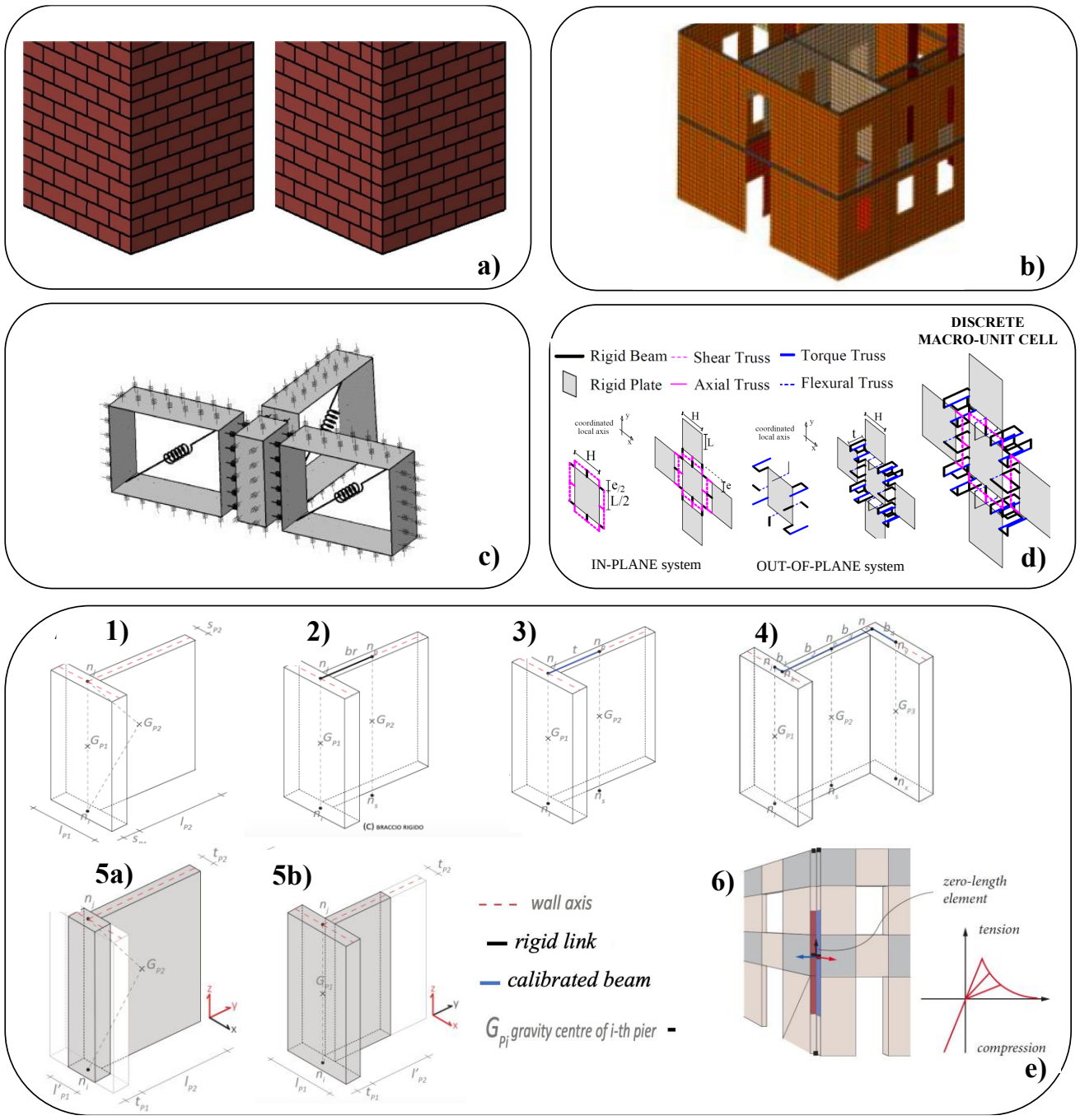

Figure 17 – Possible strategies for accounting the walls-to-walls connection varying the modeling approach: a) micromodels and block-based models (from D'Altri et al. 2020b); b) continuum models (adapted from Castellazzi et al. 2021); c) corner elements connecting adjacent discrete-macro elements (adapted from Pantò et al. 2016); d) Rigid Body Spring Model, i.e., rigid elements joined by homogenized interfaces (adapted from Bertolesi et al. 2016); e) alternative options in EF models

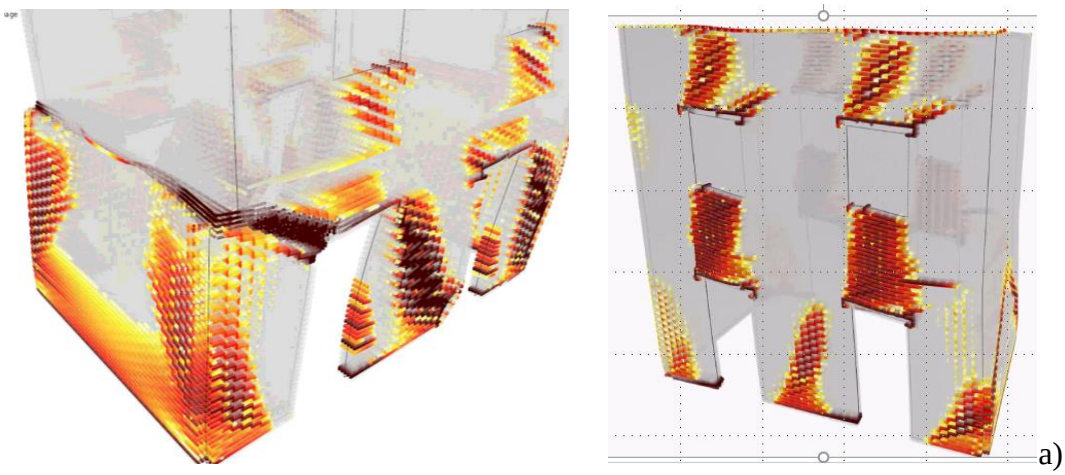

a)

b)

Figure 18 –Numerical examples of toothing behavior: (a) continuum micromodel considering the bricks and mortar separately, and (b) damaging block-based model with cohesive-frictional contact (D'Altri et al. 2019).

In the case of refined models, an alternative and effective approach to consider the degree of interlocking between perpendicular walls is the combined use of homogenization and kinematic limit analysis or an incremental approach based on the assumption of rigid elements joined by homogenized interfaces (Figure 17d). The limit analysis case will be treated in detail later on in the paper when dealing with the occurrence of local mechanisms (Section 2.6), whereas here the attention is focused on the combination of homogenization and rigid elements interconnected by nonlinear homogenized springs (Figure 19). At present, this procedure is conceived almost purely for research purposes and is hardly utilizable immediately at professional level; however, efforts are ongoing to automatize the required steps for making also practitioners able to use very sophisticated approaches.

The strategy takes advantage of a classical first-order homogenization scheme, which relies on the definition of a suitable boundary value problem able to provide the average (or homogenized) nonlinear stress-strain behavior of a so-called unit cell that generates a masonry wall by repetition. Interested readers should refer to Milani (2011) for further details on this theoretical topic applied

to masonry. The implementation at structural level occurs using a discrete element model, hereafter designated as Rigid Body Spring Model (RBSM). RBSM is an assemblage of non-linear homogenized springs and rigid bi-dimensional elements. The methodology and the main features of the model at cell and structural level are briefly summarized in Figure 19.

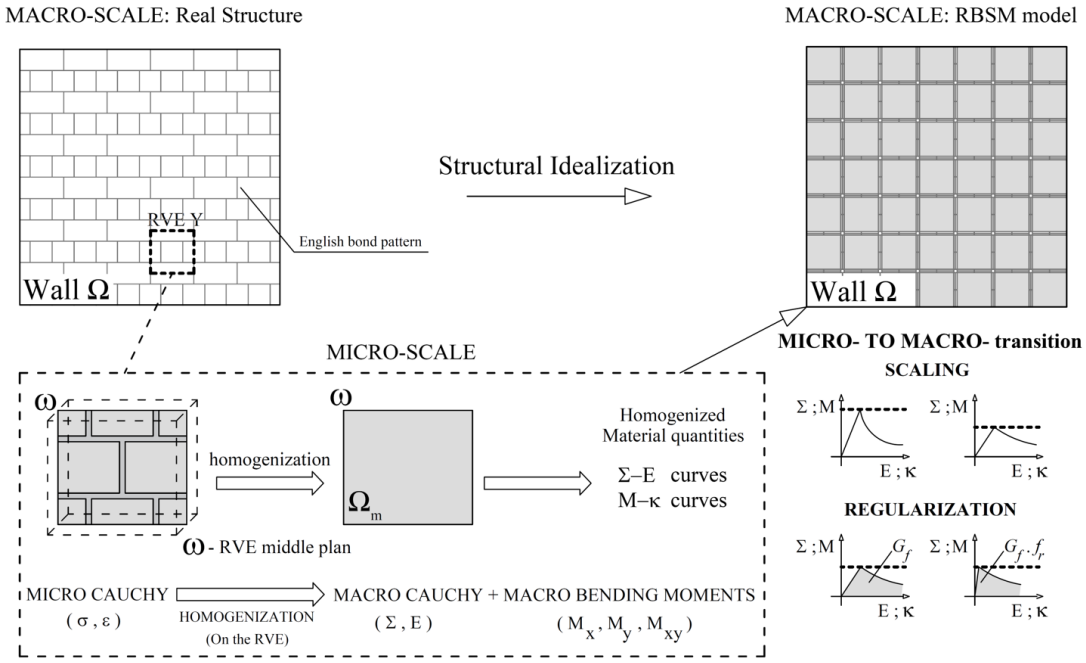

Legend of symbols:

E	Macro-scale strain	Y	Boundary of the RVE
f_r	Flexural fracture energy coefficient	e	Micro-scale strain
G_f	Fracture energy in tension	k	Macro-scale curvature
M	Macro scale moment	σ	Micro-scale Cauchy stress
M_x	Horizontal macro scale bending moment	w	Unit cell volume
M_y	Vertical macro scale bending moment	Σ	Macro-scale Cauchy stress
M_{xy}	Macro-scale torsion	W	Macro-scale wall area
RVE	Representative Element of Volume	W_m	Micro-scale unit cell area

Figure 19 –Methodology of a typical two-step numerical procedure to study 3D structures. Homogenization model and transition from micro to macro-scale.

Moving from micro-scale to macro-scale, some *ad-hoc* steps are developed for a correct upscaling, *i.e.*, the scaling and regularization of the homogenized quantities. This is a critical step since it is necessary for assuring that the macro-input is independent from the macro-mesh (Silva et al. 2020). Indeed, accounting for the interlocking between perpendicular walls complicates the formulation to a great extent. For illustrative purposes, Figure 20 shows how such approach has proven effectiveness in the numerical simulation of experimental tests carried out under both static (Figure 20a) and dynamic conditions (Figure 20b). In particular, Figure 20a illustrates an application to a wall specimen with openings tested by Griffith et al. (2007) that exhibited a good interlocking with perpendicular walls; interested readers to more details on this numerical simulation should refer to Bertolesi et al. (2016) and Bertolesi et al. (2019). Instead, Figure 20b shows an extract of some numerical simulations performed by Bertolesi et al. (2018): it deals with a two-story masonry

building lab prototype tested in the nonlinear dynamic field by Bothara et al. (2010). In particular, Figure 20b2 depicts a comparison between control point experimental and numerical displacements during the application of a real accelerogram (Taft earthquake) with maximum acceleration scaled to 0.5g. Figure 20b3 shows the damage cumulated on out-of-plane loaded walls for horizontal/vertical bending at ground acceleration peak.

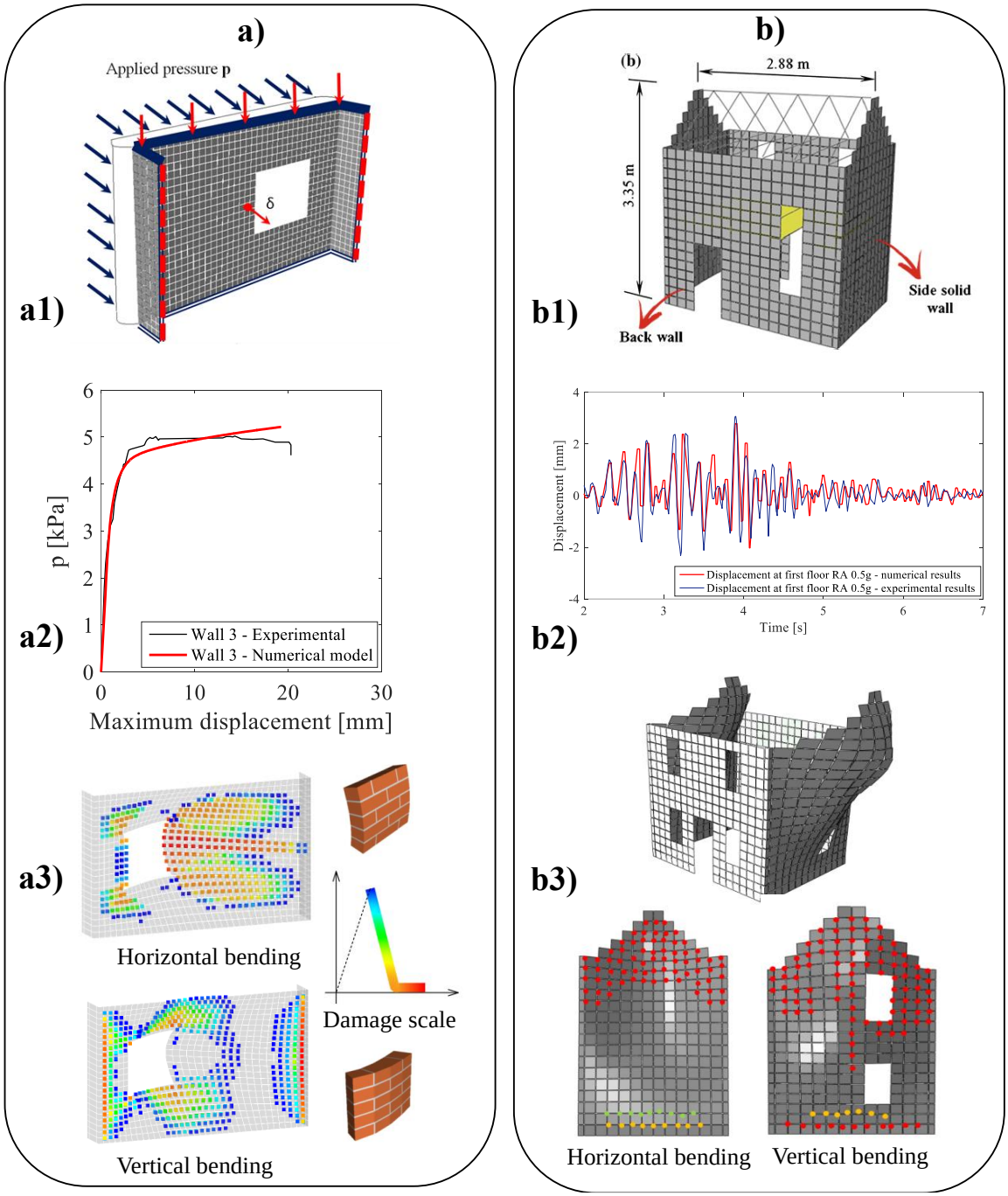

Figure 20 –Examples of application of homogenization combined with a Rigid Body and Spring Model (RBSM) in: a) the non-linear static case by simulating the wall with opening tested by Griffith et al. (2007); b) the non-linear dynamic case by simulating the two-story masonry building tested by Bothara et al. (2010) (figures of the numerical simulation adapted from Bertolesi et al. 2016 and 2019 in case a) and from Bertolesi et al. 2018 in case b). In both cases the damage for horizontal/vertical bending are reported (a3 and b3) together with the comparison in terms of pushover curves (a2) or displacement at the first floor (b2)

Finally, it is worth mentioning that in the EF approach, the connection among intersecting walls is simulated through various implementation strategies varying with the software packages used (as depicted in Figure 17e).

Considering the general case of Figure 17e case 4), of which cases 1), 2) and 3) are particular cases, a kinematic coupling among incident walls can be simulated through different solutions such as the use of kinematic constraints and the consequent condensation of the degrees of freedom (Figure 17 case 1 or case 2). In general, this option, frequently adopted as default by commercial software packages (as discussed in Cattari and Magenes 2021), can be then edited, allowing: (i) the passage from the perfect kinematic coupling to the use of "equivalent" elastic beams of finite stiffness (Figure 17e3) and (ii) the deletion of the rigid link (thus downgrading the full coupling to a null wall-to-wall connection). When "equivalent elastic beams" are adopted, the effectiveness of wall-to-wall connections may be managed through a proper calibration made by the user of the stiffness parameters of the coupling beam (as discussed in more detail in Ottonelli et al. 2021). In the general case of Figure 17e case 4) where more than two panels are intersecting to form a complex section, a common option is to define one simple vertical element per each panel (three in the particular case of the figure). The nodes at the top of each element can be connected to each other via rigid links (kinematic constraints) or calibrated beams (links or elements b_1, b_2, b_3 and b_4 in the figure) creating hence composite actions among the panels (the same can be applied for the bottom nodes of the elements). When such a solution is adopted, it is very important to consider that, unless rotational releases are introduced at nodes n_k between links b_1 and b_2, and at node n_z between links b_3 and b_4, the free warping of the composite section would be restrained, increasing dramatically (and fictitiously) the stiffness of the composite wall (especially the torsional stiffness).

When using the EF approach in general-purpose software packages, the equivalent frame model is implemented directly by the user, and a common practical way to simulate the collaboration effect among intersecting walls must be defined. Depending on the direction of loading, an "effective flange width" must be considered collaborating with the "web" of the composite section. The section properties of the equivalent frame element are thus defined in terms of moment of inertia, cross-sectional area, effective shear area, as it would be done for T- o I-shaped sections. Such approach clearly produces different section properties depending on the direction of loading (as shown in Figure 17e, cases 5a for a shear force in the y-direction, and 5b for the x-direction). Finally, Figure 17e6 presents the approach adopted in the equivalent frame model by Vanin et al. (2020a, 2020b) and implemented in OpenSees (McKenna et al. 2000). In this case, the connection between orthogonal walls is modeled through zero-length elements. Such connection can also

exhibit a nonlinear behavior (thus giving the possibility to reproduce the development of a vertical crack as also discussed in section 2.6, Figure 23) and can be modeled either through point connections at the corner nodes (to which appropriate tensile properties are then assigned) or through the use of fiber sections.

When the strategy presented in Figure 17e3 is adopted, the calibration of the equivalent beams used to simulate different degrees of effectiveness of the wall-to-wall connections becomes quite difficult since it should account for the geometry and properties of the incident piers and the masonry typology (*i.e.*, dimensions of block and bond type). Despite that, there are no specific indications in the literature to properly calibrate the stiffness of such beams, which is usually determined through empirical approaches. In Ottonelli et al. (2021), the "starting reference value" of the stiffness of the equivalent beams has been calibrated in order to reproduce the same solution obtained in the case of perfect coupling; then, from that value, a progressive reduction of the moments of inertia has been applied in order to reproduce various levels of effectiveness of the wall-to-wall connection (see also Milosevic et al. 2020).

The effective width to be considered for the flange (essential for applying the strategy of Figure 17d5a/b and also for the equivalent beam calibration) still represents a critical open issue. Most works available in the literature focus on the determination of the effective flange width in reinforced concrete and reinforced masonry shear walls (*e.g.*, Priestley and He 1995, Hassan and EI-Tawil 2003, Shi and Wang 2016), but the rationales employed are different for different materials. For example, the effective flange width of a reinforced concrete shear wall increases due to the yielding of the reinforcement, and obviously this feature cannot be applied to URM walls. Some indications specifically conceived for URM walls have been proposed in (Yi 2004, EC6 -Part 1-1 CEN 2004, MSJC 2008, Mordant 2016, and Calderoni et al. 2019b), but research into this very specific topic is still ongoing.

Regardless of these difficulties, it is worth being aware of the high potential sensitivity of the achievable results, particularly in the case of EF models.

When the connection between the orthogonal walls is managed through the perfect coupling of the vertical component or with rigid links (*i.e.*, regardless of the dimension of the flange), this may lead to an overestimation of the flange collaboration in the presence of long intersecting walls which imply very long effective flange widths (*e.g.*, the case of very long and squat walls without openings), where it seems unrealistic to consider the whole width as effective. As an example, Figure 21 shows some results referred to the case of the Fabriano Courthouse (Italy), recently discussed in Cattari et al. 2021b. This building is permanently monitored by the Department of Civil Protection (DPC, Dolce et al. 2017) and the figure shows the comparison of the experimental

modes, as evaluated from the data provided by the DPC, and those numerically simulated by the EF frame model presented in Cattari et al. (2021b).

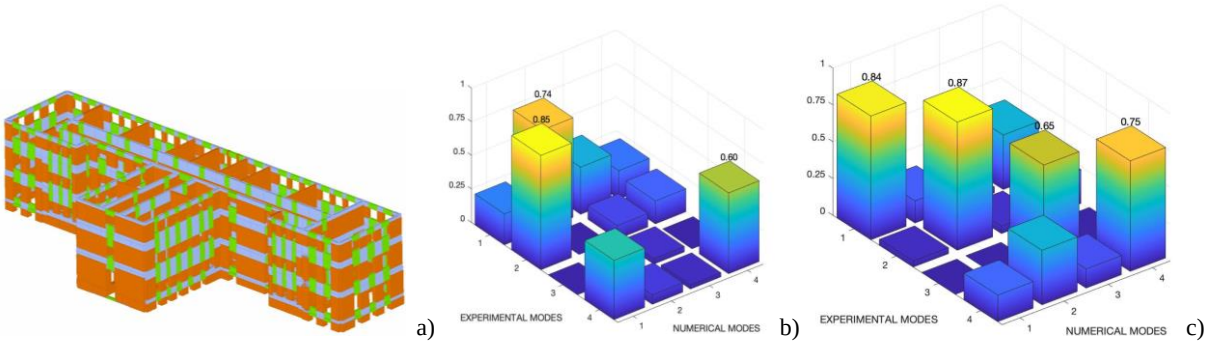

a) b) c)

Figure 21 – a) EF model of Fabriano Courthouse. Comparison of simulated and experimental modes in terms of MAC index in case of perfect (b) or calibrated (c) coupling among walls (adapted from Cattari et al. 2021b)

The comparison is made in terms of MAC (Modal Assurance Criterion) index (Allemange and Brown 1982), where values close to 1 indicate a very good agreement between experimental and numerical data, and the optimal result consists of having unitary values along the diagonal. It is interesting to observe that the option associated with the full kinematic coupling (Figure 21b) produces a very high discrepancy in terms of mode shapes. A correct prediction is obtained using equivalent beams of finite stiffness calibrated to simulate a good quality of connection. This latter hypothesis is in agreement with the actual configuration of the building, where strengthening interventions were introduced to improve such specific structural aspect.

Finally, Figure 22 provides a more comprehensive overview on the potential repercussions of alternative assumptions on the quality of the wall connections by assuming as reference the benchmark structure (BS5) inspired by the “P. Capuzi” school of Visso (MC, Italy) and analysed in Ottonelli et al. (2021) within the scope of the *URM Nonlinear modeling*-Benchmark project.

Passing from the perfect connection to the poor connection assumption among walls, the results show a significant variation in terms of: (1)pushover curves (Figure 22b); (2) value of the axial load on piers composing the flange system (Figure 22c), referring to both the initial value, after the application of gravity loads, and its variation due to the application of horizontal forces; (3) mode shapes and participant masses (Figure 22d, considering the first three modes). Results presented in Figure 22b have been obtained using three different software packages (SWs) that adopt different strategies to simulate the walls-to-walls connection. Such outcome also demonstrates that the numerical procedures depicted in Figure 17e3 (used in SW1 and SW2) and in Figure 17e5 (used in SW7) may produce analogous predictions, if consistently implemented. Further details on this issue may be found in Ottonelli et al. (2021). Of course, it is worth specifying that the actual variation in the results depends on the specific structural configuration of each building.

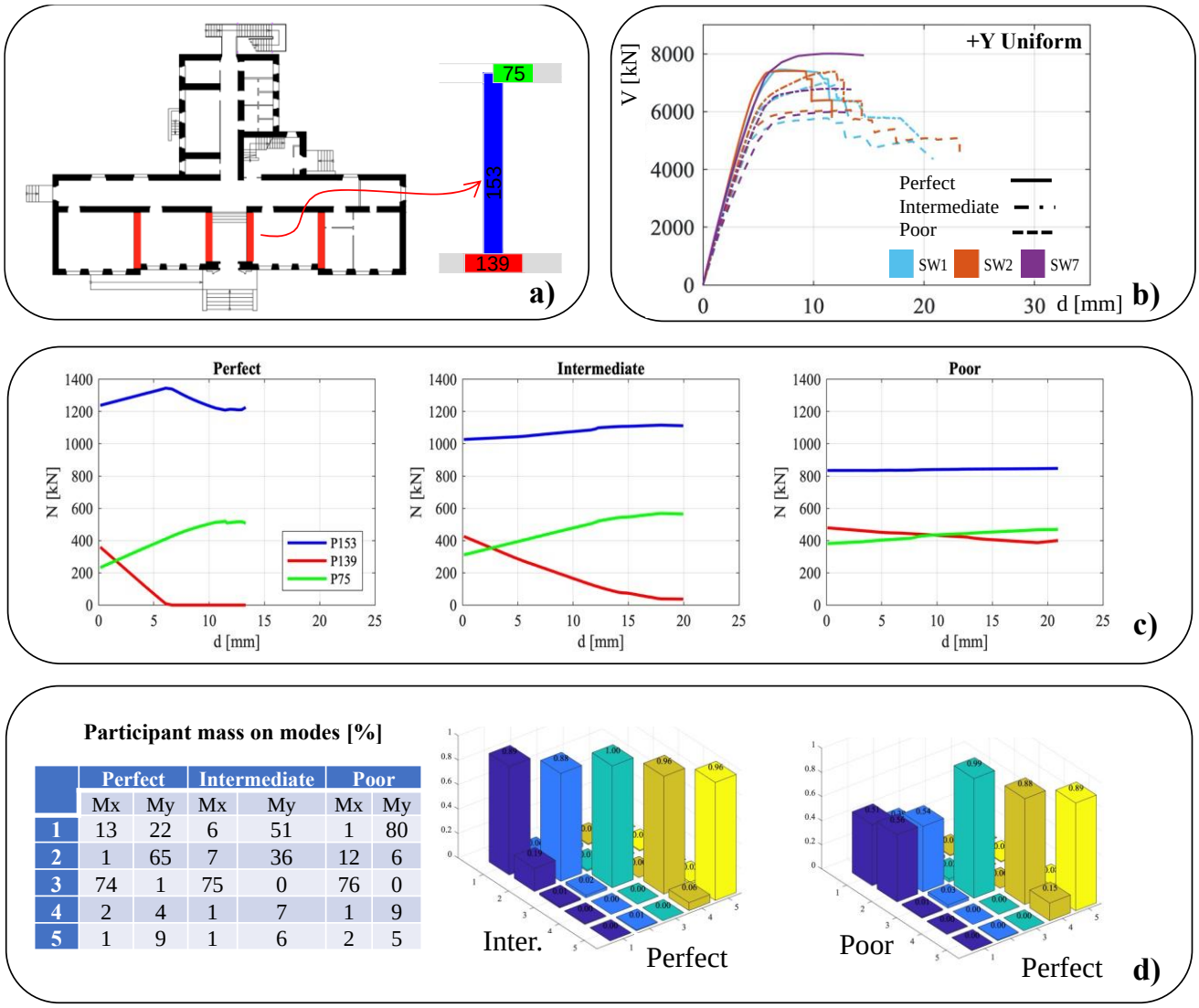

	Perfect		Intermediate		Poor	
	Mx	My	Mx	My	Mx	My
1	13	22	6	51	1	80
2	1	65	7	36	12	6
3	74	1	75	0	76	0
4	2	4	1	7	1	9
5	1	9	1	6	2	5

Figure 22 – Overview of potential repercussions of alternative assumptions on the quality of wall connections for BS5 (figures adapted and integrated from Ottonelli et al. 2021): a) in plan view of the BS5 and identification of piers analysed in c); b) pushover curves; c) axial load variation on piers; d) mode shape variation.

2.5 Critical issues in modeling the out-of-plane response of masonry walls

Modeling the out-of-plane response of URM walls in full 3D seismic analyses involves two main issues. The first deals with the contribution of the out-of-plane stiffness and pier strength to the overall horizontal force equilibrium. The second deals with properly accounting for the possible activation of out-of-plane failure mechanisms of walls (usually called “local mechanisms”, for whose an overview of the most recurring ones is provided in D’Ayala and Speranza 2003), which, at collapse, are ruled more by the loss of equilibrium rather than the attainment of the material strength limits. Particularly in the second case, the difficulty lies in modeling both the in-plane and

1039 out-of-plane responses in an integrated, efficient, and accurate way to also account for their
1040 possible combined effects.
1041 In the following, these issues are first discussed for EF models.
1042 The pier out-of-plane stiffness and strength are included in most commercial software packages
1043 based on this modeling approach (see also Cattari and Magenes 2021). For the strength, similarly
1044 to the in-plane flexural response, the ultimate bending out-of-plane capacity is usually computed
1045 based on the axial load applied to the panel, neglecting the masonry tensile strength and assuming
1046 an equivalent rectangular stress block distribution of stresses. Since this contribution depends on
1047 the axial load, it has to be highlighted that the latter is also dependent on the modeling of the flange
1048 effect. As also discussed in Ottonelli et al. (2021), for traditional buildings and for wall thicknesses
1049 lower than 0.40 m, the incidence of such out-of-plane contribution can be considered as not
1050 particularly significant, and it is conservative to ignore it. Conversely, for thicknesses greater than
1051 0.40 m, the contribution of the out-of-plane response becomes progressively more significant, and
1052 neglecting it could lead to appreciable variations not only on the overall base shear capacity but
1053 also on the initial stiffness and ultimate displacement capacity. In Ottonelli et al. 2021, for the
1054 complex URM building of Figure 22, the incidence of both the out-of-plane contribution and the
1055 flange effect is discussed by considering alternative options for each single modeling hypothesis
1056 and by considering their combination.
1057 Passing to the second issue (*i.e.*, the simulation of "local mechanisms"), according to the most
1058 common procedures accepted by the scientific community, EF approaches are considered
1059 unsuitable for directly dealing with the partial collapses of out-of-plane loaded masonry walls and
1060 for the hybrid in- and out-of-plane failures of portions of entire buildings. In general, it is assumed
1061 that the EF approach alone can provide reliable and exhaustive information only when the out-of-
1062 plane response is not critical, for example, if the walls are tied together at all story levels.
1063 Conversely, if local mechanisms are likely to occur, a common approach is to adopt the method
1064 of rigid body limit analysis with pre-assigned failure mechanisms (as discussed in the following).
1065 Then the results of the global in-plane response made by the EF model and those provided by the
1066 rigid body limit analysis have to be combined. The simplest approach is to consider the final safety
1067 index as the worst between the two ones (see for example Simoes et al. 2014), but in the context
1068 of developing fragility curves some attempts to integrate the two failures modes in a more accurate
1069 way – even if still analysing them in a separate way - have been also developed (see for example
1070 Angiolilli et al. 2021).
1071 A preliminary attempt to fill the gap between EF limitations and the possibility to predict out-of-
1072 plane collapses (albeit in an approximative way) has been recently provided in the approach
1073 implemented by Vanin et al. (2020a, 2020b) and already introduced in Section 2.5. This approach

couples equivalent frames with possible out-of-plane failures of single elements. Figure 23 illustrates the basis of this method with an application that highlights the sensitivity of the out-of-plane response to alternative hypotheses relative to the wall-to-wall connection. Unfortunately, this approach still does not account for very complex partial failure mechanisms observed in post-earthquake surveys, despite steps forward have been done to deal with the task in its full complexity.

After a thorough revision of the literature available, it is the Authors' opinion that the possibility to include out-of-plane failures in EF models still needs substantial improvements.

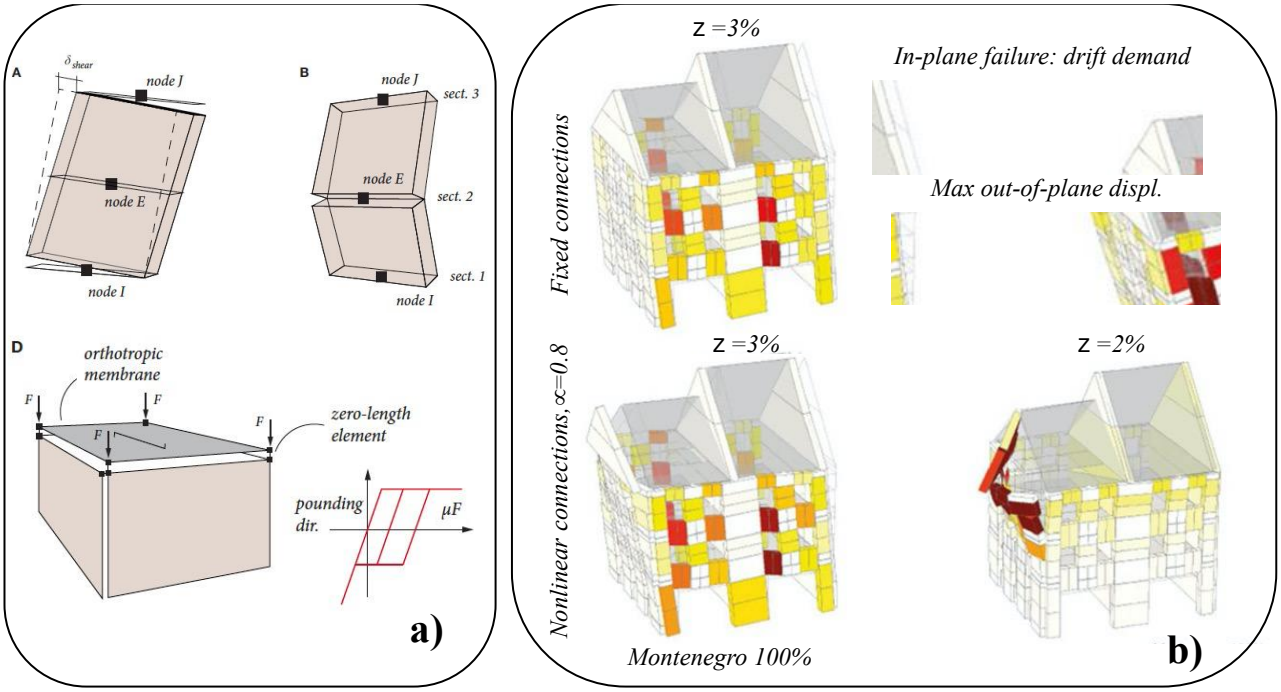

Figure 23 – a) Basics of the equivalent frame approach implemented by Vanin et al. (2020); b) sensitivity of the in-plane and out-of-plane damage simulated to the effectiveness of walls connections and damping ratio by performing NLTHA (adapted from Vanin et al. 2020b)

The main reason for these difficulties stands in the awareness that experimental tests carried out since the 70's on laterally loaded brick masonry walls show that failure occurs along crack lines, whose patterns are only in some cases consistent with the simple overturning of the walls or the formation of a horizontal cylindrical hinge (as in simple one-way vertical or horizontal bending). In the past, these results inspired the utilization of approximate analytical solutions, based on the classic yield line theory, that in practice is an application of the classic kinematic theorem of limit analysis. Interested readers may refer to Lagomarsino (2015), Giresini et al. (2015), Abrams et al. (2017), Casapulla et al. (2017), Sorrentino et al. (2017) and Degli Abbati et al. (2021), for a review of the methods proposed in the literature and Codes belonging to this approach and for some scientific studies addressed to validate them. The Italian Code (MIT 2019), for instance, explicitly requires the examination of such collapse modes and suggests the kinematic limit analysis as a

robust verification tool where masonry can be modeled as a no-tension material. Unfortunately, this last assumption on the material strength (no-tension) does not take into account a number of mechanical features of masonry that can influence the out-of-plane response. First of all, masonry is a heterogeneous composite material (made of bricks or blocks and mortar) that, according to experimental evidence, may exhibit in several cases a non-isotropic behavior both in the pseudo-elastic field (service conditions) and at failure. Additionally, masonry tensile strength is not strictly zero, and despite being low, highly scattered and with a quasi-brittle post-peak behavior, it can affect significantly the results in several cases. In addition, the infinite compression strength assumption made for rigid blocks is, in such cases, questionable, and currently, there are some approaches available that can account for these features in a reasonable manner, without excessive computational burden. In any case, brittle crushing phenomena are typically considered to be of minor importance in an out-of-plane analysis of walls at failure. Another crucial aspect that requires particular attention is the role played by the friction coefficient μ of mortar joints. According to several experiments (*e.g.* Atkinson et al. 1989 and Andreotti et al. 2019) , the friction coefficient appears relatively high, in general above 0.4 (with the exception of particular cases such as in presence of damp proof courses) thus excluding sliding phenomena (at least out-of-plane) in the majority of the cases, favoring the formation of torsional and flexural hinges. In such case classic limit analysis can be applied without the risk to obtain inaccurate results from an engineering standpoint. The role of the stabilizing role of the friction between interlocked walls compared to other extrinsic or intrinsic loading capacity (e.g. the effect of tie-rods and simply supported horizontal diaphragms with frictional resistance) has been discussed in Casapulla and Argiento (2016). Moreover, in Casapulla et al. (2021) a macro-block model accounting for frictional resistance has been used to calculate the onset load factors in multi-storey buildings for two classes of local mechcanisms which are particularly useful in engineering applications, like as the rocking-sliding and the flexure mechanisms.

Finally, the use of heterogeneous approaches or macroscopic nonlinear orthotropic models is at present too demanding at professional level due to the excessive computational effort needed and the expected weak background of the typical user in the definition of the many material parameters needed for blocks, mortar or the macroscopic materials representing masonry to apply in the non-linear range.

Despite the aforementioned approximations and the awareness that masonry does not behave as a rigid-plastic material, limit analysis remains a possible tool that is fast and simple enough for assessing both the ultimate load capacity of masonry walls and the corresponding active failure mechanisms. Thanks to its simplicity and the very limited number of parameters required, limit

analysis was selected over the last few decades as a standard procedure for evaluating failure modes and ultimate bearing capacity of masonry in bending.

According to the Authors' opinion, the main issues to investigate are the following: (1) to maintain the analysis with a limited computational burden, (2) to accurately reproduce the crack pattern developing during the formation of an out-of-plane failure mechanism, (3) to use a model that is easily understandable by practitioners and finally (4) to take into account the most important features of the masonry material under consideration, such as orthotropy, irregular assemblages of stones/blocks, and the possible presence of multi-leaf walls.

Recently, a first attempt has been made to define the pre-assigned failure mechanisms by drawing the mesh with CAD. The mesh is imported in a standard FEM software using refined discretization and recursively applying the principle of virtual works on a number of different mechanisms to closely approximate the actual failure mechanism. It is important also to account for the real geometry,load distribution and internal dissipation of the masonry material (Milani 2019). The approach proved to be efficient for masonry towers, but additional work is needed to deal with more complex historical structures.

The most recent literature in the general field of existing structures moves in another direction. It suggests using numerical models conceived *ad-hoc*, where masonry is assumed as rigid plastic, so the classic theorems of limit analyses still hold, *i.e.*, choosing to delegate the detection of the failure mechanism to a numerical algorithm (Chiozzi et al. 2017). To circumvent the important drawback of applying the kinematic approach of limit analysis, which needs to assign *a-priori* a failure mechanism, recent literature proposes using very rough Finite Element FE meshes of the particular portion of the structure that needs to be investigated. It also suggests a possible progressive adjustment of the nodes in order to overlap step-by-step the plastic dissipation of the numerical model with the actual one, thus accurately reproducing the actual failure mechanism with a realistic assumption of the material properties to assign for masonry, deduced from heuristic, compatible, or rigorous homogenization techniques. Examples can be found in some seminal papers in the field (see, *e.g.*, Chiozzi et al. 2019a and 2019b), where adaptive curved/NURBS finite elements with orthotropic behavior have been used to reproduce with a good level of accuracy the activation of two way bending mechanisms for walls as in Figure 24 (Chiozzi 2019b), churches as in Figure 25a (Chiozzi et al. 2019a), domes with complex geometries as in Figure 25b (Grillanda et al. 2019), and masonry aggregates as in Figure 25c (Grillanda et al. 2020a). The adaptation has been carried out either with Sequential Linear Programming or with non-standard Genetic Algorithms and Meta-Heuristic approaches in general. The interested reader should refer to (Milani 2015) and (Grillanda et al. 2020b) for further details. This approach could also be

coupled with displacement-based evolutive analysis strategies, as successfully carried out in (D'Altri et al. 2020b), to perform pushover analysis.

Passing to other refined approaches (see Figure 26*)*, like as FE models, masonry walls are often modeled with shell elements to reduce the computational cost (*e.g.*, Petracca et al. 2017b). This seems to be a reasonable simplification when the wall is not extremely thick. However, most FEM codes adopt a plane-stress formulation for the nonlinear material in each layer (through-the-thickness integration point) of the shell. For thick shells (shear-deformable), the out-of-plane shear is modeled elastically (and un-coupled from the in-plane and bending response). The transverse shear strain can be considered negligible up to the onset of strain location and only if the model is homogeneous. However, in micro-models, even if the overall wall can be considered as thin, the mortar joints are not. The overall crack in the out-of-plane failure can be seen as a rotational hinge at the global level, but locally (in a micro-model), there is a high concentration of transverse shear deformation in the joints. Therefore, it is mandatory to use a full 3D constitutive model (except when the normal stress is equal to zero) in each layer of the shell.

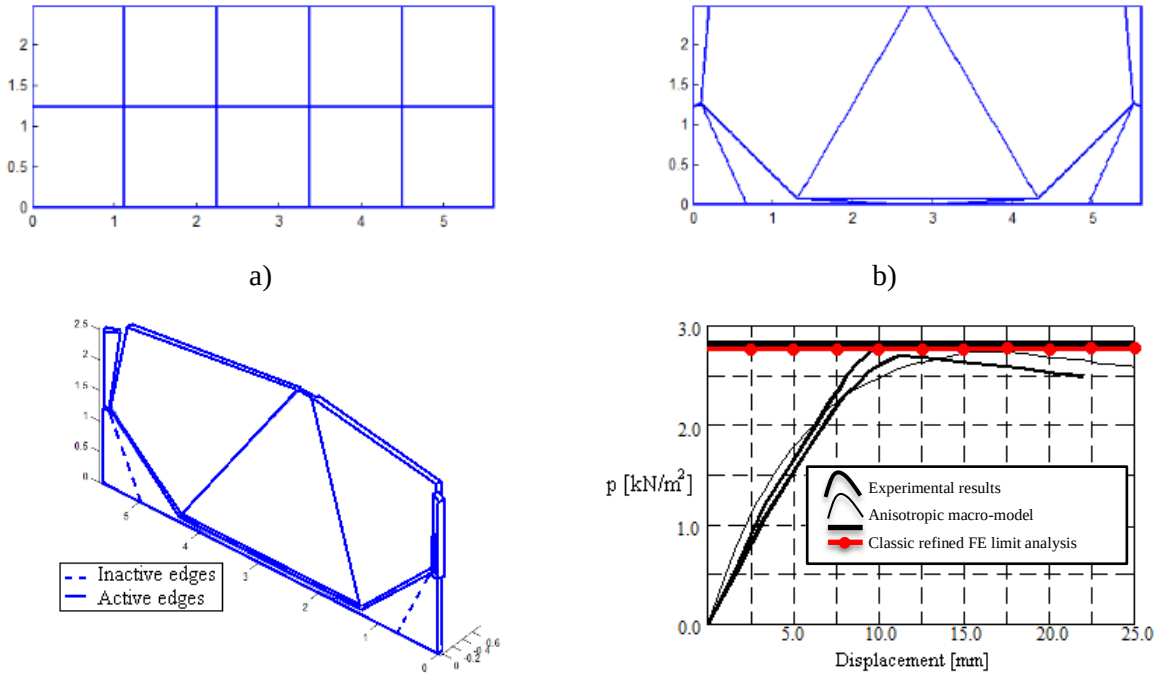

Figure 24. Masonry panel without openings in two way bending: a) initial rough mesh and b*)* final mesh obtained with a Genetic Algorithm optimization approach. c) Failure mechanism with overturning obtained at the optimization procedure. d) Comparison among adaptive limit analysis (red horizontal line), standard refined limit analysis (black horizontal line), and a variety of non-linear force-displacement approaches available in the literature

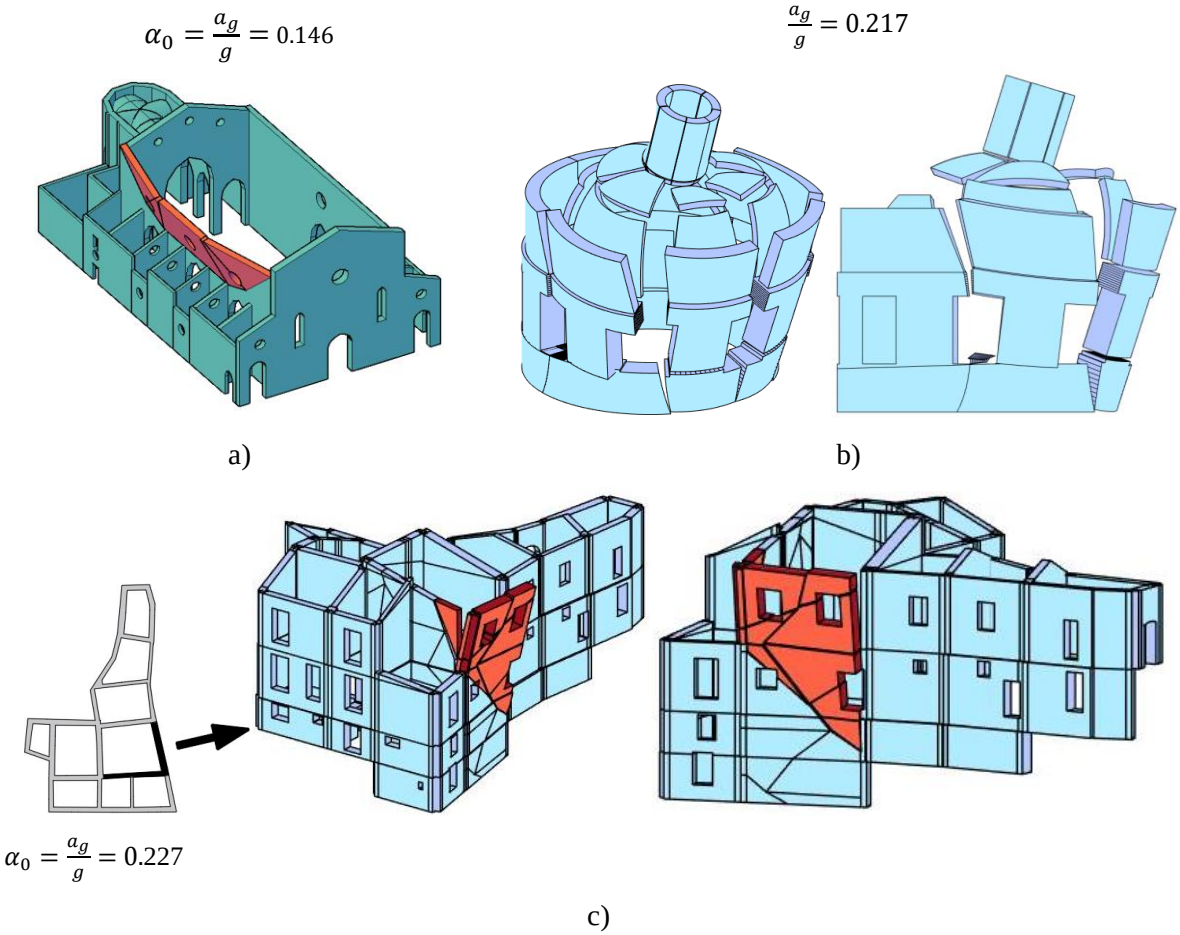

Figure 25. Examples of optimized failure mechanisms found with an adaptive kinematic limit analysis: a) a medium-scale masonry church in Italy; b) a masonry dome subjected to horizontal load up to failure; c) a masonry aggregate with good interlocking between perpendicular walls

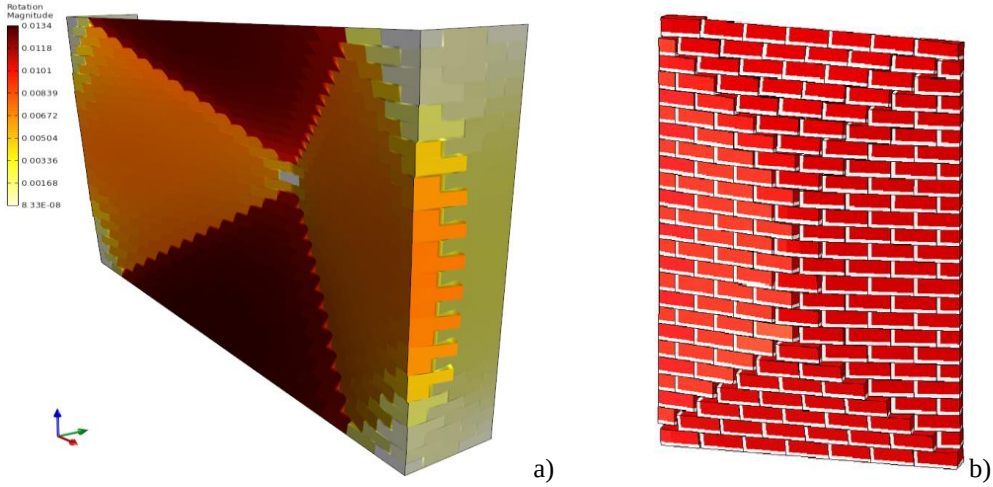

Figure 26 –Numerical modeling of the out-of-plane failure of masonry walls: (a) using layered shell elements with a full 3D constitutive model (Petracca et al. 2017b), (b) using a 3D detailed micro-model (D'Altri et al. 2018).

In the discrete macro-element approach (DMEM), the 2D macro-element allows for the simulation of a masonry wall in its own plane but ignores the out-of-plane response (Caliò et al. 2012). To overcome this significant restriction, a third dimension and the relevant needed additional degrees

of freedom have been introduced in a 3D macro-element (Panto et al. 2016, Pantò et al. 2017; Chácara et al. 2018). Figure 27 reports the 3D macro-element obtained as the extension to the space of the plane element first introduced in (Caliò et al. 2005).

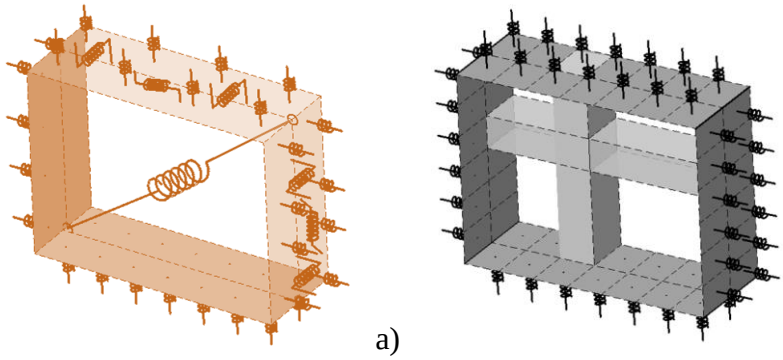

a) b)

Figure 27 - 3D macro-element. (a) simplified mechanical scheme; (b) a typical fiber discretization of the element.

The kinematics of the spatial macro-element is governed by just seven degrees-of-freedom and can describe the in- and out-of-plane rigid body motions of the quadrilateral as well as the in-plane shear deformability. The interaction of the spatial macro-element with the adjacent elements or the external supports is ruled by 3D-interfaces. Each 3D-interface possesses *m* rows of *n* orthogonal (*i.e.*, perpendicular to the planes of the interface) nonlinear links. Consequently, each interface is discretized in *m*×*n* sub-areas (Figure 27b), similarly to what is done in classical fibre models. The 3D interfaces are endowed with additional shear-sliding springs, required to control the in-plane and out-of-plane sliding mechanisms and the torsion around the axis perpendicular to the plane of the interface. The number of Nlinks adopted in the 3D-interfaces is selected according to the desired level of accuracy of the nonlinear response. A detailed description of the spatial macro-element's mechanical calibration and its numerical and experimental validation is reported in (Pantò et al. 2017). This model has been also applied for the simulation of infilled frame structures accounting for the in- and the out-of-plane behaviour of infills (Pantò et al. 2018).

Figure 28 reports a recent numerical and experimental validation of the DMEM with reference to a shaking table test carried out on a U-shaped prototype and discussed in Mendes et al. (2017). In the figure, the gray color map represents the activation of plastic deformations in the nonlinear links orthogonal to the interfaces and the red lines indicate the sliding motions along the in-plane and out-of-plane directions.

Although the DMEM possesses a spatial element able to account for the in-plane and the out-of-plane behaviour of masonry walls, its use in engineering practice still presents some limitations due to the following issues. Unlike the in-plane behaviour, the simulation of the out-of-plane mechanisms requires the use of a mesh of macro-elements that increases the computational burden for large models. The a priori definition of the interfaces does not allow for the accurate reproduction of the crack pattern developed during the formation of an out-of-plane failure

mechanism. Aiming at improving the kinematics of the spatial element in (Minga et al. 2020), a further degree of freedom for simulating the out-of-plane diagonal cracking modes has been introduced to represent, in a phenomenological approach, the respective deformation modes of the inner block.

Figure 29 reports a simulation of the nonlinear behaviour of a masonry church, via push-over analyses obtained with the DMEM.

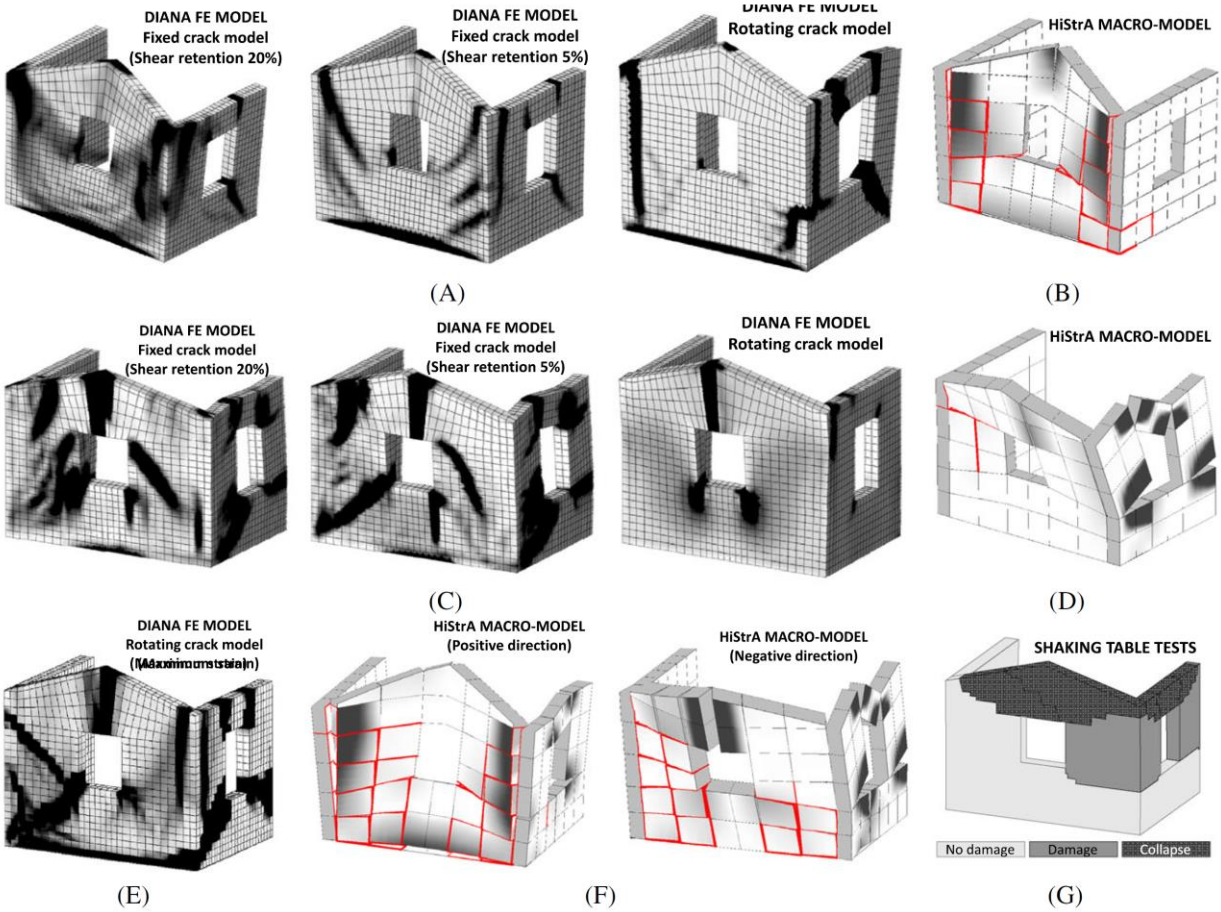

Figure 28 - Compilation of collapse mechanisms of brick masonry prototype: positive (pushing) direction of (A) finite element (FE) models and (B) DMEM macromodel; negative (pulling) direction of (C) FE models and (D) DMEM macromodel; and dynamic response analysis of (E) FE, (F) DMEM macromodels, and (G) experimental campaign (adapted from Chácara et al. 2018).

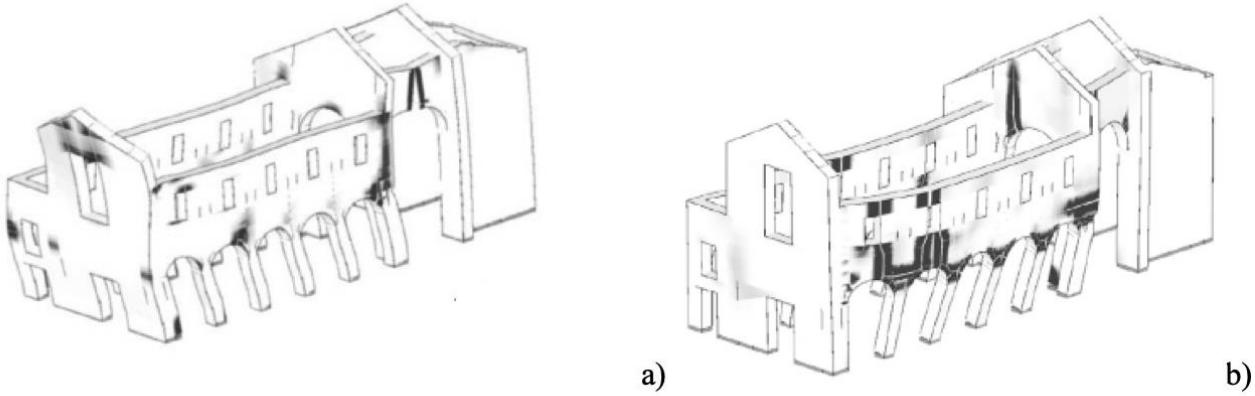

Figure 29 –Failure mechanism and damage distribution obtained with the DMEM for longitudinal (a) and transversal (b) directions of a basilica plan church subjected to mass proportional push-over analyses (adapted from Pantò et al. 2016).

2.6 Critical issues in diaphragm modeling

Diaphragm stiffness and strength, as well as its connections to the masonry walls, have a crucial role in the seismic behavior of masonry structures.

As introduced in Section 1, statistical studies (Del Gaudio et al. 2019, Rosti et al. 2020), based on a large amount of data on the seismic damage caused by the 2009 L'Aquila earthquake, pointed out the importance of the in-plane deformability of floor diaphragms in the seismic response of URM buildings. These research efforts have highlighted the greater seismic vulnerability of buildings (worsened by out-of-plane actions in the absence of retaining steel tie-rods) with vaults and, in general, deformable floors. On the contrary, it is well established that the in-plane stiffness of floor diaphragms positively influences the global dynamic behavior of the structure, ensuring the lateral load redistribution, restraining out-of-plane mechanisms and promoting a box-like behavior. Diaphragms transfer horizontal loads to the vertical elements depending on their in-plane stiffness. The latter should be considered in the model because it affects the distribution of horizontal forces on the vertical elements. Numerical studies, based on nonlinear static and dynamic analyses, have also proved that the seismic assessment is considerably sensitive to the variation of the diaphragm stiffness (Nakamura et al. 2017), with further potential repercussions on the definition of the damage limit states on the pushover curve (Cattari et al. 2015b, Marino et al. 2019). The assumption made on the in-plane stiffness assigned to the floor diaphragms can significantly influence the safety assessment evaluations, also according to the recommendations of Codes. Extremely flexible diaphragms are not able to transfer in-plane shear forces, so that lateral forces acting on each vertical element (wall) mainly depend on the corresponding tributary area. Therefore, the element capacity can be assessed independently and the building could be modeled as a set of independent subsystems.

Figure 30a illustrates the main components of the diaphragms influencing their response: membrane (or horizontal trusses), which carry the in-plane shear; drag strut members that transfer the load to the masonry walls; chords which resist the compression and tensile forces that develop in the diaphragm; and connections between the membrane, the chords, and masonry walls (a review on the typologies that may characterize masonry buildings is presented in Solarino et al. 2019).

Various modeling strategies can be adopted, and the elements should reproduce both the diaphragm capacity and stiffness. Diaphragm stiffness and strength can be modeled with 1D elements, beams, and/or trusses (Figure 30b), or 2D elements, shell or membrane (Figure 30c) combined, if necessary, with beam elements (Figure 30d). If the diaphragm is very stiff, it is reasonable to adopt kinematic constraints to reproduce its effect, thus reducing the number of degrees of freedom of the model (Figure 30f). Even when simplified, a quite effective strategy

often adopted in the case of EF models is to simulate the diaphragm in terms of an equivalent orthotropic membrane (Figure 30e).

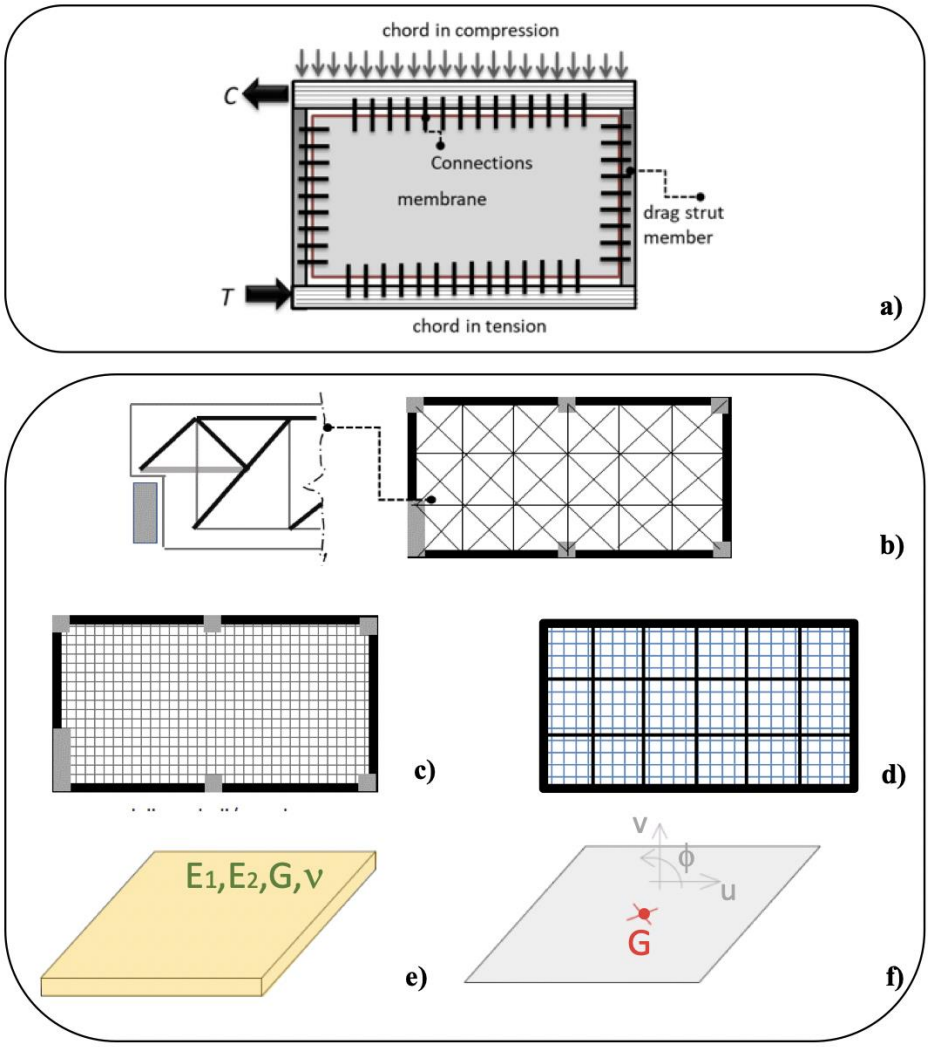

Figure 30 – Diaphragm components a) and possible modeling strategies: b) 1D element model (with springs and struts); c) 2D element model (with shell/membrane elements); d) with combined 2D element models and beams; e) through equivalent orthotropic membranes; f) through a simple kinematic constraint (rigid floor).

According to this strategy, the crucial point becomes the assignment of equivalent elastic moduli that are as reliable as possible. To this end, the support of structural diagnostic investigations becomes very useful. However, even if several in situ tests are available to investigate the material properties (as for example discussed in Krzan et al. (2015)), fewer experimental techniques are available to evaluate the stiffness of floor diaphragms and the attention to this issue is quite recent. For further details, interested readers may refer to: Giongo et al. (2015), Rizzi et al. (2020) and NZSEE 2017, more specifically for timber floors; Rossi et al. (2016, 2017) and Cattari et al. (2008b), more specifically for vaults; Sivori et al. (2021), in general for the use of ambient vibration measurements to address the hypothesis on diaphragm stiffness.

The model of the diaphragm can be linear or nonlinear. When a linear behavior is assumed, an effective reduced stiffness should be considered depending on the expected damage of the diaphragm (*i.e.*, cracking or slip among the elements). Moreover, in a linear hypothesis, the shear capacity of the diaphragm must be checked after the analysis to ensure that it is higher than the corresponding demand. The nonlinear behavior can be modeled with zero-length or fiber elements in the case of 1D models and with continuum nonlinear models for 2D models. The models should be conceived to correctly predict the in-plane stiffness and shear capacity of the membrane as well as the chord and drag strut member capacities.

The connections can be modeled explicitly with 1D elements or springs or, if not modeled, their capacity should be checked against the in-plane shear demand.

Finally, it is worth noting that, while in theory, the problem appears simple to solve, it is actually unrealistic to assume it is always possible to reliably define the stiffness and the resistance capacity of a real floor of an existing building. For this reason, in professional applications, it is sometimes advisable to consider both the limit conditions of a completely flexible floor and, if the case may be, of a completely rigid floor.

3 Challenging issues in the use of URM nonlinear modeling for the seismic assessment based on nonlinear static analyses

3.1 Convergence issues in highly nonlinear analyses and algorithmic aspects

It is well known that the numerical modeling of brittle materials, such as masonry, is often very challenging. The softening nature of masonry leads to highly nonlinear responses with many instabilities, making the rigorous numerical simulation of such responses very difficult, mostly due to convergence problems.

It is mandatory to use methods, such as Displacement-Control or Arc-Length, to overcome the local and global instabilities that can be found during the analysis in order to trace the correct equilibrium path.

At the same time, convergence problems should be mitigated in order to trace the equilibrium path beyond the peak resistance point. Constitutive models are often equipped with algorithms that aim to reduce the strong nonlinearity of the problem to achieve a better convergence. These kinds of algorithms, such as viscoplastic regularization (see the Concrete Damage Plasticity CDP model in ABAQUS) or IMPL-EX Mixed Implicit-Explicit integration (Oliver et al. 2008), are however artificial, and their algorithmic parameters are non-physical, thus hard to calibrate. If not calibrated properly, they can lead to highly different results. It is therefore necessary to adopt procedures where the error is maintained under a reasonable threshold.

Another possible approach, particularly suitable for overcoming convergence difficulties, is the so-called "Sequentially linear analysis" (*e.g.*, Rots 2001), which adopts a simplified saw-tooth stress-strain softening law for masonry. In detail, a series of linear analyses is performed where the elastic modulus of the elements reaching the tensile strength is reduced following the saw-tooth stress-strain law adopted. It is worth noting that the sequentially linear analysis, due to its intrinsic simplicity, can be used in most commercial FE programs even without specific customization capabilities, making it particularly interesting for practitioners. As an example, Figure 31 shows the results obtained with a sequentially linear analysis applied to the Palladio's Tempietto Barbaro, where the elements reaching threshold values in tension are marked in red, indicating potential cracking areas (see Berto et al. 2017).

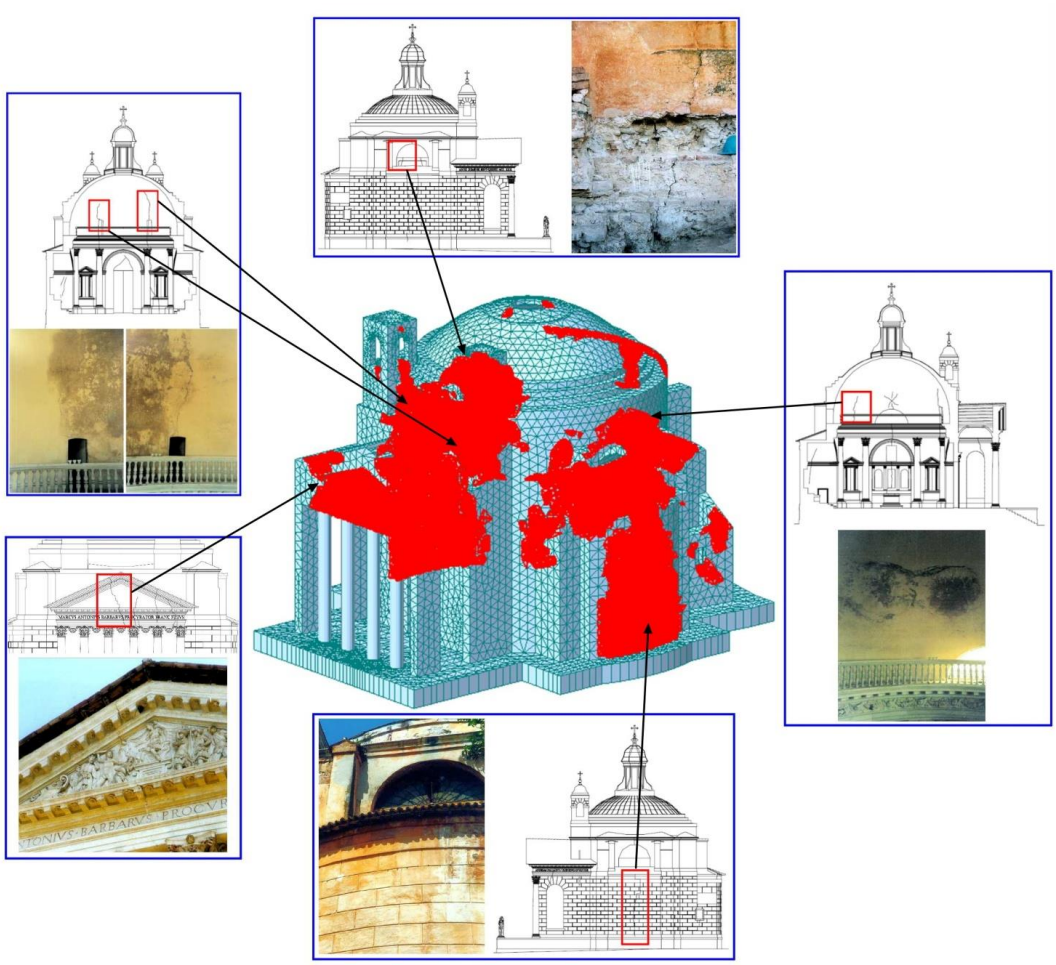

Figure 31 – Palladio's Tempietto Barbaro: results of sequentially linear analysis compared with crack pattern (Berto et al. 2017)

3.2 Horizontal load application in pushover analysis

The application of the horizontal load pattern in pushover analyses represents a conventional aspect that may induce additional sources of differences in results passing from EF to refined models.

https://www.saxion.edu/programmes/exchange-programme/industrial-sustainable-buildingA first issue, indeed common to both modeling approaches, concerns the choice of the load pattern simulating the seismic action through static incremental horizontal forces. Possible options for the distribution to apply are the following (see Aydinoglu and Onem 2010 for an overall overview): (1) proportional to masses (obtained from a uniform displacement shape); (2) obtained from a triangular displacement shape (pseudo-triangular) (3) proportional to the fundamental modal shape (modal); (4) given by a proper combination of different modes (e.g. SRSS-based or as proposed in Reyes and Chopra 2013 or Azizi-Bondarabi et al. 2019, among others); (5) load pattern adapted to the current displacement shape (adaptive, e.g. as originally proposed in Antoniou and Pinho 2004). The first three distributions correspond to the ones most frequently adopted in engineering practice, but depending on the geometric and mass features of the building to analyze, the typologies of diaphragms (if rigid or not), the in plan and in elevation irregularities, etc., the most reliable choice deserves careful attention. A critical discussion on the use of these various possibilities in the case of URM buildings is reported in Lagomarsino and Cattari (2015b). Once a certain load pattern is assumed (*e.g.*, proportional to masses), the horizontal load can be considered lumped at the floor level (lumped actions) or distributed along the entire height of the building (distributed actions). Although this last scheme better represents the inertial forces that can actually arise in the structure, the simplified use of lumped actions at the floor level is generally assumed in EF models.

The distribution of horizontal loads could have a non-negligible impact on the pushover curve and on the peak base shear. Lumped actions are expected to produce a lower peak base shear than distributed actions, as shown in Figure 32, where the pushover curves referred to a benchmark structure, namely the Benchmark Structure BS5 inspired by “P. Capuzi” school in Visso (already discussed in Figure 22, see Castellazzi et al. 2021 for further details), are comparatively represented. The curves have been obtained by using a continuum constitutive law model and a general increase of up to 22% of the maximum load when moving from lumped actions to distributed actions at floor level has been registered. To further confirm this potential effect in Figure 33 the results of the 3D two-story single unit building (Benchmark Structure 4 in the *Nonlinear URM modeling* – Benchmark project), discussed in Cannizzaro et al. 2021, are presented. As it could be expected, the larger the wall thickness, the bigger the differences are in terms of pushover curves between lumped and distributed actions.

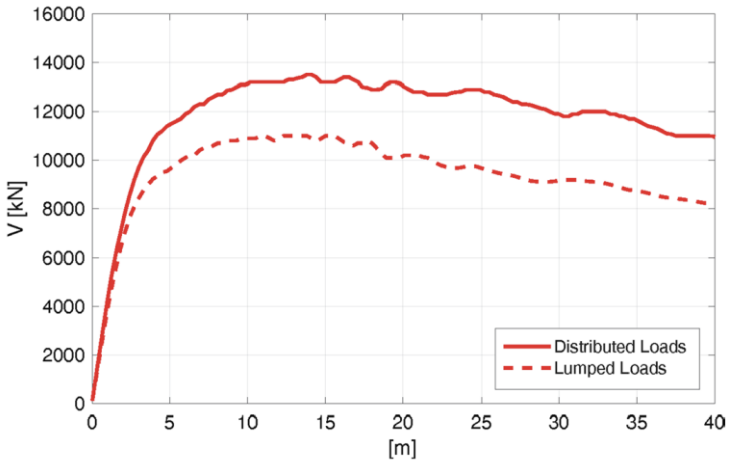

Figure 32 –Influence of the type of horizontal load application (distributed actions versus lumped actions) on the BS5 analyzed in Nonlinear URM modeling – *Benchmark project* reproduced by using a continuum model (from Castellazzi et al. 2021)

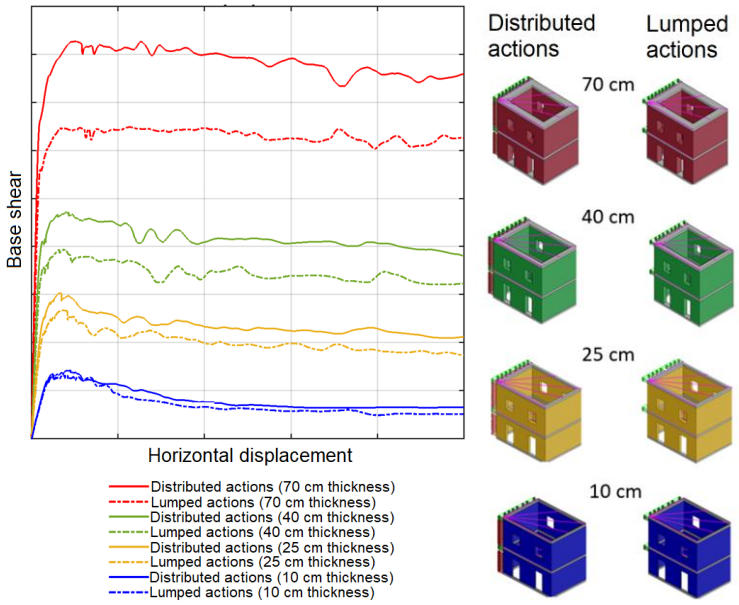

Figure 33 –Influence of the type of horizontal load application (distributed actions versus lumped actions) depending on the thickness of the walls for the BS4 analyzed in *Nonlinear URM modeling* – Benchmark project (adapted from Canizzaro et al. 2021)

3.3 Definition of displacement thresholds in the pushover curve associated to ultimate limit states

Seismic verification, according to the performance-based approach, requires to associate given limit states (LS) to specific performance conditions characterizing the structure under consideration. Usually, LSs do not refer only to the structural damage but also to other performances (such as reusability, immediate occupancy, operational functions, economic issues, etc.). The quantification of the performance requirements usually needs the introduction of conventional criteria to correlate them to proper engineering demand parameters that can be estimated and monitored by the numerical models. To this aim, different criteria are proposed in

the literature and codes. In some cases, the definition of LSs is treated by checking the attainment of corresponding damage levels in each single element (ASCE 41-17 2017) or by considering inter-storey drift thresholds and/or heuristic criteria on the stiffness and strength degradation of the pushover curve (EC8-3 2005, MIT 2019). More specifically, and referring to ultimate limit states, in (MIT 2019), various criteria are integrated with those based on the strength degradation, and for example, consist of defining the attainment of the ultimate drift in all the masonry piers of one level of the building as the ultimate condition or, for very deformable floors, of one level of one masonry wall. Further limitations are put in terms of maximum ductility demand (expressed equivalently through a maximum force reduction ratio) differentiated for Life Safety and for Near Collapse limit state. The logic and benefit of such a multi-criteria approach are also discussed in (Lagomarsino and Cattari 2015a). An in-depth review of these criteria is out of the scope of this paper, and those interested may refer to (Marino et al. 2019). Whatever the rule adopted, the definition of an ultimate condition of the structure (in terms of ultimate displacement) is fundamental, also because in most nonlinear static procedures, like for instance the N2 Method proposed by (Fajfar 2000) and recommended in both (EC8-3 2005) and (MIT 2019), it also affects the derivation of the bilinear equivalent curve that is at the basis of the assessment procedure.

Ideally, the adoption of coherent criteria and rules should be required for all the various modeling strategies discussed in the paper.

Despite that, heuristic criteria based exclusively on the strength degradation rule (*i.e.*, when the base shear decreases at 80% of the maximum base shear) are not always easy to apply in the case of refined models. In fact, while in EF models the collapse condition at element scale is usually automatically implemented in terms of attainment of given drift thresholds and, consequently, the softening phase on the overall pushover curve is detected thanks to the progressive failure of piers, in more refined models such a pronounced softening cannot be reached systematically. This may be the consequence of either convergence issues in a strong nonlinear phase or damaging and failure modes of the structure that are not always associated with a significant softening behavior (*e.g.*, when dominated by the flexural response). Moreover, as already introduced in Section 2.2, it is useful to recall that the above-mentioned checks at element scale are not directly managed by refined models and require some post-processing of the results. As an example, Figure 34 shows two pushover curves obtained for the masonry wall of Figure 5 by (Occhipinti et al. 2021). In such analyses, two different configurations have been considered, namely with or without floor reinforced concrete beams. The case with floor beams shows a significant softening after the diagonal shear failure of the masonry panel at the bottom level. Conversely, the case without floor beams shows the formation of an overturning mechanism of the right part, which is associated with a long plateau in the pushover curve (*i.e.*, no softening behaviour is observed).

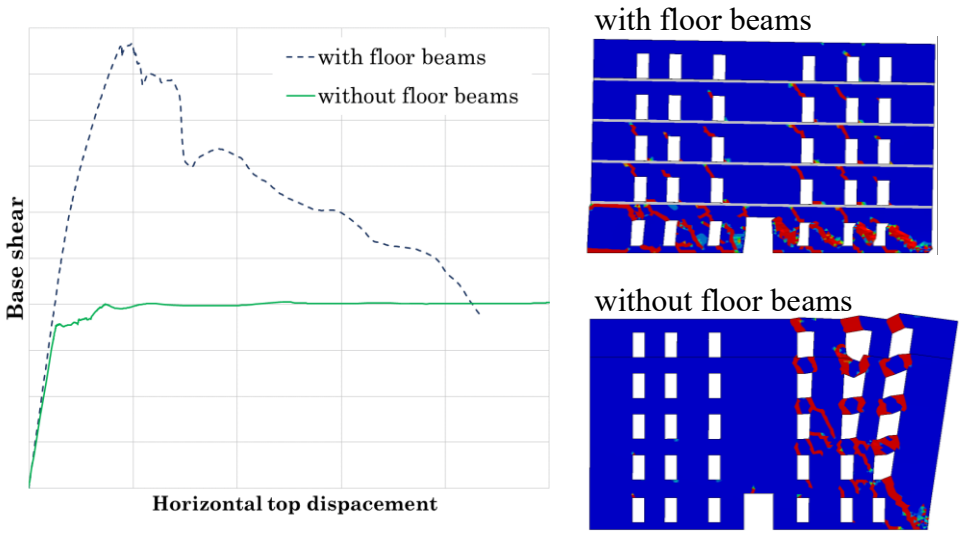

Figure 34 – Example of a masonry structure that shows softening behavior when floor beams are present, while no softening is observed without floor beams (adapted from Occhipinti et al. 2021)

When no significant softening is observed in the pushover curve, the alternative above-mentioned solutions, that refer to performing checks on single elements or sets of elements (e.g., those at the same level) are very effective and useful, see also for instance Figure 32 for model B.

However, as already briefly mentioned in Section 2.2, such an approach implies various steps to be done *ex-post* like identifying the most representative structural elements, interpreting their failure modes, and computing derived parameters on selected sections through integration operations (*e.g.*, computing the drift). Some examples are illustrated in (Castellazzi et al. 2021).

Various uncertainties characterize the conventional ultimate drift and influence the results achievable with EF models. As also discussed in (Cattari and Magenes 2021), the main issue is whether rigid body motion is detracted from the angular deformation demand on the pier. The result is that different variables may be associated with the same general concept of "drift," like the angular deformation, the simple ratio between the difference of horizontal displacements at the end sections and the panel height, the chord rotation, and its equivalence with the plastic component of the rotation. This arbitrariness follows the fact that most codes recommend thresholds for the "drift" of a wall element to check the attainment of the collapse without clarifying the criteria adopted to compute it, and still, there are no unanimous criteria shared in the scientific community. Since these criteria are then autonomously defined by the software packages without allowing users to change them, this may result in a scatter of the ultimate displacement capacity on pushover curves obtained by different software. As shown in Figure 35, this has been highlighted in all the benchmark structures examined in the *URM nonlinear modeling*-Benchmark project, somehow independently from their complexity as documented in (Manzini et al. 2021) for BS4, (Ottonelli et al. 2021) for BS5, and (Degli Abbati et al. 2021) for BS6. More specifically, the variation illustrated in the figure (ΔSRP) refers to the difference between the value computed for

a given software package and a reference value equal to the average estimated from the numerical predictions made by the entire SW set considered. The results demonstrate that this variation systematically decreases only for specific idealized conditions (*e.g.*, in the shear-type idealization, named /D in Figure 35), which makes the rotation component at the end sections of elements irrelevant. Conversely, in structural configurations associated with weak spandrel behavior (named /A in Figure 35) or even with the systematic presence of r.c. beams at floor level (named /C in Figure 35), the dispersion on the ultimate displacement capacity is substantially comparable.

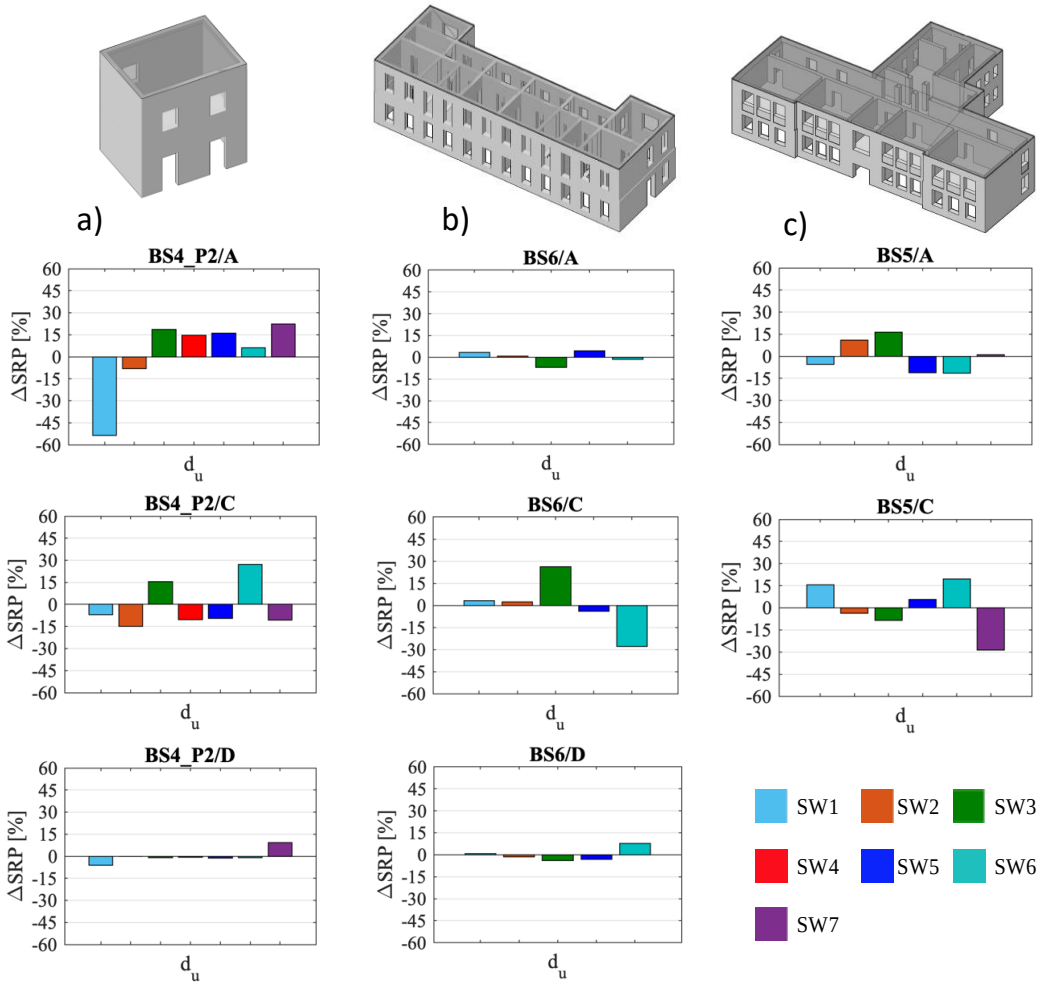

Figure 35 – Variation of the ultimate displacement estimated by various software packages used in the *URM nonlinear modeling*-Benchmark project across various benchmark structures (adapted from Manzini et al. 2021 for BS4, from Ottonelli et al. 2021 for BS5, and Degli Abbati et al. 2021 for BS6)

4 Conclusions

The overview outlined in the paper on the nonlinear seismic modeling of URM structures has revealed the complexity of the topic and has shown the significant scientific advancements obtained in the last years. Considering the first applications of non-linear seismic analysis on masonry buildings dating back to the 1970s (Tomazevic 1978), today the available numerical tools really have the potential to simulate much more accurately the actual seismic response. This allows to overcome the numerous simplifying hypotheses of models used in the past, that in many cases

did not reflect the actual behaviour of existing buildings. Furthermore, significant progress has been made in transferring many of the research advances into commercial software packages, making them available to professionals. However, given the variety of available choices, the analysts, when using the software packages, still need a solid expertise regarding the seismic response of the buildings, and need to be aware of what the available software is able to simulate and how. To provide a contribution in this direction, in this paper the advantages, limitations and open problems related to the use of different modeling techniques of URM buildings in engineering practice have been discussed, with particular regard to the nonlinear static seismic analysis. Possible criteria and methods for the critical comparison of different models/software packages have been suggested, in particular when simplified equivalent frame model results are compared with more refined models, with reference also to code-prescribed performance limit states.

Despite the current significant level of progress of the available nonlinear modeling techniques for masonry structures, the review presented in the paper has pointed out several open issues in which scientific advancements are needed.

Regarding equivalent frame models, the areas of future development are primarily the following:

- The integration of the in-plane response with the out-of-plane one (mainly referring to the activation of local mechanisms) into the same equivalent frame 3D representation of a building.
- The availability of more standardized and sound rules to account for the epistemic uncertainties involved in the modeling process. Among the others, the two most important issues are the following: (1) the idealization of URM walls into equivalent frames, especially in the case of irregular opening layouts (since results may be very sensitive to the alternative options currently available in the literature); (2) the development of sufficiently reliable criteria to account for the wall-to-wall connections and composite sections, accounting, if possible, for different degrees of effectiveness. This would be very useful, particularly for professionals, to reduce the significant scatter of results generated by such epistemic uncertainties and, moreover, to avoid inappropriate choices, potentially leading to strong underestimation/overestimation of the actual capacity of existing buildings.

As regards refined models, the paper has highlighted how they can be very effective also in guiding the calibration of simplified models. In principle, they have the advantage of allowing the modeling of any type of geometry without the approximations implied in simplified models such EF. In theory, virtually every detail of the structure, including connections and interfaces, could be modeled, nonlinearly when needed, with a suitably calibrated constitutive law. However, in

engineering practice, some recommendations and guidelines are necessary and needed since their use requires a very high level of expertise and a proper calibration of the parameters of the models. Nowadays, their use in engineering practice is thinkable only when the resources needed (human and computational) to produce reliable results justify their cost.

Thus, as regards refined models, the outlined areas of future development are primarily:

- To increase their robustness in allowing practitioners to use very sophisticated approaches reducing as much as possible the risk of incurring in large errors due to the lack of knowledge about how all the parameters should be calibrated, allowing thus the professional to focus on the knowledge of the physical object that is studied (the building), which is always and anyway an essential step of the assessment procedure.
- To improve their reliability, addressing efforts towards the following tasks: (1) in calibrating the constitutive model parameters to match code-defined macromechanical properties, an issue which can affect tremendously the results (and the convergence of the solution); (2) in properly describing the orthotropic nature of masonry; (3) in relating damage patterns to code-defined performance limits (these last difficulties in good part are also related to the oversimplification implied in code-prescribed limits).

Regardless of the modeling approach adopted, it has been noted how criteria to guide the nonlinear modeling of floor and roof diaphragms are very scarce both in the literature and in design/assessment guidelines. Moreover, the potential repercussions of improvements in the modeling of diaphragms on performance assessments based on nonlinear static or dynamic analyses are still unclear (*e.g.*, criteria for the definition of limit states).

Some issues more specifically related to nonlinear static modeling of URM structures have also been discussed in the paper, given the increasing use of this method for seismic assessment in everyday engineering practice. Among these, the paper has highlighted the issues related to the representation of the seismic action in distributed mass systems (the effect of lumping the seismic forces vs. using distributed load patterns) and to the definition of displacement/deformation based criteria and thresholds for a performance based assessment depending on the type of model that is being used (simplified or refined).

Finally, some issues have not been covered by the review presented in the paper, and could be the subject of future reviews. Among these are some complex issues typical of the execution of nonlinear time history analyses. Just to mention a few of them: the simulation of the cyclic response, which would give rise to additional issues such as the computational efficiency; the capability of reproducing energy dissipation associated to different failure modes; and, last but not least, the proper interpretation of the large and complex amount of data obtained from the analyses.

Surely, EF models have a great potential if extended to cyclic modeling, taking advantage of the

reduced computational effort needed, with respect to refined nonlinear models. Some examples already exist in the literature, but they need to be further consolidated and developed before they can be accessible to professionals in commercial software packages.

Acknowledgements

The study presented in the paper was developed within the research activities carried out in the frame of the 2014-2018 ReLUIS Project (Topic: Masonry Structures; Coord. Proff. Sergio Lagomarsino, Guido Magenes, Claudio Modena, Francesca da Porto) and of the 2019-2021 ReLUIS Project - WP10 "Code contributions relating to existing masonry structures" (Coord. Guido Magenes). The projects are funded by the Italian Department of Civil Protection.

Moreover, the Authors acknowledge the whole group of research teams (RT) that participated to this research activity: UniGE RT (University of Genova; Coord. Prof. Serena Cattari; Participants: Stefania Degli Abbati, Daria Ottonelli); UniPV RT (University of Pavia: Coord. Guido Magenes, Participants: Carlo Manzini, Paolo Morandi); UniCH RT (University of Chieti-Pescara; Coord. Prof. Guido Camata, Participants: Corrado Marano); UniCT RT (University of Catania–Coord. Prof. Ivo Caliò; Participants: Francesco Canizzaro, Giuseppe Occhipinti, Bartolomeo Pantò); UniNA RT (University Federico II of Naples– Coord. Prof. Bruno Calderoni; Participants: Emilia Angela Cordasco, Gaetana Pacella); UniBO RT (University of Bologna- Coord. Prof. Stefano de Miranda – Participants: Giovanni Castellazzi, Antonio Maria D'Altri); POLIMI RT (Polytechnic of Milan- Coord. Prof. Gabriele Milani; Participant: Nicola Grillanda); IUAV RT (University Iuav of Venice - Coord. Prof. Anna Saetta; Participants: Luisa Berto, Diego Alejandro Talledo).

Funding

The research activity "URM nonlinear modeling - Benchmark project", whose methodology and benchmark structures proposed, are presented in this paper, did not receive any grant from funding agencies in the public, commercial or not-for-profit sectors that may gain or lose financially through publication of this work.

Conflicts of interest/Competing interests

The authors declare that they have no known competing financial interests or personal relationships that could have appeared to influence the work reported in this paper.

Availability of data and material

The benchmark structures mentioned in the paper can be replicated by other interested researchers and analysts thanks to the input data provided in Cattari and Magenes (2021) as supplementary electronic material (Annex I-*Benchmark Structures Input Data*). The results on these benchmark structures are discussed in other scientific papers of the Special Issue "*URM nonlinear modeling* - Benchmark project" published on *Bulletin of Earthquake Engineering*.

Authors' contributions

SC: conceptualization, methodology, original basis of scientific results presented in the examples discussed in the paper, writing-original draft; BC/IC/GC/SDM/GM/GM/AS: conceptualization, methodology, original basis of scientific results presented in the examples discussed in the paper, writing-review.

References

ABAQUS®, theory manual, version 6.14.

Abrams D.P., AlShawa O., Lourenço P.B., Sorrentino L (2017) Out-of-plane seismic response of unreinforced masonry walls: conceptual discussion, research needs and modelling issues, *International Journal of Architectural Heritage*, 11(1),22-30

Allemange RJ, Brown DL (1982) A correlation coefficient for modal vector analysis, Proceedings 1st international modal analysis conference, November 8–10 1982, Orlando, Florida, 110-116.

Andreotti G, Graziotti F, Magenes G (2019) Expansion of mortar joints in direct shear tests of masonry samples: implications on shear strength and experimental characterization of dilatancy. Mater Struct, 52, 64.

Angiolilli M, Lagomarsino S, Cattari S, Degli Abbati S (2021) Seismic fragility assessment of existing masonry buildings in aggregate, Engineering Structures, under review (second round).

Antoniou S, Pinho R (2004) Development and verification of a displacement-based adaptive pushover procedure. *J Earthq Eng* 8(5), 643–661

Aydinoglu MN, Onem G (2010) Evaluation of analysis procedures for seismic assessment and retrofit design. *In Garevsky M, Ansal A (eds) Earthquake engineering in Europe*. Springer, Dordrecht, Netherlands,171–198.

ASCE 41-17 (2017) Seismic Evaluation and Retrofit of Existing Buildings. American Society of Civil Engineers.

Atkinson RH, Amadei BP, Saeb S, Sture S (1989) Response of masonry bed joints in direct shear. *J Struct Eng ASCE,* 115(9), 2276–2296.

Augenti N (2006) Seismic behavior of irregular masonry walls. *Proc.of the 1st European Conference on Earthquake Engineering and Seismology*, Geneva, Switzerland.

Augenti N, Parisi F (2010) Learning from Construction Failures due to the 2009 L'Aquila, Italy, Earthquake, *Journal of Performance of Constructed Facilities*, 24(6), 536–555.

Augenti, N., Parisi, F., Acconcia, E. (2012) MADA: online experimental database for mechanical modelling of existing masonry assemblages *Proc. of the 15th World Conference on Earthquake Engineering*, Lisbon.

Azizi-Bondarabadi H, Mendes N, Lourenco, PB (2019) Higher mode effects in pushover analysis of irregular masonry buildings. *Journal of Earthquake Engineering*, 25(8), 1459-1493.

Belmouden Y, Lestuzzi P (2009) An equivalent frame model for seismic analysis of masonry and reinforced concrete buildings. *Construction and Building Materials*, 23, pp: 40–53.

Belytschko T, Loehnert S, Song JH (2008) Multiscale aggregating discontinuities: a method for circumventing loss of materialstability. Int J Numer Methods Eng 73(6):869–894

Berke PZ, Peerlings RHJ, Massart TJ, Geers MGD. A homogenization-based quasi-discrete method for the fracture of heterogeneous materials. Comput Mech 2014;53(5):909–23.

Berti M, Salvatori L, Orlando M, Spinelli P (2017) Unreinforced masonry walls with irregular opening layouts: reliability of equivalent-frame modelling for seismic vulnerability assessment, *Bulletin of Earthquake Engineering*, 15(3), 1213-1239.

Berto L, Saetta A, Scotta R, Vitaliani R (2002)An orthotropic damage model for masonry structures, *International Journal for Numerical Method in Engineering*, 55 (22),127-157.

Berto L, Saetta A, Scotta R, Vitaliani R (2004) Shear behaviour of masonry panel: parametric F.E. analyses, *International Journal of Solids and Structures*, 41/16-17, 4383-4405

Berto L, Doria A, Faccio P, Saetta A, Talledo D (2017) Vulnerability Analysis of Built Cultural Heritage: A Multidisciplinary Approach for Studying the Palladio's Tempietto Barbaro, *International Journal of Architectural Heritage*, 11(6), 773-790

Bertolesi E, Milani G, Lourenço PB (2016) Implementation and validation of a total displacement non-linear homogenization approach for in-plane loaded masonry. *Computers & Structures*,176,13-33.

Bertolesi E, Milani .G, Casolo S (2018). Homogenization towards a mechanistic Rigid Body and Spring Model (HRBSM) for the non-linear dynamic analysis of 3D masonry structures. *Meccanica*; 53,1819–1855.

Bertolesi E, Silva LC, Milani G (2019)Validation of a two-step simplified compatible homogenization approach extended to out-plane loaded masonries, *International Journal of Masonry Research and Innovation*, 4(3),265-296.

Beyer K (2012) Peak and residual strengths of brick masonry spandrels, *Engineering Structures*,41, 533-547.

Beyer K, Dazio A (2012) Quasi-static cyclic tests on masonry spandrels, *Earthquake Spectra*,28(3), 907-929.

Beyer K, Mangalathu S (2013)Review of strength models for masonry spandrels,*Bull Earth Eng*,11,521–542.

Borri A, Corradi M, Castori G, De Maria A (2015) A method for the analysis and classification of historic masonry, *Bulletin of Earthquake Engineering*, 13(9),2647-2665.

Boschi S, Bernardini C, Vignoli A (2021) The Tuscany masonry database website, *Heritage* 4(1), 230-248.

Bosco E, Kouznetsova V, Geers M (2015) Multi-scale computational homogenization-localization for propagating discontinuities using x-fem. Int J Numer Methods Eng 102(3–4):496–527

Bothara JK, Dhakal RP, Mander JB (2010) Seismic performance of an unreinforced masonry building: an experimental investigation. *Earthq Eng Struct Dyn*, 39,45–68

Bracchi S, Rota M, Penna A, Magenes G (2015) Consideration of modelling uncertainties in the seismic assessment of masonry buildings by equivalent-frame approach, *Bullettin of Earthquake Engineering*, 13(11), 3423-3448.

Bracchi S, Galasco A, Penna A (2021) A novel macroelement model for the nonlinear analysis of masonry buildings.Part 1: Axial and flexural behaviour, *Earthquake Engineering and Structural Dynamics*, 50(8), 2233-2252.

Bracchi S, Penna A (2021) A novel macroelement model for the nonlinear analysis of masonry buildings.Part 2: Shear behavior, *Earthquake Engineering and Structural Dynamics*, 50(8), 2212-2232.

Brignola A, Frumento S, Lagomarsino S, Podestà S (2008) Identification of shear parameters of masonry panels through the in-situ diagonal compression test, *International Journal of Architectural Heritage*, 3(1),52-73.

Calderini C, Cattari S, Lagomarsino S (2009) In-plane strength of unreinforced masonry piers, *Earthquake Engineering and Structural Dynamics*, 38, 243-267

Calderoni B, Cordasco EA, Lenza P, Pacella G. (2011) A simplified theoretical model for the evaluation of structural behavior of masonry spandrels, *International Journal of Material and Structural Integrity*, 5,192–214.

Calderoni B, Cordasco EA, Pacella G, Onotri V (2016) Critical issues in the assessment of seismic vulnerability of historical masonry buildings: a study case. *Proc. of 16th International Brick and Block Masonry Conference*, Padua, Italy, 26-30 June 2016.

Calderoni B, Cordasco EA, Musella C, Sandoli A (2017) La modellazione delle pareti murarie in relazione alle irregolarità geometriche: problemi aperti. *Proc. of XVII ANIDIS Conference*, 17-21 September, Pistoia, Italy (in Italian).

Calderoni B, Cordasco EA, Pacella G, Simoniello P (2019a) The spandrel of masonry buildings: Experimental tests and numerical analysis. *International Journal of Masonry Research and Innovation*; 4(1/2):123–149.

Calderoni B, Cordasco EA, Pacella G, Sandoli A, Musella C, Festosi A (2019b) L'influenza del grado di connessione tra le pareti ortogonali sul comportamento sismico degli edifici in muratura. *Proc. of XVIII ANIDIS Conference,* Ascoli Piceno, Italy, 15-19 September 2019 (In Italian).

Caliò I and Pantò B (2014) A macro-element modelling approach of infilled frame structures', *Computers & Structures*, 143,91–107.

Caliò I, Marletta M, Pantò B (2005) A simplified model for the evaluation of the seismic behaviour of masonry buildings, in *Proc. of the Tenth International Conference on Civil, Structural and Environmental Engineering Computing*, ed. B. H. V. Topping (Stirlingshire: Civil-Comp Press), 195.

Calio I, Marletta M, Panto B, (2012) A new discrete element model for the evaluation of the seismic behaviour of unreinforced masonry buildings *Engineering Structures*,40, 327-338.

Calvi GM, Magenes G (1994) Experimental research on response of URM building system. Proceedings of U.S.-Italy workshop on guidelines for seismic evaluation and rehabilitation of unreinforced masonry buildings, D. P. Abrams, G. M. Calvi eds, State University of New York at Buffalo, NCEER-94-0021, 3-41/57, Pavia.

Cámara M, Romero M, Pachón P, Compán V, Lourenço PB (2021) Integration of disciplines in the structural analysis of historical constructions. The Monastery of San Jerónimo de Buenavista (Seville-Spain). Engineering Structures, 230, DOI: 10.1016/j.engstruct.2020.111663.

Camilletti D, Cattari S, Lagomarsino S (2018) In plane seismic response of irregular URM walls through equivalent frame and finite element models, *Proc. of 16th European Conference on Earthquake Engineering*, Thessaloniki, 18-21 June 2018.

Camilletti D (2019) Equivalent Frame modelling of URM buildings: numerical validation and rules, PhD Thesis, PhD Program in Civil, Chemical and Environmental Engineering, Curriculum in Structura and Geotechnical Engineering, Mechanics and Materials, Genoa, May 2019.

Cannizzaro F and Lourenço P B (2017) Simulation of Shake Table Tests on Out-of-Plane Masonry Buildings. Part (VI): Discrete Element Approach, *International Journal of Architectural Heritage*, 11 (1), 125-142.

Cardani G , Binda L (2015) Guidelines for the evaluation of the load-bearing masonry quality in built heritage, *Rearch for Development*, 127-139.

Casapulla C, Argiento LU. (2016) The comparative role of friction in local out-of-plane mechanisms of masonry buildings. Pushover analysis and experimental investigation. Eng Struct. 126,158-173.

Casapulla C, Giresini L, Lourenço PB. (2017) Rocking and kinematic approaches for rigid block analysis of masonry walls: state of the art and recent developments. Buildings, 69.

Casapulla C, Argiento L U, Maione A, Speranza E (2021) Upgraded formulations for the onset of local mechanisms in multi-storey masonry buildings using limit analysis, Structures, 31, 380 – 394.

Castellazzi G, Pantò B, Occhipinti G, Talledo D, Berto L, Camata G (2021) A comparative study on a complex URM building. Part II: issues on modelling and seismic analysis through continuum and discrete-macroelement models, Submitted to Bulletin of Earthquake Engineering, 10.1007/s10518-021-01183-0

Cattari S, Lagomarsino S (2008a) A strength criterion for the flexural behavior of spandrel in un-reinforced masonry walls. *Proc. of the 15th World Conference on Earthquake Engineering*, Beijing, China.

Cattari S, Resemini S and Lagomarsino S (2008b) Modelling of vaults as equivalent diaphragms in 3D seismic analysis of masonry buildings, in Structural Analysis of Historic Construction: Preserving Safety and Significance, Two Volume Set, 537-544, CRC Press.

Cattari S. and Lagomarsino S. (2013) Masonry structures, 151–200. in T. Sullivan and G. M. Calvi (ed.) Developments in the Field of Displacement Based Seismic Assessment. IUSS Press and EUCENTRE, Pavia, Italy, p 524, ISBN, 978-88-6198-090-7.

Cattari S, Beyer K (2015) Influence of spandrel modelling on the seismic assessment of existing masonry buildings. Proceedings of the 10th Pacific Conference on Earthquake. Engineering Building an Earthquake-Resilient Pacific, 6-8 November, Sydney, Australia

Cattari S, Lagomarsino S, Bosiljkov V, D'Ayala D (2015a) Sensitivity analysis for setting up the investigation protocol and defining proper confidence factors for masonry buildings, *Bull Earthquake Eng*, 13 (1), 129–151.

Cattari S, Lagomarsino S, Karatzetzou A, Pitilakis D (2015b) Vulnerability assessment of Hassan Bey's mansion in Rhodes, *Bulletin of Earthquake Engineering*, 13(1),347-368.

Cattari S, Camilletti D, Lagomarsino S, Bracchi S, Rota M, Penna A (2018) Masonry Italian Code-conforming Buildings. Part 2: Nonlinear Modelling and Time-History Analysis, *Journal of Earthquake Engineering*, 22(sup2), 2010-2040.

Cattari S, Degli Abbati S, Ottonelli D, Marano C, Camata G et al. (2019) Discussion on data recorded by the Italian structural seismic monitoring network on three masonry structures hit by the 2016-2017 Central Italy earthquake. *Proc. of COMPDYN conference*, 24-26 June 2019, Crete, Greece.

Cattari S, Magenes G (2021) Benchmarking the software packages to model and assess the seismic response of unreinforced masonry existing buildings through nonlinear static analyses, *Bulletin of Earthquake Engineering*, 10.1007/s10518-021-01078-0.

Cattari S, Camilletti D, D'Altri A M, Lagomarsino S (2021a) On the use of Continuum Finite Element and Equivalent Frame models for the seismic assessment of masonry walls, *Journal of Building Engineering*, 43,102519.

Cattari S, Degli Abbati S, Alfano S, Brunelli A, Lorenzoni F, Da Porto F (2021b) Dynamic calibration and seismic validation of numerical models of URM buildings through permanent monitoring data, *Earthquake Engineering and Structural Dynamics*, 50(10), 2690-2711.

Cavalagli N, Cluni F, Gusella V (2013) Evaluation of a statistically equivalent periodic unit cell for a quasi-periodic masonry. Int J Solids Struct 50(25–26):4226–4240

CEN (2005) Eurocode 8: Design of structures for earthquake resistance – Part 3: Assessment and retrofitting of buildings. EN1998 – 3, Comité Européen de Normalisation, Brussels.

CEN (2004) Eurocode 6: Design of masonry structures, Part 1: General rules for reinforced and unreinforced masonry structures. EN 1996-1-1, Comité Européen de Normalisation, Brussels.

Chácara C, Cannizzaro F, Pantò B, Caliò I, Lourenço PB (2018) Assessment of the dynamic response of unreinforced masonry structures using a macro-element modelling approach, *Earthquake Engineering & Structural Dynamics*, vol. 47(12), 2426-2446.

Chen SY, Moon FL, Yi T (2008) A macroelement for the nonlinear analysis of in-plane unreinforced masonry piers, *Engineering Structures*, 44, 3625–41.

Chiozzi A, Grillanda N, Milani G, Tralli A (2018) UB-ALMANAC: an adaptive limit analysis NURBS-based program for the automatic assessment of partial failure mechanisms in masonry churches, *Engineering Failure Analysis*, 85,201-220.

Chiozzi A, Milani G, Grillanda N, Tralli A (2018b) A fast and general upper-bound limit analysis approach for out-of-plane loaded masonry walls. *Meccanica*; 53, 1875–1898.

Chiozzi A, Milani G, Tralli A (2017) A Genetic Algorithm NURBS-based new approach for fast kinematic limit analysis of masonry vaults, *Computers & Structures*,182,187–204.

CNR-DT 212/2013 (2014) Guide for the Probabilistic Assessment of the Seismic Safety of Existing Buildings, National research council of Italy, Rome, Italy, 2014.

Costley AC, Abrams DP (1996) Dynamic response of unreinforced masonry buildings with flexible diaphragms. *NCEER-96-0001*, University of Buffalo, Buffalo, N.Y., USA.

D'Altri AM, de Miranda S, Castellazzi G, Sarhosis V (2018) A 3D detailed micro-model for the in-plane and out-of-plane numerical analysis of masonry panels, *Computers & Structures*, 206,18-30.

D'Altri AM, Messali F, Rots J, Castellazzi G, de Miranda S (2019) A damaging block-based model for the analysis of the cyclic behaviour of full-scale masonry structures, *Engineering Fracture Mechanics*, 209,423-448.

D'Altri AM, Sarhosis V, Milani G, Rots J, Cattari S, Lagomarsino S, Sacco E, Tralli A, Castellazzi G, de Miranda S (2020a) Modeling strategies for the computational analysis of unreinforced masonry structures: review and classification, *Archives of Computational Methods in Engineering*, 27,1153-1185.

D'Altri AM, de Miranda S, Milani G, Castellazzi G.(2020b) A numerical procedure for the force-displacement description of out-of-plane collapse mechanisms in masonry structures, *Computers & Structures*, 233, 106-234.

D'Altri AM, Cannizzaro F, Petracca M, Talledo D (2021) Nonlinear modelling of the seismic response of masonry structures: Calibration strategies, Submitted to *Bulletin of Earthquake Engineering*, 10.1007/s10518-021-01104-1.

D'Ayala D, Speranza E (2003) Definition of collapse mechanisms and seismic vulnerability of historic masonry buildings, Earthquake Spectra, 19(3), 479-509.

D'Ayala D.F., Paganoni S. (2011) Assessment and analysis of damage in L'Aquila historic city centre after 6th April 2009, *Bulletin of Earthquake Engineering*, 9(1), 81–104.

De Felice G (2011) Out-of-plane seismic capacity of masonry depending on wall section morphology, *International Journal of Architectural Heritage*, 5 (4-5),466-482.

De Bellis ML, Addessi D (2011) A cosserat based multiscale model for masonry structures. Int J Multiscale Comput Eng9(5):543–563

Degli Abbati S, Cattari S, Lagomarsino S (2021) Validation of displacement-based procedures for rocking assessment of cantilever masonry elements, *Structures*, 33,3397-3416.

Del Gaudio C, De Martino G, Di Ludovico M, Manfredi G, Prota A, Ricci P, Verderame G M (2019) Empirical fragility curves for masonry buildings after the 2009 L'Aquila, Italy, earthquake, *Bulletin of Earthquake Engineering*, 17(11), 6301- 6330.

Dolatshahi K.M., Nikoukalam M.T., Beyer K. (2018) Numerical study on factors that influence the in-plane drift capacity of unreinforced masonry walls, *Earthquake Engineering and Structural Dynamics*, 47(6), 1440–1459

Dolce M (1991) Schematizzazione e modellazione degli edifici in muratura soggetti ad azioni sismiche, L'industria delle costruzioni, 25 (242), pp. 44-57 (in Italian).

Dolce M, Nicoletti M, De Sortis A, Marchesini S, Spina D, Talanas F. (2017) Osservatorio sismico delle strutture: the Italian structural seismic monitoring network, *Bull Earthquake Eng*, 15(2), 621-641.

Dolce M, Speranza E, Giordano F, Borzi B, Bocchi F, Conte C, Pascale V (2019) Observed damage database of past Italian earthquakes: the Da.D.O WebGIS, *Bollettino di Geofisica Teorica ed Applicata*, 60(2), https://doi.org/10.4430/bgta0254

Fajfar P (2000) A nonlinear analysis method for performance-based seismic design. *Earthq Spectra*, 16(3), 573–92.

Giresini L, Fragiacomo M, Lourenço PB. (2015) Comparison between rocking analysis and kinematic analysis for the dynamic out-of-plane behavior of masonry walls. Earthq Eng Struct Dyn. 44,2359-2376.

Giongo I, Dizhur D, Tomasi R, Ingham J. M. (2015) Field testing of flexible timber diaphragms in an existing vintage URM building, *Journal of Structural Engineering*, 141(1),D4014009.

Grande E, Imbimbo M, Sacco E (2011) A beam finite element for nonlinear analysis of masonry elements with or without fiber-reinforced plastic (FRP) reinforcements, *International Journal of Architectural Heritage*, 5, 693–716.

Graziotti F, Magenes G, Penna A. (2012) Experimental cyclic behaviour of stone masonry spandrels. *Proc. of the 15th World Conference on Earthquake Engineering*. Lisboa. PT.

Griffith M C ,Vaculik J, Lam N T K, Wilson J, Lumantarna E (2007) Cyclic testing of unreinforced masonry walls in two-way bending, *Earthquake Engineering and Structural Dynamics*, 36, 801-821.

Grillanda N, Chiozzi A, Milani G, Tralli A (2019) Collapse behavior of masonry domes under seismic loads: An adaptive NURBS kinematic limit analysis approach, *Engineering Structures*, 200: 109517.

Grillanda N, Chiozzi A, Milani G, Tralli A (2020b) Efficient meta-heuristic mesh adaptation strategies for NURBS upper–bound limit analysis of curved three-dimensional masonry structures. *Computers & Structures*, 236:106271.

Grillanda N, Valente M, Milani G (2020a) ANUB-Aggregates: a fully automatic NURBS-based software for advanced local failure analyses of historical masonry aggregates, *Bulletin of Earthquake Engineering*, 18, 3935–3961.

Hassan M, Ei-Tawil S (2003) Tension Flange Effective Width in Reinforced Concrete Shear Walls, *ACI Structural Journal*, 100 (3), 349-356.

Khanmohammadi M, Benham H, Marefat MS (2014) Seismic behavior prediction of flanged Unreinforced Maosnry (FURM) walls, *Journal of Earthquake Engineering*, 18,759-784.

Krzan M, Gostic S, Cattari S, Bosiljkov V (2017) Acquiring reference parameters of masonry for the structural performance analysis of historical building, *Bull. Earth. Eng*, 13(1), 203-236.

Kouznetsova V, Geers M, Brekelmans W (2004) Multi-scale second-order computational homogenization of multi-phase materials: a nested finite element solution strategy. Comput Methods Appl Mech Eng 193:5525–5550 advances in computational plasticity

Lagomarsino S (2015) Seismic assessment of rocking masonry structures. Bull Earthq Eng, 13, 97-128.

Lagomarsino S, Abbas N, Calderini C, Cattari S, Rossi M. Ginanni Corradini R, Marghella G, Mattolin F, Piovanello V (2011) Classification of cultural heritage assets and seismic damage variables for the identification of performance levels. *Proc. of 12th STREMAH conference*, 5-7 September 2011, Chianciano Terme (Italy), WIT Trans Built Environ, Vol 118: 697-708, doi:10.2495/STR110581

Lagomarsino S, Penna A, Galasco A, Cattari S. (2013) TREMURI program: an equivalent frame model for the nonlinear seismic analysis of masonry buildings. *Engineering Structures*, 56,1787-1799.

Lagomarsino S, Cattari S (2015a) PERPETUATE guidelines for seismic performance-based assessment of cultural heritage masonry structures, *Bulletin of Earthquake Engineering*, 13(1), 13-47.

Lagomarsino S, Cattari S (2015b) Seismic performance of historical masonry structures through pushover and nonlinear dynamic analyses. Perspectives on European earthquake engineering and seismology Springer International Publishing, 265–292, https://doi.org/10.1007/978-3-319-16964-4_11.

Lagomarsino S, Cattari S, Ottonelli D (2021) The Heuristic vulnerability model: fragility curves for masonry buildings, *Bulletin of Earthquake Engineering*, 19(8),3129-3163.

Lee J and Fenves GL (1998) Plastic-Damage Model for Cyclic Loading of Concrete Structures, *Journal of Engineering Mechanics*, 124(8), 892–900.

Lorenzoni F, Salvalaggio M, Valluzzi MR, Boaga J, Deiana R (2020) A multidisciplinary approach for the assessment of the dynamic and seismic behaviour of archaeological structures in hierapolis of Phrygia, Turkey, *Proc. of the 11th EURODYN Conference*, 2, 4340-4348.

Lourenço, PB (1997) Computational strategies for masonry structures. PhD thesis, TU Delft.

Lourenço, PB (2002) Computations on historic masonry structures, Progress in Structural Engineering and Mat., 4(3), 301-319.

Magenes G, Calvi GM, Kingsley GR (1995) Seismic Testing of a Full-Scale, Two-Story Masonry Building: Test Procedure and Measured Experimental Response, in *Experimental and Numerical Investigation on a brick Masonry Building Prototype - Numerical Prediction of the Experiment*, Report 3.0 - G.N.D.T., January 1995

Magenes G, Calvi GM (1997) In plane seismic response of brick masonry walls, *Earthquake Engineering and Structural Dynamics*,26,1091-1112.

Magenes G, Della Fontana A (1998) Simplified non-linear seismic analysis of masonry buildings. *Proc British Masonry Soc* 1998:1, 190-195.

Magenes G, Bolognini D, Braggio C (2000) Metodi semplificati per l'analisi sismica non lineare di edifici in muratura, CNR-Gruppo Nazionale per la Difesa dai Terremoti, Roma, 2000, 99 pp. ISBN 88-88151-03-6 (in Italian), https://emidius.mi.ingv.it/GNDT2/Pubblicazioni/Magenes_copertina_con_intestazione.htm

Manzini C, Ottonelli D, Degli Abbati S, Marano C, Cordasco EA (2021) Modelling the seismic response of a 2-storey URM benchmark case study. Comparison among different equivalent frame models, *Bull Earthquake Eng*, https://doi.org/10.1007/s10518-021-01173-2.

Marino S, Cattari S, Lagomarsino S. (2019) Are the nonlinear static procedures feasible for the seismic assessment of irregular existing masonry buildings?, *Engineering Structures*, 200, 109700.

Massart TJ, Peerlings RHJ, Geers MGD (2007) An enhanced multi-scale approach for masonry wall computations with localization of damage. Int J Numer Methods Eng 69(5):1022–1059

McKenna F, Fenves G L, Scott, MH, and Jeremic B (2000) Open System for Earthquake Engineering Simulation (OpenSees). *Technical Report*, University of California, Berkeley, CA.

Mendes N, Costa A A, Lourenço PB, Bento R, Beyer K, de Felice G, Gams M, Griffith M, Ingham JM, Lagomarsino S, Lemos JV, Liberatore D, Modena C, Oliveira DV, Penna A, Sorrentino L (2017) Methods and Approaches for Blind Test Predictions of Out of-Plane Behavior of Masonry Walls: A Numerical Comparative Study, *International Journal of Architectural Heritage*, 11:1, 59-71

Messali F, Rots JG (2018) In-plane drift capacity at near collapse of rocking unreinforced calcium silicate and clay masonry piers. *Engineering Structures*, 164, 183-194.

Mercatoris B,Massart T(2011) A coupled two-scale computational scheme for the failure of periodic quasi-brittle thin planar shells and its application to masonry. Int J Numer Methods Eng 85(9):1177–1206

Milosevic J, Cattari S, Bento (2020) Definition of fragility curves through nonlinear static analyses: procedure and application to a mixed masonry-RC building stock, *Bulletin of earthquake engineering*, 18(2), 513-545.

Milani G (2011) Simple homogenization model for the non-linear analysis of in-plane loaded masonry walls, *Computers & Structures*, 89,1586–1601.

Milani G (2015) Upper Bound Sequential Linear Programming mesh adaptation scheme for collapse analysis of masonry vaults. *Advances in Engineering Software*, 79, 91-110.

Milani G (2019) Fast vulnerability evaluation of masonry towers by means of an interactive and adaptive 3D kinematic limit analysis with pre-assigned failure mechanisms. *International Journal of Architectural Heritage*, 13(7), 941–962.

Minga E, Macorini L, Izzuddin BA, Caliò I (2020) 3D macroelement approach for nonlinear FE analysis of URM components subjected to in-plane and out-of-plane cyclic loading, *Engineering Structures*, 220, 110951.

MIT 2019, Ministry of Infrastructures and Transportation, Circ. C.S.Ll.PP. No. 7 of 21/1/2019. Istruzioni per l'applicazione dell'aggiornamento delle norme tecniche per le costruzioni di cui al Decreto Ministeriale 17 Gennaio 2018. G.U. S.O. n.35 of 11/2/2019 (In Italian).

Morandi P, Albanesi L, Graziotti F, Li Piani T, Penna A, Magenes G (2018) Development of a dataset on the in-plane experimental response of URM piers with brick and blocks, *Construction and Building Materials*, 190, 593-611.

Mordant C (2016) Unreinforced clay masonry structures: advanced characterization of the seismic behavior including acoustic issues. PhD Thesis, University of Liege, Belgium.

MSJC (2008) Building Code Requirements for Masonry Structures (TMS 402/ACI 530/ASCE 5). American Concrete Institute, Structural Engineering Institute, The Masonry Society (Masonry Standard Joint Committee) Boulder, CO, USA.

Nakamura Y, Derakhshan H, Magenes G,Griffith MC (2017) Influence of diaphragm flexibility on seismic response of unreinforced masonry buildings, *Journal of Earthquake Engineering*, 21(6), 935-960.

NTC18 (2018). Italian Technical Code, Decreto Ministeriale 17/1/2018. "Aggiornamento delle Norme tecniche per le costruzioni". Ministry of Infrastructures and Transportation, G.U. n.42 of 20/2/2018 (In Italian).

NZSEE (2017) The Seismic Assessment of Existing Buildings (the Guidelines), Wellington, New Zealand; 2017.

Occhipinti G, Caliò I, D'Altri AM, de Miranda S, Grillanda N, Milani G, Spacone E (2021). Nonlinear Finite and Discrete element simulations of multi-storey masonry walls, *Bulletin of Earthquake Engineering*, submitted to the SI on *URM non modelling* – Benchmark Project.

Oliver J, Huespe AE, Sánchez PJ (2006) A comparative study on finite elements for capturing strong discontinuities: E-FEM vs X-FEM Computer Methods, *Applied Mechanics and Engineering* 195(37-40), 4732-4752.

Oliver J, Huespe A E, Lay J C (2008) Year implicit/explicit integration design to increase computability of non-linear material and contact/friction problems, *Computer Methods in Applied Mechanics and Engineering*, 197,1865-1889.

Ottonelli D, Marano C, Manzini C, Calderoni B, Cattari S (2021) A comparative study on a complex URM building. Part I: sensitivity of the seismic response to different modelling options in the equivalent frame models. *Bulletin of Earthquake Engineering*, https://doi.org/10.1007/s10518-021-01128-7.

Page AW (1981) The biaxial compressive strength of brick masonry. Proc. of the Institution of Civil Engineers.

Pantò, B, Caliò, I, Lourenço, PB (2018) A 3D discrete macro-element for modelling the out-of-plane behaviour of infilled frame structures, *Engineering Structures*, 175, 371-385.

Pantò B, Cannizzaro F, Caddemi S, Caliò I (2016) 3D macro-element modelling approach for seismic assessment of historical masonry churches, *Advances in Engineering Software*, 97, 40-59.

Pantò B, Cannizzaro F, Caliò I, Lourenço,PB (2017) Numerical and experimental validation of a 3D macro-model element method for the in-plane and out-of-plane behaviour of unreinforced masonry walls, *Int. J. Archit. Herit.*, 11(7), 946-964.

Paquette J, Bruneau M (2003) Pseudo-dynamic testing of unreinforced masonry building with flexible diaphragm, *Journal of Structural Engineering*, 129(6), 708-716.

Parisi F, Augenti N (2013) Seismic capacity of irregular unreinforced masonry walls with openings, *Earthquake Engineering and Structural Dynamics*, 42, 101–121.

Pelà L, Cervera M, Roca P (2013) An orthotropic damage model for the analysis of masonry structures, *Constr Build Mater*, 41:957–967.

Penna A, Morandi P, Rota M, Manzini C.F., da Porto F., Magenes G. (2014a) Performance of masonry buildings during the Emilia 2012 earthquake, *Bulletin of Earthquake Engineering*, 12, 2255–2273.

Penna A, Lagomarsino S, Galasco A (2014b) A nonlinear macroelement model for the seismic analysis of masonry buildings, *Earthquake Engineering and Structural Dynamics*, 43(2), 159–179.

Petracca M., Pelà L., Rossi R., Oller R., Camata G., Spacone E. (2016) Regularization of first order computational homogenization for multiscale analysis of masonry structures, *Computational Mechanics*, Springer. ISSN:0178-7675 vol. 57

Petracca M, Pelà L, Rossi R, Oller R, Camata G, Spacone E (2017b) Multiscale computational first order homogenization of thick shells for the analysis of out-of-plane loaded masonry walls, *Computer Methods in Applied Mechanics and Engineering*, 315, 273-301, DOI: 10.1016/j.cma.2016.10.046

Petracca M, Pelà L, Rossi R, Zaghi S, Camata G, Spacone E (2017a) Micro-scale continuous and discrete numerical models for nonlinear analysis of masonry shear walls, *Construction and Building Materials*, 149, 296-314. DOI: 10.1016/j.conbuildmat.2017.05.130

Petry S, Beyer K (2014) Influence of boundary conditions and size effect on the drift capacity of URM walls, *Engineering Structures*, 65,76–88.

Ponte M, Bento R, Vaz SD (2021) A Multi-Disciplinary Approach to the Seismic Assessment of the National Palace of Sintra. *International Journal of Architectural Heritage*, 15(5), 757–778.

Priestley MJ, He L (1995) Seismic Response of T-Section Masonry Shear Walls, *The Masonry Society Journal*, 9 (1), 10-19.

Quagliarini E, Maracchini G, Clementi F (2017) Uses and limits of the equivalent frame model on existing unreinforced masonry buildings for assessing their seismic risk: a review, *J. Build. Eng.*, 10, 166–182.

Raka E, Spacone E, Sepe V, Camata G (2015) Advanced frame element for seismic analysis of masonry structures: model formulation and validation, *Earthquake Engineering and Structural Dynamics*, 44(14),2489-2506.

Reyes JC, Chopra AK (2013) Three-Dimensional Modal Pushover Analysis of Unsymmetric-Plan Buildings Subjected to Two Components of Ground Motion, *Geotechnical, Geological and Earthquake Engineering*, 24, 203–217.

ReLuis – Task 4.1 Workgroup (2018) edited by: S. Cattari, S. Degli Abbati, D. Ottonelli, D. Sivori, E. Spacone, G. Camata, C. Marano, C. Modena, F. Da Porto, F. Lorenzoni, A. Calabria, G. Magenes, A. Penna, F. Graziotti, R. Ceravolo, E. Matta, G. Miraglia, D. Spina, N. Fiorini. Report di sintesi sulle attività svolte sugli edifici in muratura monitorati dall'Osservatorio Sismico delle Strutture, Linea Strutture in Muratura, ReLUIS report, Rete dei Laboratori Universitari di Ingegneria Sismica (In Italian), 2018.

Rezaie A, Godio M, Beyer K (2020) Experimental investigation of strength, stiffness and drift capacity of rubble stone masonry walls, *Construction and Building Materials*, 251, 118972.

Rizzi E, Giongo I, Ingham J M, Dizhur D (2020) Testing and Modeling InPlane Behavior of Retrofitted Timber Diaphragms, *Journal of Structural Engineering*, 146(2), 04019191.

Roca P, Cervera M, Griup G, Pelà L (2010) Structural analysis of masonry historical constructions. Classical and advanced approaches, *Archives of Computational Methods in Engineering*, 17 (3), 299-325.

Rossi M, Barentin C C, Van Mele T, Block P (2017) Experimental study on the behaviour of masonry pavilion vaults on spreading supports, *Structures*, 11, 110-120.

Rossi M, Calderini C, Lagomarsino S (2016) Experimental testing of the seismic in-plane Displacement capacity of masonry cross vaults through a scale model, *Bulletin of Earthquake Engineering*, 14(1), 261-281.

Rosti A, Rota M, Penna A (2021) Empirical fragility curves for Italian URM buildings, *Bulletin of Earthquake Engineering*. 19(8),3057-3076.

Rota M, Penna A, Magenes G (2014) A framework for the seismic assessment of masonry buildings taking into account different sources of uncertainty, *Earthquake Engineering and Structural Dynamics*, 43(7), pp:1045–1066.

Rots JG (2001) The role of structural modeling in preserving Amsterdam architectural city heritage, *Proc. of the 3rd Int. Seminar on Historical Constructions*, 7-9 November.

Russell AP, Ingham JM (2010) The influence of flanges on the in-plane seismic performance of URM walls in New Zealand buildings, *Proc. of New Zealand society of Earthquake Engineering Conference*, paper n.38.

Russell AP, Elwood KJ, Ingham JM (2014) Lateral force-displacement response of Unreinforced Masonry walls with flanges, *Journal of Structural Engineering*, 140(4).

Sacco E (2009) A nonlinear homogenization procedure for periodic masonry. Eur J Mech-A/Solids 28(2):209–222

Sajid HU, Mohammad A, Qaisar A, Sikandar HS (2018) Effects of vertical stresses and flanges on seismic behavior of unreinforced brick masonry, *Engineering structures*, 155, 394-409.

Saloustros S, Cervera M, Pelà L (2019) Challenges, Tools and Applications of Tracking Algorithms in the Numerical Modelling of Cracks, *Concrete and Masonry Structures Archives of Computational Methods in Engineering*, 26(4), 961-1005

Saloustros S, Pelà L, Cervera M, Roca P (2018) An Enhanced Finite Element Macro-Model for the Realistic Simulation of Localized Cracks, in: Masonry Structures: A Large-Scale Application, *International Journal of Architectural Heritage* 12(3),432-447

Sandoli A, Musella C, Lignola GP, Calderoni B, Prota A (2020a) Spandrel panels in masonry buildings: Effectiveness of the diagonal strut model within the equivalent frame mode, *Structures*, 27, 879-893.

Sandoli A, Pacella G, Lignola GP, Calderoni B, Prota A (2020b). FRP-reinforced masonry spandrels: experimental campaign on reduced-scale specimens. *Construction and Building Materials*, 261,119965.

SIA 266:2015 Masonry, Swiss Standard, Swiss Society of Engineers and Architects (SIA), Zurich (in German),

Siano R, Sepe V, Camata G, Pelà L (2017) Analysis of the performance in the linear field of Equivalent-Frame Models for Regular and Irregular Masonry Walls, *Engineering Structures*, 145**,** 190–210.

Siano R, Roca P, Camata G, Pelà L, Sepe V, Spacone E, Petracca M (2018) Numerical Investigation of Non-Linear Equivalent-Frame Models for Regular Masonry Walls, *Engineering Structures*, 173, 512-529.

Silva L, Lourenço PB, Milani G (2020) Numerical homogenization-based seismic assessment of an English-bond masonry prototype: Structural level application. *Earthquake Engineering & Structural Dynamics*, 49, 841-862.

Simo J C, Rifai M. (1990) A class of mixed assumed strain methods and the method of incompatible modes, *International journal for numerical methods in engineering*, 29(8), 1595-1638.

Simoes A, Bento R, Cattari S, Lagomarsino S (2014) Seismic performance-based assessment of "Gaiolero" buildings , Engineerin Structures, 80,486-500.

Sivori D, Lepidi M, Cattari S (2021) Structural identification of the dynamic behavior of floor diaphragms in existing buildings, *Smart Structures and Systems*, 27(2),173-191.

Shi QX, Wang B (2016) Simplified calculation of effective flange width for shear walls with flange, *The structural design of tall and special buildings*, 25, 558-577.

Solarino F, Oliveira, D V, Giresini L (2019) Wall to horizontal diaphragm connections in historical buildings: A state of the art review, *Engineering Structures*, 199, 109559.

Sorrentino L, D'Ayala D, De Felice G, Griffith M, Lagomarsino S, Magenes G (2017) Review of out-of-plane seismic assessment tecniques applied to existing masonry buildings, *International Journal of Architectural Heritage*, 11(1), 2-21.

Sorrentino L, Cattari S., da Porto F., Magenes G., Penna A. (2019) Seismic behaviour of ordinary masonry buildings during the 2016 central Italy earthquakes, *Bulletin of Earthquake Engineering*, 2019, 17(10), 5583–5607.

Spina D, Acunzo G, Fiorini N, Mori F, Dolce M. (2019) A probabilistic simplified seismic model of masonry buildings based on ambient vibrations, *Bulletin of Earthquake Engineering*, 17, 985–1007.

Tomazevic M (1978) The computer program POR, Report ZRMK, Ljubljana, Slovenia, (in Slovenian).

Tomic I, Vanin F, Beyer K (2021) Uncertainties in the seismic assessment of historical masonry buildings, *Applied Sciences*, 11 (5), 1-36,10.3390/app11052280

Turnsek V, Sheppard P. The shear and flexural resistance of masonry walls. *Proc. of the International Research Conference on Earthquake Engineering*, June 30 - July 3 1980, Skopje, Macedonia.

Vanin F, Penna A, Beyer K (2020a) A three-dimensional macroelement for modelling the in-plane and out-of-plane response of masonry walls, *Earthquake Engineering and Structural Dynamics*, 49, 1365–1387.

Vanin F, Penna A, Beyer K (2020b) Equivalent-Frame modeling of two shaking table tests of masonry buildings accounting for their out-of-plane response, *Frontiers in Built Environment*, 6:42. doi: 10.3389/fbuil.2020.00042.

Vanin F, Zaganelli D, Penna A, Beyer K. (2017) Estimates for the stiffness, strength and drift capacity of stone masonry walls based on 123 quasi-static cyclic tests reported in the literature. *Bull. Earth. Eng*, 15(12), 5435-5479.

Wilding BV, Beyer (2018) Analytical and empirical models for predicting the drift capacity of modern unreinforced masonry walls, *Earthquake Engineering and Structural Dynamics*, 47(10), 2012–2031.

Yi T, Moon FL, Leon RT, Kahn LF (2006) Lateral load tests on a two-story unreinforced Masonry building, *Journal of Structural Engineering*, 132, 643–652.

Yi T (2004) Experimental investigation and numerical simulation of an unreinforced masonry structure with flexible diaphragms. PhD Thesis, Georgia Institute of Technology, Atlanta, GA, USA.

Zucchini A, Lourenço PB (2009) A micro-mechanical homogenization model for masonry: application to shear walls. Int J Solids Struct 46(3–4):871–886